Defects in correlated metals and superconductors

H. Alloul,* J. Bobroff,† and M. Gabay‡

Laboratoire de Physique des Solides, Université Paris-Sud 11, UMR 8502, CNRS, F-91405 Orsay Cedex, France

P. J. Hirschfeld§

Department of Physics, University of Florida, Gainesville, Florida 32611-8440, USA and Laboratoire de Physique des Solides, Université Paris-Sud 11, UMR 8502, CNRS, F-91405 Orsay Cedex, France

(Published 8 January 2009)

In materials with strong local Coulomb interactions, simple defects such as atomic substitutions strongly affect both macroscopic and local properties of the system. A nonmagnetic impurity, for instance, is seen to induce magnetism nearby. Even without disorder, models of such correlated systems are generally not soluble in two or three dimensions, and so few exact results are known for the properties of such impurities. Nevertheless, some simple physical ideas have emerged from experiments and approximate theories. Here the authors review what we can learn about this problem from one-dimensional (1D) antiferromagnetically correlated systems. Experiments on the high-T_c cuprate normal state which probe the effect of impurities on local charge and spin degrees of freedom are discussed, and compared with theories of single impurities in correlated hosts, as well as phenomenological effective Kondo descriptions. Subsequently, theories of impurities in d-wave superconductors including residual quasiparticle interactions are reviewed and compared with experiments in the superconducting state. Existing data exhibit a remarkable similarity to impurity-induced magnetism in the 1D case, implying the importance of electronic correlations for the understanding of these phenomena, and suggesting that impurities may provide excellent probes of the still poorly understood ground state of the cuprates.

DOI: 10.1103/RevModPhys.81.45 PACS number(s): 73.20.Hb, 74.62.Dh, 74.20.−z, 74.70.−b

CONTENTS

*alloul@lps.u-psud.fr
†bobroff@lps.u-psud.fr
‡gabay@lps.u-psud.fr
§pjh@phys.ufl.edu

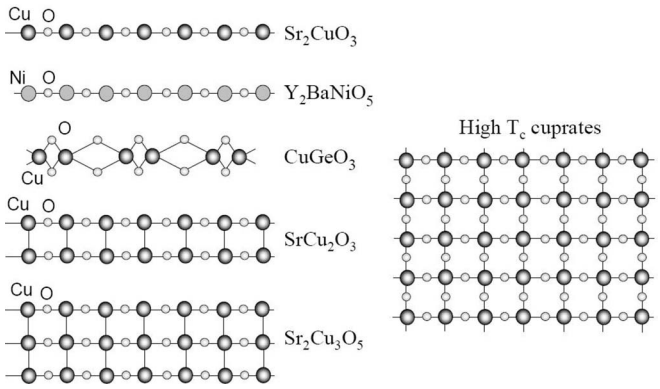

FIG. 1. A selection of actively studied inorganic oxides. Only the chain (Sr_2CuO_3, Y_2BaNiO_5, $CuGeO_3$), ladder ($SrCu_2O_3$, $Sr_2Cu_3O_5$), or planar (cuprates) unit in the molecular structure is shown.

I. INTRODUCTION

A. Aim and scope of this article

The study of "strongly correlated electron systems," materials where the typical electronic interaction energies are of order or larger than the kinetic energies, underwent a renaissance in the 1980s and 1990s after the discovery of superconductivity in organic conductors, in heavy fermions and then in copper oxides. In particular, the cuprate family has had an enduring fascination for the condensed-matter community, and not simply because of the allure of room-temperature superconductivity. Most of the important unsolved problems of quantum condensed-matter physics—the metal-insulator transition in low dimensions, breakdown of Fermi-liquid theory, the origin and behavior of unconventional superconductivity, quantum critical points, electronic inhomogeneities and localization in interacting systems, and quantum antiferromagnetism in low dimensions—are represented in the set of questions currently under active consideration in this lively field. Two factors are currently believed to underlie the anomalous properties of these materials: low dimensions and strong correlations, both of which appear to be necessary to stabilize the new types of electronic states present.

The cuprates contain as common elements CuO_2 planes (Fig. 1), which are sometimes considered to contain all the important physics. Their structure is a stacking of such planes separated by other oxide layers, which maintain charge neutrality and the cohesion of the structure essentially through ionic interactions. High-temperature superconductivity (HTSC) has been of course the physical property that has driven the interest in these systems, initially for both its fundamental aspects and its potential applications. Another aspect responsible for their appeal has certainly been the ease with which the carrier concentration can be changed by chemical heterovalent substitutions or oxygen insertion in the layers separating the CuO_2 planes, which play the important role of charge reservoirs. Electron or hole doping can then be fairly continuously controlled from zero to about 0.3 charges per unit cell, which allows one to study the evolution of the physical properties of these materials with doping. In addition to changing the concentration of charge carriers, the doping process in HTSC nearly always introduces some measure of disorder.

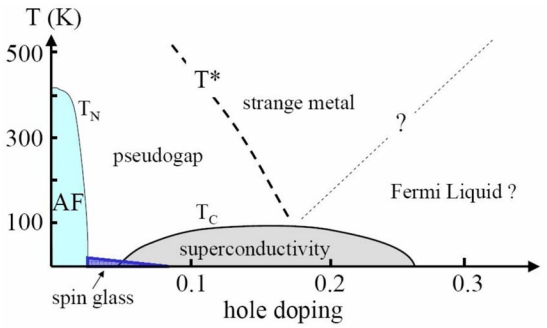

FIG. 2. (Color online) Schematic phase diagram of cuprate HTSC materials: temperature T vs hole doping n_h. AF refers to a state with long-range antiferromagnetic order, which disappears at the Néel temperature T_N. Superconductivity with d-wave symmetry sets in below a critical temperature T_c.

Despite the fact that the phase diagrams of electron- and hole-doped materials look qualitatively similar, their electronic properties in the normal and superconducting states show significant differences. To date, the hole-doped family has been more extensively studied, particularly as far as the issue of impurities is concerned, and in this review we chose to focus on this type of system. In most other classes of correlated electron materials such as quasi-one-dimensional or -two-dimensional organic compounds, one-dimensional (1D) chains, or fullerides, the number of carriers is difficult to modify, except close to some specific compositions, where pressure must be applied to modify electronic properties.

In addition to dopants, located in the charge reservoir layers, other types of impurities are sometimes intentionally introduced into the CuO_2 planes. Initially this was done to test their pair-breaking influence on superconductivity. The observation that nonmagnetic impurities such as Zn reduced T_c triggered a surge of interest in the electronic properties of impurity states in the normal metallic phases as well, and led to the discovery that even nonmagnetic impurities induce local magnetism, the central theme of this review. In the following, we highlight general features that characterize the physics of correlated electron systems, illustrating them using the phase diagram of the cuprates. We then recall why point defect impurities can be used as specific probes of the physical properties of these complex materials, where an understanding of the role of disorder has proven so crucial.

1. Correlated electron systems at a glance

Generically, at low T an insulating, magnetic phase is found in some region of the phase diagram of correlated systems, while a metallic or superconducting state is present in a neighboring (or in some cases overlapping) region. This situation is illustrated with the cuprate phase diagram of Fig. 2, which displays the different phases versus the hole content in the CuO_2 plane. Note that here zero doping corresponds to half filling, i.e., a situation where one hole is localized on each Cu atom, yielding an antiferromagnetic (AF) insulating ground state. Such a state is usually nonmetallic when the Coulomb interaction is large enough with respect to the bandwidth. In some easily compressible materials, e.g., organic systems such as the κ-$(ET)_2CuX$ salts, applying pressure increases the bandwidth and yields a Mott insulator to metal transition. In the case of cuprates and some heavy-fermion compounds, such as $CeRh_{1-x}Ir_xIn_5$, the AF order is suppressed by doping and is replaced by a metallic or a superconducting state. These types of metal-insulator transition (MIT) or superconductor-insulator transition (SIT) are archetypes of the problems encountered in correlated electron physics, which are not yet fully understood.

The phase diagram of correlated electron systems presents many novel states of matter, which in the case of cuprates includes a spin glass, a pseudogap regime, a "strange metal," a d-wave superconductor, and a putative Fermi liquid, with only the last one to be reasonably well understood theoretically (see Fig. 2). The nature of these phases has been reviewed elsewhere and will be discussed in Sec. IV. At $T=0$ the boundaries between some of these phases may correspond to quantum critical points (QCPs). In the cuprate phase diagram of Fig. 2, QCPs might be present at the end points of the superconducting dome, or at the extensions to $T=0$ of the dashed lines shown in Fig. 2, which have, however, not yet been established as true phase transitions.

Much can be learned from studies of systems with dimensions less than 2, since many theoretical results are available for 1D and quasi-1D systems. Furthermore, it is natural to imagine approaching the 2D system, where few exact results are known, by adjoining chains to form ladders and successively increasing the number of legs. Many physical situations encountered in one dimension, such as the separation of spin and charge degrees of freedom yielding the concepts of spinons and holons can be conceptually followed if one progressively increases the dimensionality of the system from 1 to 2. Although this was initially considered as a purely theoretical approach, the skills of researchers in materials science have allowed the synthesis of systems implementing the theoretical strategy. Indeed, inorganic realizations of quasi-1D spin chains are represented, e.g., by Sr_2CuO_3 (spin 1/2), Y_2BaNiO_5 (spin 1), and $CuGeO_3$ (spin 1/2, spin Peierls). The Sr_2CuO_3 material contains CuO chains which are similar to those found in the 2D cuprate $YBa_2Cu_3O_{6+x}$ (YBCO). The ladder compounds consisting of coupled spin-1/2 CuO chains, e.g., $SrCu_2O_3$ (two legs) and $Sr_2Cu_3O_5$ (three legs), are natural low-dimensional analogs of the cuprates (see Fig. 1). We discuss these systems in Sec. III.

2. Impurities as probes of correlated electron systems

To gain insight into the complex problems which arise in correlated electron systems, all possible tools and techniques have been extensively used and improved. One particular approach has been to study the modifications of the physical properties induced by the con-

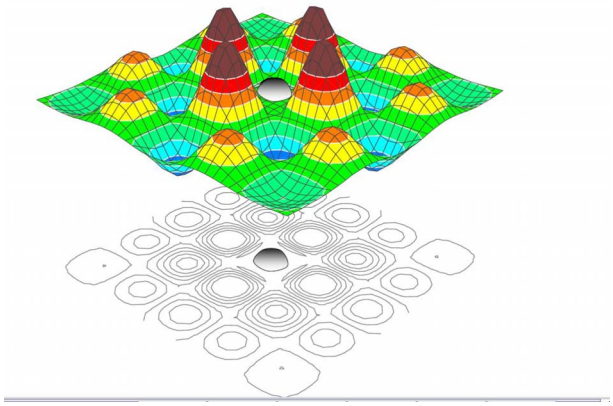

FIG. 3. (Color online) Cartoon of the staggered paramagnetic polarization induced by a nonmagnetic defect (dot at center) in a correlated 2D material. Such oscillations of the local susceptibilities are directly detectable by spin probe experiments such as NMR, since the NMR shifts of the various shells of neighbors of the defects can be resolved.

trolled introduction of point defects in the materials. We report studies of impurity substitutions, and of defects created by electron irradiation, and of defects which occur naturally even in the purest available materials synthesized so far. This approach combines material science investigations with the use of the most advanced local probe techniques.

Impurities are known to modify superconductivity in crucial ways. In conventional *s*-wave BCS materials, disorder causes changes in the penetration depth λ and in the coherence length ξ. For superconductors with non-*s*-wave symmetry, different effects are expected since impurities break Cooper pairs. It is therefore quite natural to probe the influence of defects on most matters linked with superconductivity.

In conventional metals, impurity effects constitute a relatively well-understood subject. The essence of the observed phenomena is that an impurity is a local screened Coulomb potential, which ideally is a uniform perturbation in $\mathbf{q}$ space, inducing a response which is inhomogeneous in real space but which reflects the response to all $\mathbf{q}$ values. So if some singularity occurs at a specific $\mathbf{q}$ value for a system, this singular response will dominate the modifications introduced by the impurity. In a classical metallic system, since the response is homogeneous up to $|\mathbf{q}|=k_F$, the main detected feature comes from this truncation of the response at k_F, which yields the well-known Friedel oscillations in the local density of states for a charge defect, and the Ruderman-Kittel-Kasuya-Yosida (RKKY) oscillation for a spin defect. This idea can be naturally generalized to any type of material. For instance, in magnetic materials for which AF correlations can be important at a wave vector $\mathbf{q}=\mathbf{q}_{\mathrm{AF}}$, a staggered magnetic response at this wave vector is expected (Fig. 3). This is exemplified in the case of an AF spin chain, in which a staggered paramagnetic response appears near chain ends. So quite generally an impurity potential is a fundamental tool to probe the specific response of a system.

The potential importance of this property was captured by experimentalists who developed local probe techniques, such as NMR and scanning tunnel microscopy (STM), to map out the spatial changes occurring around extrinsic defects. For instance, NMR experiments performed on the cuprates over the past 15 years or so, using a variety of nuclei, have developed a fairly clear picture of how a nominally "nonmagnetic" impurity creates a cloud of local staggered polarization on nearby Cu sites, and have characterized the response as a function of doping and temperature, for different materials.

These results triggered a growing interest in the theory community as well. The enormous theoretical effort devoted to solving problems of homogeneous 2D correlated Fermi systems by approximate methods has been occasionally applied as well to impurity problems or even to finite disorder. While there is currently no generally accepted theoretical description of an impurity in a strongly correlated 2D system (as there is no generally accepted theory for the homogeneous problem), a qualitative picture captured by many different approaches has emerged and will be summarized in this review. By contrast, the impurity problem has been quantitatively studied in the case of 1D systems, since exact analytical techniques are available, and the defect's influence on transport, magnetism, and thermal properties is known. The best studied and understood example of this phenomenon is the nonmagnetic impurity in spin chain systems, which is equivalent to a chain end in a noninfinite spin chain. Here it can be shown in a controlled fashion that a single (even weak) potential defect induces a paramagnetic net moment and staggered magnetism in its vicinity, and that the decay of this magnetism directly measures the spin correlation functions of the *pure* state. Observations done on 2D cuprates have been successfully extended to quasi-1D systems, where impurities have been used to probe magnetic correlations in a wide variety of materials. The behavior of these states depends on whether the pure host system manifests a spin gap, which in turn depends on the number of coupled chains and whether the spins are integer or half integer.

Studies of impurities in correlated electron systems are also important to help us understand the influence of (intrinsic) disorder that is present in nominally pure systems. As pointed out before, in cuprate materials and heavy-fermion systems, one can easily change the carrier concentration and thus explore a wide range of the phase diagram using the same system. However, the very doping process introduces disorder. The importance of this phenomenon has only been recently appreciated by much of the community, as local techniques such as STM have imaged impurity states directly and brought to the fore the study of disorder as a key issue in correlated electron systems. The efforts that have been made so far to understand the influence of controlled disorder and impurities are good reference points to try to under-

stand those due to the intrinsic disorder. So, although this is not the main aim of the present review, we try hereafter to recall as well some of the established facts which should help to separate out in the materials problems those that might be attributed to the intrinsic disorder.

B. Structure of the paper

We first give some preliminary background in Sec. II, discussing the basic ideas of strongly correlated electron physics, introducing the simplest and most popular models like the Hubbard and *t-J* Hamiltonians, along with some words about current methods employed to solve them. We then begin our main theme in the strange world of one dimension: in Sec. III we summarize recent progress on the conceptually simplest problem in the field, that of an impurity in a 1D spin chain. We first attempt to explain qualitatively the physical phenomena expected, discuss the theoretical background for this expectation, and justify the use of NMR to study such effects. We describe the most studied materials and models first in their idealized homogeneous form in terms of their physical properties (Haldane gap, quasi-long-range order). In the disorder-free limit, one finds correlated quantum ground states, called spin liquids, and we define the concepts of the resonating valence bond (RVB) phase, and of spinon or holon excitations. These notions will be quite useful when we turn to the 2D case. We then introduce models of defects and the concept of end-chain excitations, and show why NMR is particularly useful for studying such effects. The discussion is then broadened to include ladder compounds and models, which are in certain well-defined senses steps on the road to two dimensions. For the most part we restrict ourselves to pure spin models, as there are few relevant experiments on doped ladder or chain compounds.

In passing to two dimensions in Sec. IV, we focus on the cuprate family, and first discuss the various types of point defects that occur or can be induced in these materials. We then make contact with what we have learned from spin chains, by focusing on the undoped antiferromagnetic cuprate insulators. The analogy is not completely straightforward, since, although the cuprate planes are sometimes regarded as idealized 2D Heisenberg spin systems, the interplane couplings and small spin anisotropies must be accounted for as well. In addition, few experiments have been performed on local properties of defects in the insulating systems, and so we pass quickly to the underdoped pseudogap state, in the metallic regime. Here the suppression of the single-particle density of states (DOS) and magnetic susceptibility suggest that impurity-induced magnetism should have a large relative effect, and indeed the first observation of moment formation around impurities was made in underdoped YBCO. We review these experiments, and the measurement and interpretation of the temperature dependence of the local susceptibilities. We compare the similarities and differences between impurities, in the cases of Zn, nominally nonmagnetic, Ni, nominally spin 1, and Li, nominally nonmagnetic but charged. We review the changes in local susceptibility found to occur when the system is doped further to optimal doping, and discuss the behavior of the impurity Curie-Weiss temperature, and a simple interpretation in terms of Kondo screening. Finally, we discuss other measurements that do not give local information but are relevant to understanding the physics of disorder in these materials, particularly transport measurements.

In Sec. V we review theoretical efforts to understand the remarkable phenomenology described in higher dimensions. Some of the ideas and relevant calculations about moment formation in correlated systems are not new, and we therefore begin by reminding the reader of early work on nearly magnetic alloys and phosphorus-doped silicon. More recent work related to the properties of Zn and Ni in cuprates, which describes these ions as localized potentials embedded in a 2D Hubbard treated within the random-phase approximation, is the intellectual heir of these early works. We describe the basic ideas, which involve the buildup of antiferromagnetic correlations on the lattice due to the Hubbard repulsion, and the mode-mode coupling induced by the impurity between this staggered response and the homogeneous response actually measured in NMR in the normal state. These theories provide a remarkably good description at optimal doping, but it is not clear how to extend them to describe the effects in underdoped samples. We then discuss several theoretical approaches which begin at strong coupling with a *t-J* model, and moment formation in the spin gap state. For the most part, such theories have described spontaneous moment formation, enhanced by the presence of a pseudogap, and do not discuss the paramagnetic state in detail.

Section VI presents our understanding of the impact of superconductivity on the effects described above. To place the discussion in context, we begin by reviewing the basic ideas concerning the properties of a single impurity and many-impurity interference in a *d*-wave superconductor. We then describe how the predictions of theories described in Sec. V are modified in the presence of a gap. Finally, we discuss experiments on impurities in the superconducting state which directly probe the local density of states and magnetic correlations, and attempt to compare the results to these ideas and predictions.

II. MODELS OF CORRELATED FERMI SYSTEMS

To set the stage for our discussion of defects, we first give an account of the physics of homogeneous correlated systems and the models used to describe them. We refer the reader to more extensive reviews on the subject (Fazekas, 1999; Fulde *et al.*, 2006). From a theoretical perspective, transport, thermal, and magnetic observables can be obtained in strongly correlated systems once one has constructed a Hamiltonian containing all essential ingredients characterizing these systems, yet simple enough to be amenable to analytical or numerical computations. By and large, the model of choice is the Hubbard model, which was introduced in the early 1960s

to describe magnetism and metal-insulator transitions in narrowband transition metals (Gutzwiller, 1963a; Hubbard, 1963; Kanamori, 1963). The model consists of a kinetic term describing the hopping dynamics of electrons (or holes) with site creation operators $a_{i,\sigma}^{\dagger}$ and a potential term accounting for on-site Coulomb interactions,

$$\mathcal{H}_{\mathrm{Hubb}} = \sum_{\langle i,j\rangle,\sigma} t_{i,j}(a_{i,\sigma}^{\dagger}a_{j,\sigma} + \mathrm{H.c.}) + \tfrac{1}{2}U\sum_{i,\sigma} n_{i,\sigma}n_{i,\bar{\sigma}}. \quad (1)$$

In the simplest version, the hopping amplitude $t_{i,j}$ is limited to nearest neighbors and σ is one of the spin-$\frac{1}{2}$ eigenstates, while $\bar{\sigma}$ is the other one. $n_i = \Sigma_\sigma n_{i,\sigma}$ fermions occupy site i. The case $U>0$ corresponds to repulsive interactions, while $U<0$ mimics effective attractive interactions (mediated, for instance, by electron-phonon or electron-paramagnon processes). For the special case $U=0$ the state is either metallic or (band) insulating, depending on the filling factor. The Hubbard model was introduced originally to study the Mott transition which occurs when the bandwidth of a system narrows sufficiently in the presence of repulsive U. The basic physics can be understood by considering a lattice of atomic orbitals which can overlap to allow conduction. If there is one orbital per site, and one electron per orbital, the system is a metal if $U=0$ according to conventional electronic structure theory. Thus electrons may hop from orbital to orbital, provided all states satisfy the Pauli principle allowing only one $\uparrow$ and one $\downarrow$ spin per orbital, i.e., the Hilbert space for each site consists of $|0\rangle$, $|\uparrow\rangle$, $|\downarrow\rangle$, and $|\uparrow\downarrow\rangle$. As $U>0$ is increased, however, the Coulomb cost of doubly occupied sites $|\uparrow\downarrow\rangle$ increases, so that in the limit $U\to+\infty$ such configurations are no longer allowed, or are "projected out" of the Hilbert space. If no doubly occupied sites are present, electrons are effectively prevented from hopping in the half-filled case, and if a small number of holes is introduced one can easily see that, although conduction can now take place, it is drastically reduced due to the Coulomb repulsion. This is the primary effect of electronic "correlations" that will be considered here.

More generally, if U is nonzero, depending on its sign, the size of the ratio U/W (W is the bandwidth), and the filling factor, one expects to promote various instabilities of magnetic, metal-insulator, or superconducting types, or even phase separation. These transitions may occur at finite temperature or at zero temperature depending on the spatial dimensionality. Only a few exact results are available for this model, mostly in the one-dimensional case (Eggert, 1993). In that limit, fluctuations prevent the occurrence of ordered phases at finite temperature. At $T=0$ and for half filling, the ground state is insulating and has quasi-long-range antiferromagnetic order when $U>0$, or on-site singlet ordering when $U<0$ (Auerbach, 1994; Giamarchi, 2004). By quasi-long-range order we mean that the expectation value of the staggered magnetization is zero in the thermodynamic limit, but that the corresponding coherence length is infinite (the alternating part of the spin-spin correlation function decays as a power law at large distances). For any other band filling, the chain is a non-Fermi-liquid paramagnetic metal, when Coulomb interactions are repulsive, or a quasiordered s-wave superconductor when interactions are attractive. For higher dimensions, only a handful of methods allow analytic treatments of the Hubbard model. The simplest is the Hartree-Fock approximation, including random-phase approximation (RPA) extensions and beyond to include fluctuation effects (Kanamori, 1963; Hertz, 1976; Hirsch, 1980; Bickers *et al.*, 1989; Pao and Bickers, 1995; Aryanpour *et al.*, 2002). Its validity corresponds essentially to the weakly correlated regime (U/W much less than 1). When U is large and positive, one may use the Gutzwiller variational wave function to determine the $T=0$ properties of the model (Gutzwiller, 1963b), the Hubbard X operators (Ovchinnikov and Val'kov, 2004), or alternatively auxiliary field methods developed, for instance, by Kotliar and Ruckenstein (1986) and Lee and Nagaosa (Lee *et al.*, 2006), based on slave bosons (Barnes, 1976, 1977; Read and Newns, 1983; Coleman, 1984; Read, 1985; Bickers, 1987). Note, however, that the Gutzwiller wave function accounts for on-site correlations but neglects intersite correlations, such as the Heisenberg AF interactions, which play an important role in the large-U limit (Kaplan *et al.*, 1982). In the $d=\infty$ limit, many results pertaining to the Hubbard model can be obtained by a diagrammatic treatment, thanks to the fact that many terms vanish (Metzner and Vollhardt, 1989), and the predictions are in agreement with those obtained by Gutzwiller and Kotliar and Ruckenstein. Closely related is dynamical mean-field theory, a combination of analytic and numerical tools allowing quantitative and accurate determinations of metal-insulator transitions (Georges *et al.*, 1996; Kakehashi, 2004; Kotliar *et al.*, 2006; Kyung *et al.*, 2006).

In the $U=+\infty$ limit, double occupancy of the sites becomes energetically unfavorable, and carriers perform only virtual hops onto neighboring sites. A canonical transformation then maps the Hamiltonian Eq. (1) onto the so-called t-J model (Harris and Lange, 1967; Chao *et al.*, 1977; Hirsch, 1985),

$$\mathcal{H}_{t\text{-}J} = \sum_{\langle i,j\rangle,\sigma} t_{i,j}(a_{i,\sigma}^{\dagger}a_{j,\sigma} + \mathrm{H.c.}) + J\sum_{\langle i,j\rangle} (\vec{S}_i\cdot\vec{S}_j - \tfrac{1}{4}n_i n_j). \quad (2)$$

Here creation and annihilation operators are not the canonical ones, but are projected onto the subspace of non-doubly-occupied states. The exchange $J=4t^2/U$ is the AF coupling between spins. In the half-filled case, the kinetic term has to be zero, and one is left with a Heisenberg Hamiltonian for localized spins. As mentioned, in one dimension one gets quasi-long-range AF order at $T=0$. After much debate, it is now generally agreed that the ground state is antiferromagnetic in two dimensions at $T=0$ (fluctuations destroy the order at finite temperatures). Away from half filling, one may treat the kinetic term as a perturbation (Brinkman and Rice, 1970; Kampf, 1994). The bandwidth is strongly narrowed due to the interaction between the carrier motion and spin dynamics, and the energy scale is not governed by t,

as one might expect, but rather by J (Xu *et al.*, 1991). This property is also seen in exact diagonalization of finite-size clusters (Dagotto, 1994; Leung and Gooding, 1995) and experiments are consistent with theoretical prediction (Wells *et al.*, 1995; Damascelli *et al.*, 2003). We note that the Hamiltonian (2), if derived from Eq. (1), should also include an additional kinetic contribution of order t^2/U involving three sites (ijk),

$$\mathcal{H}_{3\ \text{sites}} = -2\frac{t^2}{U}\sum_{\langle i,j,k\rangle,\sigma}(a^{\dagger}_{i,\sigma}a_{k,\sigma}n_{j,\bar{\sigma}} - a^{\dagger}_{i,\sigma}a_{k,\bar{\sigma}}a^{\dagger}_{j,\bar{\sigma}}a_{j,\sigma}). \quad (3)$$

For nonzero doping and when carriers are mobile, one can rewrite the Hamiltonian Eq. (3) in terms of effective Heisenberg interactions involving second- and third-neighbor spin couplings (Inui *et al.*, 1988). A variety of phases can be obtained when the model—in its Hubbard or t-J form—is generalized to include more complicated kinetic or correlation terms, or else to include several orbitals or hybridizations between different bands. The restriction of Coulomb interactions to on-site terms is a drastic approximation, and several have examined the influence of an additional coupling between nearest neighbors in Hubbard chains and ladders (Fabrizio, 1993; Orignac and Giamarchi, 1997); in addition to the Hamiltonian (1), where (in the case of ladder compounds) the hopping amplitude $t_{i,j}$ can take on different values along the chains and rungs, one includes an extra Coulomb contribution:

$$\mathcal{H}_{\text{nnc}} = V\sum_{i,p} n_i n_{i+p}. \quad (4)$$

Here p is the neighbor of i on the *same* chain. For chains, this term stabilizes insulating commensurate phases for less than half filling. For ladders, it promotes an interesting orbital antiferromagnetic order. In organic materials, the molecular bonding is responsible for a pronounced quasi-1D character [for instance, in the Bechgaard or Fabre salt series (Bourbonnais and Jérome, 1999)], or a quasi-2D band structure character [for instance, in the BEDT series (Limelette *et al.*, 2003)]. In the former case, the hopping amplitude t_{ij} in Eq. (1) has a value $t_a \simeq 1000$ K along the conducting chains, $t_b \simeq t_a/10$ in one of the directions perpendicular to the chains, and $t_c \simeq t_a/100$ in the third direction. In the latter case $t_a \simeq t_b$. Since doping has not been successfully achieved for these materials, the main tuning parameter is pressure: it is applied either externally or internally when (halogen) atoms are chemically substituted into the structure and this changes the ratio t/U.

Heavy-fermion compounds are generally discussed in the framework of a periodic Anderson Hamiltonian which reads (Stewart, 2001; Sun and Kotliar, 2005)

$$\mathcal{H}_{\text{HF}} = \sum_{i,N} E^f_N n^f_{i,N} + \tfrac{1}{2}U \sum_{i,N,N',N'\neq N} n^f_{i,N}n^f_{i,N'} + \sum_{\vec{k},N}\epsilon_{\vec{k}}c^{\dagger}_{\vec{k},N}c_{\vec{k},N} + V\left(\sum_{i,N} f^{\dagger}_{i,N}c_{i,N} + \text{H.c.}\right). \quad (5)$$

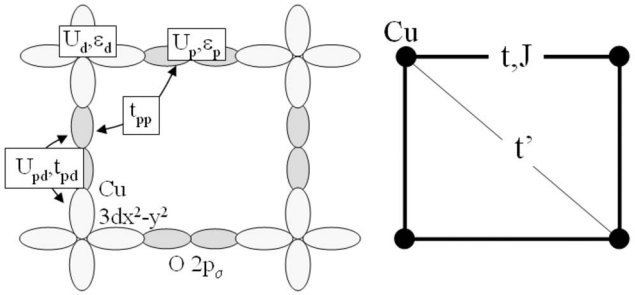

FIG. 4. Cu and O orbitals in the copper-oxide planes; relevant site, hopping, and correlation energies are included. Integrating out the O variables yields a t,t'-J model for the effective Cu lattice (right side). The notation is defined in the text.

The first two terms represent the limiting form of $\mathcal{H}_{\text{Hubb}}$ Eq. (1) for f-electron states with creation operators $f^{\dagger}_{i,N}$, since the band is so narrow that it can be approximated by a simple atomic level. The last term models the hybridization of the f state on site i with a wide band of electrons with creation operators $c^{\dagger}_{\vec{k},N}$. Their Coulomb interactions can be neglected and the kinetic part corresponds to the third term on the right-hand side of Eq. (5). Note that the summation over N runs over an *a priori* degenerate spin-orbit multiplet (although crystal-field effects and Hund's rule might of course reduce the number of terms).

An important extension of the previous model concerns cuprate materials. We focus upon this case in more detail, since these compounds will serve as our preferred example for our discussion of impurities in strongly correlated material. It is generally accepted that modeling electronic states in the copper-oxide planes allows one to capture the most remarkable and relevant properties of these high-temperature superconductors. In this case, a narrow Cu d band hybridizes with a wide O p band. In the undoped compound, the (electron) $d_{x^2-y^2}$ orbital is half filled while the p orbitals are fully occupied, and we denote their energies by E_d and E_p, respectively. Since the difference $E_d - E_p$ is small, the $d_{x^2-y^2}$, p_x, and p_y orbitals hybridize strongly (Fig. 4) and form the basis of the three-band model. The p_z and $d_{3z^2-r^2}$ wave functions couple to the buffer (or reservoir) out-of-plane oxide layers and are usually not included in a model of the CuO_2 planes. However, they have been shown to significantly renormalize the effective parameters in a one-band model (Pavarini *et al.*, 2001). Conventionally, one introduces *hole* creation operators $d^{\dagger}_{i,\sigma}$ and $p^{\dagger}_{j,\sigma}$ for the Cu and O orbitals, respectively. The most relevant site energies, hopping amplitudes, and Coulomb U are shown in Fig. 4; their values have been obtained through computer studies (Hybertsen *et al.*, 1989; McMahan *et al.*, 1990; Eskes and Sawatzky, 1991; Kampf, 1994). Using

$$\epsilon_d = -E_d - U_d - 2U_{pd}, \quad \epsilon_p = -E_p - U_p - 2U_{pd}, \quad (6)$$

the model Hamiltonian reads

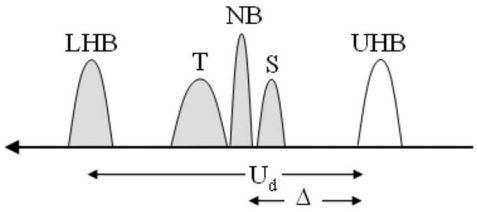

FIG. 5. Schematic rendition of the main energy hole states for the three-band and *t-J* models. The UHB (upper Hubbard band), NB (nonbonding band), and LHB (lower Hubbard band) pertain to the former while the *S* (Zhang-Rice singlet band) and *T* (Zhang-Rice triplet band) refer to the latter. Δ is the charge-transfer gap between the UHB and *S* bands. In the absence of doping, the UHB is completely filled with holes.

$$\mathcal{H}_{3\ \mathrm{band}} = \epsilon_d \sum_{i,\sigma} n^d_{i,\sigma} + \epsilon_p \sum_{j,\sigma} n^p_{j,\sigma} + \sum_{\langle i,j\rangle,\sigma} t^{pd}_{i,j}(p^\dagger_{j,\sigma} d_{i,\sigma} + \mathrm{H.c.}) + \sum_{\langle j,j'\rangle,\sigma} t^{pp}_{j,j'}(p^\dagger_{j,\sigma} p_{j',\sigma} + \mathrm{H.c.}) + U_d \sum_i n^d_{i,\uparrow} n^d_{i,\downarrow} + U_p \sum_j n^p_{j,\uparrow} n^p_{j,\downarrow} + U_{pd} \sum_{\langle i,j\rangle} n^d_i n^p_j. \quad (7)$$

The on-site and kinetic parts of $\mathcal{H}_{3\ \mathrm{band}}$ yield three bands, as shown in Fig. 4. In the hole basis, the lowest energy band (called antibonding in reference to electron states) is mainly of *d* character with a small admixture of *p*. It is half filled, since one has one hole per CuO_2 unit. The highest (bonding) band, mainly of *p* character, is empty, and the charge transfer gap between the two is $\Delta = \epsilon_p - \epsilon_d$. An empty (nonbonding) *p* band is centered around ϵ_p. Since U_d is large, the splitting of the antibonding states induced by the Coulomb energy U_d pushes the $3d^9 \rightarrow 3d^8$ band (again in reference to electron states) far above the bonding band. Since U_p and U_{pd} are significantly smaller than U_d, they do not affect the bonding and nonbonding bands too strongly. Thus the "upper" ($3d^9 \rightarrow 3d^{10}$) Hubbard band is filled with holes and constitutes the ground state; it is separated from the nonbonding excited states by a charge transfer gap of order Δ (Fig. 5). Zhang and Rice (1988) proposed a further reduction of the three-band model to an effective single-band model: a hole injected into the plane goes into an oxygen orbital since U_d is more than two times larger than Δ. In fact, it lives on the four oxygen sites surrounding a copper site, but its spin forms a so-called Zhang-Rice singlet with the copper spin. On that particular plaquette, one has a charge but no spin. Only one singlet can occupy a given plaquette at a time. The Zhang-Rice singlet then hops from one plaquette to a neighboring one, carrying charge and restoring a spin $\frac{1}{2}$ on the first plaquette. The low-energy physics is then minimally described in terms of a *t-J* model, Eq. (2), on a lattice (each site corresponds to the original CuO_2 unit), where *t* is of order 0.4 eV and *J* of order 0.1 eV, as shown in Fig. 4 (Dagotto, 1994; Kampf, 1994). The Zhang-Rice states are shown in Fig. 5. Such a reduction is not universally accepted, and there are many proposals that require three or more bands (Emery, 1987; Varma, 2006). On the other hand, early NMR experiments suggested that magnetic fluctuations on Cu and O sites track each other, when the temperature or the doping is varied, lending support to the Zhang-Rice scenario (Alloul *et al.*, 1989; Takigawa *et al.*, 1991). Still, angle-resolved photoemission spectroscopy (ARPES) experiments which are used to assign values to t_{ij} reveal that, in general, one needs to include at least second-neighbor Cu-Cu hoppings (Schabel *et al.*, 1998; Damascelli *et al.*, 2003). Neutron and Raman scattering allow one to determine *J* and show that nearest-neighbor couplings dominate. As such, a popular model used to discuss the strongly correlated limit is the *t-t′-J* Hamiltonian,

$$\mathcal{H}_{t\text{-}t'\text{-}J} = -t \sum_{\langle i,j\rangle,\sigma} (c^\dagger_{i,\sigma} c_{j,\sigma} + \mathrm{H.c.}) - t' \sum_{\langle i,i'\rangle,\sigma} (c^\dagger_{i,\sigma} c_{i',\sigma} + \mathrm{H.c.}) + J \sum_{\langle i,j\rangle} (\vec{S}_i \cdot \vec{S}_j - \tfrac{1}{4} n_i n_j), \quad (8)$$

where i' is a second neighbor of i and $c^\dagger_{i,\sigma}$ are hard-core operators indicating that any site can be occupied either by a charge or by a spin, but not both. The sign of t' controls the topology of the Fermi surface (Martins *et al.*, 2001; Damascelli *et al.*, 2003) and when $t' < 0$ one obtains a shape qualitatively similar to that seen in ARPES for hole-doped cuprates. A negative value also lowers the probability for phase separation (between hole-rich and hole-poor regions) to occur. While exact solutions of the homogeneous strongly correlated models introduced above are not available in two dimensions, most practitioners in the correlated systems field agree on the qualitative aspects of their intermediate- to high-energy spectroscopic features. In the crucial low-energy regions, attention is currently focused on questions such as whether or not they support superconductivity without the addition of couplings to the third dimension, or other ingredients. Enough understanding has been developed in recent years to embolden some to study inhomogeneous states within such models, using the approximate techniques cited above. The great need for such studies is driven by phenomena displayed by defects in 1D systems, as well as by a compelling series of experiments on 2D cuprates, discussed below.

III. IMPURITIES IN SPIN CHAINS AND LADDERS

A. Overview

One of the biggest challenges that condensed-matter physicists are still facing today is the lack of a clear understanding of the low-energy properties of correlated two-dimensional electronic systems. A route to the study of correlations uses the spatial dimension as a parameter. In one dimension, generic interacting electronic systems belong to the strong-coupling limit (Luttinger or Luther-Emery) (Luttinger, 1963; Luther and Emery, 1974; Luther, 1976). In three dimensions, weak-coupling physics appears to describe electronic systems well. Two-

dimensional systems stand at a dimensional crossroads between the strongly and weakly correlated limits. Since the scope of this review is focused on strongly correlated systems, we work our way from one dimension to two dimensions: we recall key features of 1D physics and, adding chains in parallel, forming ladders, we gradually construct planar systems. This approach will help us gain insight into the physics of the 2D case, providing properties evolve smoothly as a function of the interchain couplings.

B. The 1D world

One of the great advantages of considering the 1D case is that many exact or quasiexact results can be obtained in that limit, using different techniques. Bethe ansatz or transfer matrix methods allow us to solve such seminal models as the XXZ chain or the Hubbard model, revealing the nature of the ground state and elementary excitations. They allow us to compute thermodynamic properties, and in some instances correlation functions (Lieb and Wu, 1968; den Nijs, 1988; Cardy, 1990). Bosonization and mapping to nonlinear sigma models are methods which give access to the low-energy properties of 1D quantum problems, when the energy spectrum is linearized in the vicinity of the Fermi points (Cabra and Pujol, 2004; Giamarchi, 2004); combined with conformal theory, these two methods allow one to identify universality classes, to compute critical indices and correlation functions accurately, and to give expressions for the corrections to scaling due to boundary conditions or to thermal effects. The functional renormalization group gives access to multiple energy scales and is thus able to capture important features when impurities are present (Meden *et al.*, 2002; Andergassen *et al.*, 2004). In conjunction with the above analytical methods, a number of powerful numerical techniques have been developed: density matrix renormalization group (DMRG) or exact diagonalization provide information on the ground-state properties and on correlations of ordered or quasiordered phases. Quantum Monte Carlo calculations (QMC) yield the temperature dependence of various observables and correlation functions, but for fermionic variables the infamous "sign problem" prevents one from simulating temperatures much less than the bare kinetic energy (Davidson, 1993; Grotendorst *et al.*, 2002; Schollwöck, 2005). From these studies, one may identify two generic types of system: those that fall into the Luttinger universality class and those that belong to the Luther-Emery class. The former case corresponds to a critical regime where correlation functions decay as power laws of the distance; the system is compressible and excitations are gapless. The latter case pertains to a gapped regime; some or all of the excitations are gapped (incompressible state) and the corresponding correlation functions decay exponentially with distance. Many concepts that apply to 1D systems and that one may hope to extend to higher dimensions can be expressed in the language of bosonization. We restrict our presentation to the material that is necessary to that end and refer the reader to reviews on one-dimensional problems (Affleck and Marston, 1988; Mattis, 1993; Tsvelik, 1995; Voit, 1995; Gogolin *et al.*, 1999; Giamarchi, 2004; Lecheminant, 2004; Schollwöck *et al.*, 2004). In the case of a single-band fermionic problem, low-energy modes correspond to excitations close to the Fermi surface which consists of two points. One then defines (real space) annihilation operators with spin σ ($\sigma=\uparrow,\downarrow$), $\psi_{r,\sigma}(x)$, for right-moving fermions whose momentum is close to $+k_F(r=+1)$ and for left-moving fermions whose momentum is close to $-k_F(r=-1)$,

$$\psi_{r,\sigma}(x) = (1/\sqrt{2\pi\alpha})\,\eta_{r,\sigma} e^{irk_F x} e^{-i[r\phi_\sigma(x)-\theta_\sigma(x)]}. \tag{9}$$

The bosonic phase operators $\phi_\sigma(x)$ and $\Pi(x) = (1/\pi)\nabla\theta_\sigma(x)$ are canonically conjugated. The Klein factors (Majorana fermions) $\eta_{r,\sigma}$ ensure proper anticommutation of ψ's with different σ or r. In Eq. (9) only the lowest harmonics ($+k_F$ and $-k_F$) are included. To study commensurability effects or the influence of a nonlinear energy-momentum dispersion one would include higher harmonics. At this stage, we highlight some similarities and differences between one and two dimensions:

- Interaction terms in the Hamiltonian mix low-energy fluctuations associated with topologically distinct portions of the Fermi surface ($+k_F$ and $-k_F$). These backward scattering contributions are often relevant, i.e., significantly affect the thermodynamic and transport properties of the system.
- Introducing the particle density operator $\hat{\rho}_\sigma(x) = [k_F - \nabla\phi_\sigma(x)]/\pi$, one may rewrite Eq. (9) as

$$\psi_{r,\sigma}(x) = (1/\sqrt{2\pi\alpha})\,\eta_{r,\sigma} \exp\left(i\left[r\int dy\,\hat{\rho}_\sigma(y) - \theta_\sigma(x)\right]\right). \tag{10}$$

  This form is the 1D analog of the expression for fermion operators used in the context of the 2D fractional quantum Hall effect (Fradkin, 1991; Pham *et al.*, 2000). The "Jordan-Wigner" term

$$\exp\left(i\left[r\int dy\,\hat{\rho}_\sigma(y)\right]\right) \tag{11}$$

  is equivalent to the topological Chern-Simons term. This analogy was made more precise by Pham *et al.* (2000) who showed that the eigenfunctions of the Luttinger liquid are 1D Laughlin wave functions (Seidel and Lee, 2006).
- If one defines charge (c) and spin (s) phase operators for the ϕ fields,

$$\phi_c(x) = \frac{1}{\sqrt{2}}[\phi_\uparrow(x) + \phi_\downarrow(x)],$$

$$\phi_s(x) = \frac{1}{\sqrt{2}}[\phi_\uparrow(x) - \phi_\downarrow(x)], \tag{12}$$

and similarly for the θ fields, one finds that the bosonized form of the low-energy Hamiltonian of the interacting fermionic system is the sum of two terms, one describing charge fluctuations,

$$H_c = \frac{1}{2\pi} u_c \int_0^L dx \left(K_c [\pi \Pi_c]^2 + \frac{[\nabla \phi_c(x)]^2}{K_c} \right) + \frac{2g_3}{(2\pi\alpha)^2} \int_0^L dx \cos[\sqrt{8}\phi_c(x) - 4k_F x], \tag{13}$$

and one describing spin fluctuations,

$$H_s = \frac{1}{2\pi} u_s \int_0^L dx \left(K_s [\pi \Pi_s]^2 + \frac{[\nabla \phi_s(x)]^2}{K_s} \right) + \frac{2g_1}{(2\pi\alpha)^2} \int_0^L dx \cos \sqrt{8}\phi_s(x). \tag{14}$$

Since the charge and spin phase fields commute, we have spin-charge separation. Furthermore, one may rewrite Eq. (9) as

$$\psi_{r,\sigma}(x) = (1/\sqrt{2\pi\alpha})\, \eta_{r,\sigma} e^{ik_F x} \times e^{(-i/\sqrt{2})\{r\phi_c(x) - \theta_c(x) + \sigma[r\phi_s(x) - \theta_s(x)]\}}. \tag{15}$$

The fermion operator Eq. (15) is the product of a charge field times a spin field. In the Luttinger regime, if the spin part has SU(2) symmetry, one may identify the spin field with the spinon operator, such that applying it to the ground-state wave function creates the elementary quantum of spin excitation. By contrast, the charge part is not a simple holon operator (applying the holon operator to the ground-state wave function would create the elementary quantum of charge excitation).

This feature is reminiscent of the slave-boson $[c_\sigma(x) = b^\dagger(x) f_\sigma(x)]$ or slave-fermion $[c_\sigma(x) = f^\dagger(x) b_\sigma(x)]$ decomposition of the electron in two dimensions, but we have to keep in mind the fact that the pseudoboson (b) and pseudofermion (f) operators are not independent (they satisfy local constraints) so that these representations do not necessarily imply spin-charge separation. We emphasize that spin-charge separation in one dimension is mostly an asymptotic property. For instance, the Bethe ansatz solution of the Hubbard model shows that it holds only in the low-energy limit, except when U goes to infinity (the t-J model), when it applies at all energy scales (Ogata and Shiba, 1990). In the low-energy sector, we can discuss magnetic and (charge) transport properties separately, and in the following we concentrate on the former aspect.

C. 1D physics in the spin sector

1. Spin-$\frac{1}{2}$ systems

In the presence of a commensurate potential that pins one charge per lattice site, the spin Hamiltonian Eq. (14) can be mapped onto the low-energy representation of the XXZ spin-$\frac{1}{2}$ chain,

$$H_{XXZ} = J \sum_i S_i^x S_{i+1}^x + S_i^y S_{i+1}^y + \Delta S_i^z S_{i+1}^z, \tag{16}$$

where $J\Delta$ denotes the exchange energy in the z direction. This is done using a gauge transformation that changes S^x and S^y to $-S^x$ and $-S^y$ at every other site. Since $2k_F = \pi$, the g_1 term [see Eq. (14)] corresponds to an umklapp term $g_3 = -J\Delta$ as in Eq. (13) (we set the lattice spacing to unity). Keeping the $2k_F$ harmonics, the bosonized expression of the $S^z(x)$ operator at point x reads [see, for instance, Giamarchi (2004)]

$$S^z(x) = -(1/\pi)\nabla \phi + [(-1)^x/\pi\alpha]\cos 2\phi. \tag{17}$$

The first term is the uniform ($q \sim 0$) part while the second term is the staggered ($q \sim \pi$) part. The isotropic limit corresponds to $\Delta = 1$ where one recovers the Heisenberg model. For translationally and rotationally invariant spin-$\frac{1}{2}$ systems with sufficiently short-range antiferromagnetic interactions, the Marshall and Lieb-Schultz-Mattis (LSM) theorems state that the ground state has total $S^z = 0$ and either is nondegenerate, with gapless excitations of odd parity, or has degenerate ground states and breaks parity (reflection about a site), with a gap to the first excited triplet state (Lieb *et al.*, 1961). Clearly, the Heisenberg model falls into the former category and represents the paradigm of spin liquids for spin-$\frac{1}{2}$ spins (Haldane and Affleck generalized the previous theorems to arbitrary spins, see below). Elementary excitations of this spin liquid consist of pairs of (asymptotically free) spin-$\frac{1}{2}$ spinons (Bethe, 1931; des Cloizeaux and Pearson, 1962). Spin rotational symmetry implies $K_s = 1$; the g_1 term then corresponds to a marginal operator which gives logarithmic corrections to the staggered part of the correlation functions (Kosterlitz, 1974),

$$\langle S^z(x,0) S^z(0,0) \rangle = C_1 \frac{1}{x^2} + C_2 (-1)^x \left(\frac{1}{x} \right) \ln x^{1/2}. \tag{18}$$

These correlations can also be calculated at finite temperature, and they allow one to compute the uniform susceptibility per atomic site, χ (Bonner and Fisher, 1964; Eggert *et al.*, 1994). At low T, setting $k_B = 1$ and in units of $(g\mu_B)^2/J$ one finds that

$$\chi(T) \sim \frac{1}{\pi^2} \left(1 + \frac{1}{2\ln(7.7J/T)} \right). \tag{19}$$

The correlation length is given by (Nomura and Yamada, 1991; Greven *et al.*, 1996)

$$\xi_{1D} \sim \frac{1}{T} \left(\frac{1}{2 - [\ln(J/0.3733T)]^{-1}} \right). \tag{20}$$

Few experimental realizations of a truly 1D Heisenberg $S = 1/2$ chain have been achieved up to now. The best known example is the Cu chain Sr_2CuO_3 (Keren *et al.*, 1993; Ami *et al.*, 1995; Motoyama *et al.*, 1996). Magnetic susceptibility measurements by magnetization techniques and NMR show good agreement with Eq. (19) at low temperatures and with a Bonner-Fisher behavior

over the whole temperature range (Motoyama *et al.*, 1996; Thurber *et al.*, 2001). The T dependence allows one to extract an antiferromagnetic coupling between adjacent Cu sites of $J=2200\pm200$ K. Long-range order is observed only below $T_N=5$ K, confirming the strongly one-dimensional character of the chain. As shown in the following section, impurity effects enable one to determine correlation lengths compatible with Eq. (20).

The rotational symmetry of the XXZ spin-$\frac{1}{2}$ chain [Eq. (16)] is broken when $\Delta\neq1$ in the expression for H_{XXZ}. For $\Delta>1$ a long-range antiferromagnetic state is obtained in the z direction. For $|\Delta|<1$, the XXZ chain is in the Luttinger-liquid regime. Bethe ansatz methods allow one to obtain exact expressions for the spin velocity,

$$v_s=\frac{J}{2}\frac{K_s}{K_s-1}\sin\pi\left(1-\frac{1}{K_s}\right), \tag{21}$$

and the compressibility $K_s=\pi/\arccos(-\Delta)$ for all values of Δ (Luther and Peschel, 1975; Haldane, 1980). Equal time spin-spin correlation functions decay as power laws at large distances x, implying a critical behavior and infinite correlation length.

2. Spin-1 systems

The situation here is qualitatively different from that for spin-$\frac{1}{2}$ systens. Based on the study of the low-energy physics of the spin-1 Heisenberg chain, Haldane (1983) showed that the ground state of rotationally and translationally invariant integer spin systems is a nondegenerate singlet and that excitations to the first odd-parity state (triplet) are gapped. He established these properties using a nonlinear sigma model, which showed that the difference with the half-integer case stems from the presence of a Berry phase in the latter case (Haldane, 1983; Affleck, 1989). This Berry phase is the generalization of the 1D Chern-Simons term [see Eq. (11) in Sec. III.B]. Correlation functions are given by

$$\langle\vec{S}(x,0)\cdot\vec{S}(0,0)\rangle\sim(-1)^x\exp(-|x|/\xi)/\sqrt{|x|}. \tag{22}$$

Here $\xi=v_s/\Delta_{\rm Hal}$ where $\Delta_{\rm Hal}=0.4105J$ and, as $T\to0$,

$$\xi\sim6 \tag{23}$$

(Affleck, 1989; Golinelli *et al.*, 1994). Accordingly, the susceptibility varies as

$$\chi(T)\sim(1/\sqrt{T})\exp(-\Delta_{\rm Hal}/T) \tag{24}$$

(Tsvelik, 1987; Damle and Sachdev, 1998; Kim *et al.*, 1998).

Experimental realizations of the $S=1$ antiferromagnetic chain were obtained in the Ni chains $[Ni(C_2H_8N_2)_2(NO_2)]ClO_4$ (NENP) and YBa_2NiO_5 (Buttrey *et al.*, 1990). In both cases, a gap was observed, confirming Haldane's conjecture (Renard *et al.*, 1987, 1988; Darriet and Regnault, 1993; Batlogg *et al.*, 1994; Sakaguchi *et al.*, 1996; Xu *et al.*, 1996). In YBa_2NiO_5, the large intrachain coupling $J=280$ K, the small single-ion anisotropy, and the small ratio between interchain and intrachain coupling ($J'/J<5\times10^{-4}$) give this compound good 1D Heisenberg chain character, with a Haldane gap $\Delta=100$ K (Darriet and Regnault, 1993; Batlogg *et al.*, 1994; Das *et al.*, 2004). In both compounds, the temperature dependence of the susceptibility follows that given by Eq. (24).

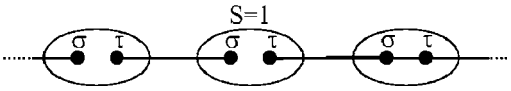

FIG. 6. Conception of a valence bond state. Each spin-1 $\vec{S}$ is written as the sum of two spin-1/2 states, $\vec{\sigma}+\vec{\tau}$; valence bonds are formed between a σ and a τ belonging to neighboring sites.

Haldane's conjecture received convincing theoretical confirmation via the mapping of the spin Hamiltonian

$$H_{s1}=J\sum_i S_i^xS_{i+1}^x+S_i^yS_{i+1}^y+\Delta S_i^zS_{i+1}^z+(D/J)(S_i^z)^2 \tag{25}$$

onto a classical 2D restricted solid-on-solid model (den Nijs and Rommelse, 1989). These authors showed that the massive phase can be understood in terms of ordering a Jordan-Wigner-like order parameter. The nature of the ground state and excitations were revealed thanks to the bosonization analysis of this model (Schulz, 1986). Each spin is written as the sum of two spin $\frac{1}{2}$, $\vec{S}_i=\vec{\sigma}_i+\vec{\tau}_i$ (Fig. 6). Insofar as singlet states on any given site are not relevant in the low-energy sector, H_{s1} is now the sum of two coupled spin-$\frac{1}{2}$ systems. The most relevant coupling is of the form

$$g\int dx\cos[2\theta_0(x)], \tag{26}$$

where θ_0 is an "optical-mode-like" phase field, related to an antisymmetric combination of θ operators [see Eq. (9)]. Since the renormalized g flows to minus infinity, θ_0 has to be either 0 or π in order to minimize the energy in the ground state. In the context of bosonization, the θ field characterizes a superfluid phase. When it acquires a finite expectation value, a Josephson superfluid current flows across the system. Thus we call the term Eq. (26) a Josephson coupling. In spin language, this term comes from kinetic contributions of the form $\sigma_i^+\tau_{i+1}^-$. The long-range ordering of this quantity is responsible for a spin gap proportional to g. It signals the formation of a RVB phase, i.e, a nondegenerate, rotationally and translationally invariant, valence bond gapped phase.

This term is the counterpart of the spinon hopping amplitude order parameter introduced in the framework of the 2D slave-boson representation of the t-J model (Kotliar and Liu, 1988; Lee and Nagaosa, 1992). Excitations break the valence bond singlets, promoting them to the triplet state. This picture emerges from the exact solution of the Affleck-Kennedy-Lieb-Tasaki (AKLT) model (Affleck *et al.*, 1987). It is the spin-1 Heisenberg model with an additional term $\frac{1}{3}J\Sigma_i(\vec{S}_i\cdot\vec{S}_{i+1})^2$. Valence bonds formed between nearest-neighbor sites and spin-spin correlation functions decay exponentially with dis-

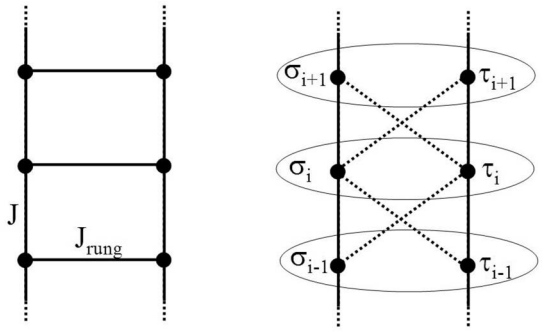

FIG. 7. The spin-1 chain as a special type of two-leg ladder. Left: A two-leg spin-$\frac{1}{2}$ ladder. Dots represent the spins with couplings J along the legs and J_{rung} along the rungs. Right: A spin-1 chain can be viewed as a two-leg spin-$\frac{1}{2}$ ladder with diagonal couplings (dotted lines).

tance, with a correlation length $\xi_{\text{AKLT}}=1/\ln 3$ (Arovas and Auerbach, 1988; Arovas and Girvin, 1992). The inclusion of the additional term does not affect the low-energy physics of the Heisenberg model. These particular valence bond states are sometimes considered to be characteristic of a bosonic RVB phase (Arovas and Auerbach, 1988; Ng, 1992) and relevant to the physics of cuprate or other strongly correlated materials. It is noteworthy that, in the $\sigma-\tau$ language, the Heisenberg Hamiltonian can be viewed as a two-leg ladder model, with intrachain and interchain couplings (see Fig. 7).

3. Higher spin states

Affleck presented a physicist's proof extending the ground-state and excitation properties of the spin-$\frac{1}{2}$ case to general half-integer spins (Affleck, 1989). Haldane also predicted that general integer spins fall into the same class as the spin-1 case. These characteristics are difficult to prove rigorously, for want of exact solutions for general spin S, but one can use the decomposition of S into $2S$ half-integer spins for integer S and $2(S-\frac{1}{2})+1$ half-integer spins for half-integer S (Schulz, 1986). Forming valence bonds between different "σ" and "τ" species on neighboring sites, one is left with a "single" spin-$\frac{1}{2}$ chain for the half-integer case. This gives an overall gapless regime, with massless spinons. For the integer spin case, one can generalize the AKLT model (Oshikawa 1992) for any S, and this gives an exact RVB (valence bond) gapped state, with a correlation length $\xi_{\text{AKLT}}=1/\ln(1+2/S)$. Again we view this latter case as a model for an S-leg ladder system in the low-energy limit (S chains with interchain couplings along rungs).

4. Coupling of the rungs

On the road to two dimensions, we now turn to spin-$\frac{1}{2}$ ladders. Two- and three-leg Cu ladder structures were experimentally realized in $SrCu_2O_3$ and $Sr_2Cu_3O_5$ oxides (Hiroi *et al.*, 1991; Azuma *et al.*, 1994). Couplings along the rung and along the leg are similar, of the order of 1000 to 1000–2000 K. In the two-leg compound, the ladders are almost decoupled from each other since the system does not show any magnetic ordering down to $T=50$ mK (Kojima, Keren, Le, *et al.*, 1995; Kojima, Keren, Luke, *et al.*, 1995). This is not the case in the three-leg compound, which orders at 52 K, probably due to weak transverse couplings. A gap is observed only for the two-leg system, as shown by macroscopic measurements and NMR (Azuma *et al.*, 1994; Ishida *et al.*, 1994, 1996). In a similar ladder cuprate $Sr_{14-x}Ca_xCu_{24}O_{41}$, hole doping could be achieved through Ca-Sr substitution, leading for high enough pressure to a superconducting behavior at $x=13.6$ (Uehara *et al.*, 1996).

In these spin ladders, exact solutions are not available, but, for low energies, we can use some of the techniques that we discussed above to determine ground states and excitation properties (Dell'Arringa *et al.*, 1997; Nersesyan *et al.*, 1998; Orignac and Giamarchi, 1998; Gogolin *et al.*, 1999; Citro and Orignac, 2002). In addition, DMRG, exact diagonalization, and quantum Monte Carlo methods (no sign problem for spins) also add useful information (Poilblanc *et al.*, 1994c; White and Noack, 1994; Greven *et al.*, 1996; Dagotto 1999; Johnston *et al.*, 2000). In the case of the two-leg ladder, bosonization is easy to perform after introducing acoustic (symmetric under the exchange of the two legs) and optical (antisymmetric) modes (Strong and Millis, 1994). Remarkably, the form is precisely that obtained by Schulz in his analysis of the Haldane spin-1 chain in terms of two coupled spin-$\frac{1}{2}$ legs (see Sec. III.C.2). Accordingly, the spin sector is fully gapped as soon as any interchain coupling is turned on. Once again [see Eq. (26) and subsequent comments], a Josephson coupling between the two chains of the form $\sigma_i^+\tau_{i+1}^-$ is relevant and provides the gap between the valence bond RVB ground state and the first triplet excited state (see Fig. 7). When comparing the spin-1 chain with a two-leg spin-$\frac{1}{2}$ ladder, one should consider the particular topology (see right panel of Fig. 7); it plays an important role, for instance, in the presence of defects or open boundary conditions (Ng, 1994; Qin *et al.*, 1995).

Similarly, the analysis of the three-leg ladder within bosonization leads to the result that one sector is gapless. As mentioned, a gap was experimentally observed in the two-leg compound $SrCu_2O_3$ while no gap was detected in the three-leg material $Sr_2Cu_3O_5$. It is possible to analyze the ladder problem with arbitrary number of legs (n_l), using the nonlinear sigma model, and one finds that an odd number of legs leads to a gapless state with power-law decay of the spin-spin correlation functions, while for an even number of legs correlations fall off exponentially, such that $\xi_{\text{lad}}\sim\exp[(\pi/2)n_l]$ (Dell'Arringa *et al.*, 1997). In the weak-coupling limit ($J_{\text{rung}}\ll J$), the gap decreases exponentially to zero with increasing number of legs: $\Delta_{\text{lad}}\sim\xi^{-1}$. These results have been confirmed, and extended to the isotropic limit ($J_{\text{rung}}=J$) using numerical work (Greven *et al.*, 1996): $\Delta_{\text{lad}}=0.50, 0.16, 0.05$ for $n_l=2,4,6$. At large distances, spin-spin correlation functions behave exactly as in the spin-1 case [Eq. (22)] and the susceptibility is given by Eq. (24)

where one substitutes $\Delta_{\rm lad}$ for $\Delta_{\rm Hal}$. Here ξ=3.2,10 for n_l=2,4.

5. Summary of 1D physics in the spin sector

A picture emerges from the above description: for (spin) rotationally and translationally invariant systems, the ground state of 1D spins chains and ladders is either a degenerate dimer phase where reflection symmetry about a site is broken, or a nondegenerate valence bond phase, also known as a resonating valence bond phase, where parity symmetry exists for *any* site (Anderson, 1997). The state consists of singlets, which resonate coherently on a length scale ξ. Since the spectrum is linearized near the Fermi points, the binding energy in this RVB state is $\Delta \sim v_s \xi^{-1}$. Within the RVB phase, quasiparticles consist of spinons. These are thus confined within a distance ξ of each other, forming bound-state singlets. An excitation breaks the singlet, leading to a triplet state. This triplet can propagate through the lattice as a magnon excitation. For strictly 1D chains at $T=0$, ξ is infinite in the spin-$\frac{1}{2}$ case, and we have a gapless spin liquid with asymptotically free spinons, while ξ is finite in the spin-1 case. For ladders, we have a gapped RVB phase and $\xi_{\rm lad} \sim \exp[(\pi/2)n_l]$ for even numbers (n_l) of legs. The limit $n_l \to \infty$ is singular, since the ground state of a 2D spin-$\frac{1}{2}$ system is believed to sustain long-range antiferromagnetic order (Chakravarty *et al.*, 1989). The RVB phase that constitutes the ground state of spin-1 and even-leg ladder systems is a strongly correlated phase in that it has long range phase coherence. This property is quite independent of the strength of the interactions. Can we actually see spinons? Simulations are of course one way to do so: a 1D ring with an odd number of spins shows a spinon extending over the entire circumference. Open chains are another way of revealing these quasiparticles. From an experimental perspective, there is a way to realize this situation, namely, to add nonmagnetic impurities, as these effectively break the 1D chain. We discuss this point in the next section. Another way to probe spinons—akin to the odd number of spins case—is to consider ladders with an odd number of legs. In that case, the "unpaired" spinons form a 1D spin-liquid phase, which is revealed in experiments. If we associate a Josephson phase (θ) with each singlet in the RVB phase, this θ field is either quasi ordered in the cases of 1D spin-liquid and odd-leg ladders or ordered for even-leg ladders: in the former situation, correlation functions of the θ field decay algebraically with distance, while in the latter they tend to a constant value for $|x| \to \infty$.

D. Defects in 1D spin chains

From an experimental perspective, intrinsic defects will modify the magnetic properties of materials. Examples of impurities are weak (magnetic coupling) links, broken chains, and magnetic or nonmagnetic atomic substitutions (Eggert *et al.*, 1994; Eggert and Affleck, 1995; Igarashi *et al.*, 1995; Zhang *et al.*, 1997, 1998; Brunel *et al.*, 1999; Rommer and Eggert, 1999, 2000). They produce spectacular effects which are direct consequences of the correlated 1D states so that we may actually use defects in a controlled way in order to probe the ground state and excitations in the spin chains introduced in the previous section. Nonmagnetic atoms suppress the couplings J between neighboring spins. Thus, in one-dimension, a finite concentration of such atoms will break the chain into disconnected segments. At low temperature, each segment is in its ground state. In the case of spin-S Heisenberg chains, Marshall's theorem tells us that the total spin is zero for an even number of spins in a chain or S for an odd number of spins in the chain. Thus odd chains will give a Curie contribution to the uniform magnetic susceptibility proportional to the concentration of impurities (assuming small concentrations and equal probability of getting even or odd chains) (Wessel and Haas, 2000; Sirker *et al.*, 2006). This property does not tell us much about the nature of the correlated state *per se*. In contrast, we show that boundaries cause additional phenomena which reveal the nature of the low-temperature phases; the reason is that the spin density in the z direction is the sum of two terms [see Eq. (17)]: a uniform part ($\propto \nabla \phi$) which is essentially unaffected by the breaking of translational invariance, except in the vicinity of the edges plus a staggered (umklapp) part giving two types of contribution, one stemming from finite-size effects and one from the boundaries (Eggert *et al.*, 2002). We first consider spin-$\frac{1}{2}$ compounds, then discuss spin-1 chains and ladders, and conclude with quasi-1D systems (Eggert and Affleck, 2004).

1. Spin-$\frac{1}{2}$ systems

We first discuss the influence of boundaries on the magnetic properties of a spin-$\frac{1}{2}$ isotropic Heisenberg chain. Bethe ansatz, conformal theory, or bosonization techniques allow one to compute all relevant observables (Cardy and Lewellen, 1991; Eggert and Affleck, 1995; Essler, 1996; Lukyanov, 1998; Fujimoto, 2000; Fujimoto and Eggert, 2004). In bosonization language, a boundary forces a condition on the $r=-1$ and $r=+1$ modes [Eq. (9)] [see, for instance, Giamarchi (2004), p. 306]. Breaking translational invariance affects spin-spin correlation functions. Far from the boundary, one recovers the usual behavior; for instance, if one applies a *uniform* magnetic field H, one gets a magnetization equal to $\chi(T)H$, where the uniform susceptibility is given by Eq. (19). Close to the boundary, the susceptibility becomes site dependent; it is the sum of two contributions. One of those has a magnitude close to $\chi(T)H$, such that in Fourier space its components are centered around $q=0$ (see Eggert and Affleck, 1995). In addition, because of the boundary, the alternating part of the spin-spin correlation function also contributes to the uniform susceptibility. This is an impurity-induced effect. For finite temperature, one gets a site-dependent, staggered magnetization of the form (Eggert and Affleck, 1995)

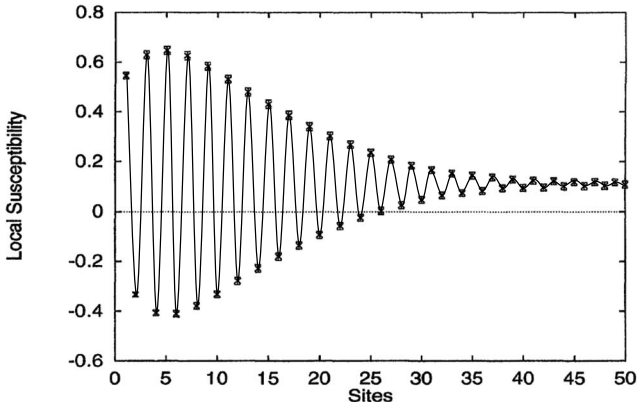

FIG. 8. Alternating magnetization caused by a boundary in a spin-1-2 chain according to Monte Carlo simulations at $T=J/15$. From Eggert and Affleck, 1995.

$$M(x) = H(-1)^x \frac{1.16}{\pi} \frac{x}{\sqrt{(J/2T)\sinh(4Tx/J)}}. \quad (27)$$

At low enough temperature $T \ll J$, the envelope of the magnetization increases initially with the distance to the impurity site, peaks at $x=0.48J/T$ in cell units, then decreases with an exponential asymptote of typical extension ξ_{imp} as shown in Fig. 8. From Eq. (27) one finds that $\xi_{\text{imp}} \sim T^{-1}$.

One needs to be careful when taking the $T=0$ limit. The expression for the magnetization given by Eq. (27) with T set to zero is restricted to "small enough" values of x. The proper form reads

$$M(x) \sim (-1)^x \sqrt{2/x} \sin(Hx/2v_S) \quad (28)$$

and shows that a finite field H produces an incommensurate oscillating magnetization [on top of the quasiuniform part]. On sites close to the boundary, the effect of the "impurity" is seen through extra contributions to the magnetization which are nonzero even at $T=0$ (Rommer and Eggert, 1999). Fujimoto and Eggert (2004) showed that one needs to include a term generated by marginally irrelevant bulk operators. It gives a quasi-Curie contribution to the susceptibility of the form $\chi_B \sim [(T\ln(T))]^{-1}$. Note that this additional piece exists for both even and odd chains, since this is a "surface" effect.

In practice, creating a boundary does not require one to cut the chain. Indeed, a weak link (a smaller exchange coupling between two neighboring spins) is a strong perturbation and, ultimately, as the temperature is reduced, renormalization and numerical techniques show that it produces similar effects on the susceptibility to the case of the open chain (Rommer and Eggert, 1999).

As stated in the introduction to this section, defects break a chain into disconnected segments. The boundaries of each segment give rise to extra surface contributions to the magnetization. In addition, there are "volume" contributions associated with finite-size effects: since the staggered coherence length diverges at $T=0$ in the thermodynamic limit, one gets a low-T finite alternating moment per site proportional to $1/\sqrt{L}$ for a chain

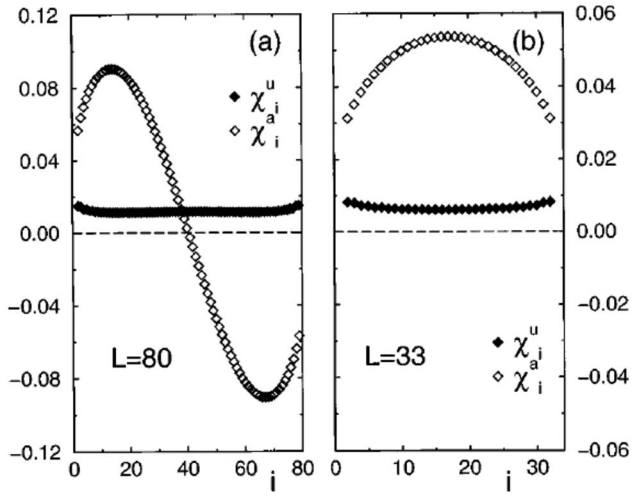

FIG. 9. Uniform (χ_i^u) and staggered (χ_i^a) components of the local susceptibility χ_i obtained with the DMRG method applied to the $S=\frac{1}{2}$ Heisenberg model on a chain with L sites and open boundaries, using m states in the iterations and studying the subspace with a total spin in the z direction equal to 1. (a) $L=80$ and $m=16$, and (b) $L=33$ and $m=32$. From Laukamp *et al.*, 1998.

of length L (Eggert *et al.*, 2002). This size dependence is a direct consequence of the r^{-1} falloff of the staggered correlation function. For odd-L chains this magnetization is a manifestation of a spin-$\frac{1}{2}$ in the ground state, and for even-L chains it accompanies a spin-1 excitation above the ground state (see Fig. 9). The local magnetic susceptibility χ_i on site i is the sum of a uniform contribution χ_i^u and an alternating contribution. Figure 9 shows χ_i^u and the staggered part of the alternating term, namely, $\chi_i^a=(-1)^i(\chi_i-\chi_i^u)$.

On the experimental side, the Sr_2CuO_3 spin chain introduced in Sec. III.C.1 is a good realization of a truly 1D Heisenberg $S=\frac{1}{2}$ system, with an antiferromagnetic coupling $J=2200\pm200$ K (Keren *et al.*, 1993; Ami *et al.*, 1995; Motoyama *et al.*, 1996). Only nonmagnetic Pd substitution was achieved on Cu site, leading to a Curie behavior of the macroscopic magnetization (Kojima *et al.*, 2004). This Curie term is a consequence of the chain segments with an odd number of sites, as argued above. Local probes such as NMR are necessary to probe the local variation of the magnetization $M(r)$. Measurements were performed only in the case of a nonsubstituted chain, taking advantage of unavoidable intrinsic defects, probably oxygen vacancies and interstitials (Takigawa *et al.*, 1997; Boucher and Takigawa, 2000). The NMR spectrum shows a central line and a broad symmetric background with sharp edges (see Fig. 10). This is evidence of an alternating polarization induced by the native defects, as shown in Fig. 14. The edges of the ΔH pattern shift in temperature, with a $1/\sqrt{T}$ dependence, as would be expected from Eq. (27) for values of x near the peak position.

In the Cu spin-$\frac{1}{2}$ chain dichlorobis (pyridine) copper (II) ($CuCl_{22}NC_5H_5$), referred to as CPC, with $J=27$ K,

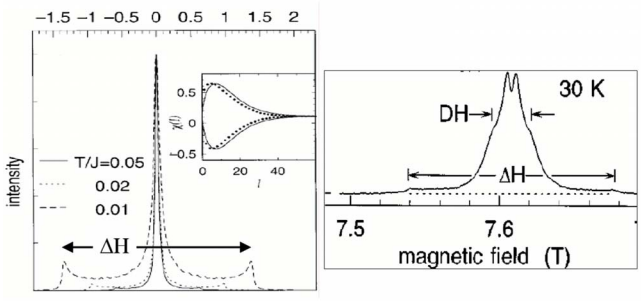

FIG. 10. (Color online) Theoretical and experimental NMR line shapes due to defects in spin chains. Left: The NMR spectrum expected for a staggered magnetization of the spin-$\frac{1}{2}$ chain displayed in the inset, corresponding to its histogram. Right: The experimental Cu NMR spectrum in Cu chain Sr_2CuO_3 displays a similar ΔH pattern. It is interpreted as induced by intrinsic defects. From Takigawa *et al.*, 1997.

muon spin resonance was performed, where implanted muons were used both as a probe of the local susceptibility and as a defect in the chains (Chakhalian *et al.*, 2003). Indeed, muons are positively charged particles which stop in the bulk of the material and then couple to the chains, according to comparisons of Knight shift measurements with DMRG computations. While this technique is valuable in order to study chains where native defects cannot be produced by simple chemistry, it is limited by the fact that the muon location is not exactly known.

2. Spin-1 chains

In many respects, it is easier to describe the response of a spin-1 system to an impurity. As discussed above, the ground state of the pure system is a nondegenerate RVB state, with long-range order (of a singlet order parameter). Introducing a nonmagnetic impurity breaks a valence bond and, in the representation of a spin 1 in terms of two spins $\frac{1}{2}$, implies that a spin $\frac{1}{2}$ is "freed" at the location of the broken valence bond, i.e., it is pinned in the vicinity of the impurity, as shown in Fig. 11 (Kennedy, 1990; Ng, 1992; Miyashita and Yamamoto, 1993a, 1993b; Laukamp *et al.*, 1998).

Monte Carlo simulations performed on chains of L sites ($L \geqslant 100$) show that the polarization oscillates with an exponential envelope $\langle S_i^z \rangle \propto e^{-[(i-1)/\xi]} + e^{-[(L-i-1)/\xi]}$, with $\xi \sim 6$. A comparison of the induced magnetization for the $S=\frac{1}{2}$ and 1 cases is shown in Fig. 12. This value of ξ is that of the undoped compound. This result suggests that the perturbation which created the impurity is localized and decays with the coherence length of the pure system; see Eq. (23). This fact is confirmed in various

FIG. 11. The introduction of a nonmagnetic impurity in the spin-1 chain displayed in Fig. 6 breaks two singlet bonds, thereby releasing two spins 1/2.

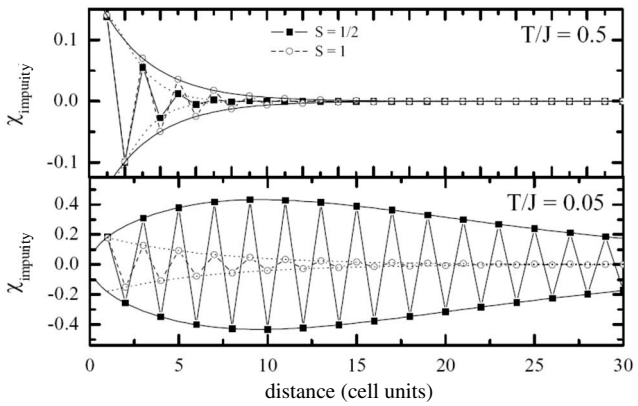

FIG. 12. Alternating magnetization in the case of spin-1/2 and spin-1 systems with a defect. The polarization for $S=1$ is normalized to that for $S=1/2$. At high temperature, the two polarizations are roughly identical, exponentially decaying. At low temperatures, for $S=1$, the polarization does not evolve further because ξ saturates. On the other hand, the extension of the polarization for $S=1/2$ systems continues to increase as T is decreasing and exhibits a nonmonotonic behavior (see Fig. 8).

DMRG and QMC studies (Miyashita and Yamamoto 1993a, 1993b; Sørensen and Affleck, 1995; Kim *et al.*, 1998; Polizzi *et al.*, 1998; Alet and Sørensen, 2000). A remarkable feature emerges from these simulations, namely, the relative sign of the polarization at the end of the chain segment formed by two impurities. Assume that we have a spin-up state at one end of the segment. The oscillation of the polarization implies that the next site is in the down state, and so on. If we extend the up-down alternation of the sites to the other end of the segment, we observe that the polarization on the site closest to the second impurity corresponds to that expected from the up-down alternation rule, *despite the fact* that the distance between the impurities is much larger than 2ξ. In other words, the singlet order parameter propagates the relative phase of the spin operators across the entire segment (see Miyashita and Yamamoto, 1993).

This observation is confirmed by a study combining theory and experiments (Hagiwara *et al.*, 1990) on a spin-1 chain with a spin-$\frac{1}{2}$ (Cu) impurity. The lowest-energy state is such that sites located on either side of the Cu are *both* in the up or down state and form a triplet with $\langle S^z \rangle = \pm 1$, as shown in Fig. 13. DMRG and QMC confirm this picture (Sørensen and Affleck, 1995; Tonegawa and Karubaki, 1995; Roos and Miyashita, 1999).

FIG. 13. Spin-1 chain with a Cu spin-$\frac{1}{2}$ defect. Spin-$\frac{1}{2}$ states are formed on either side of the Cu atom and align to form a spin-1 state.

Contrary to the case of the $S=\frac{1}{2}$ spin chain, the impurity-induced magnetization in the $S=1$ spin chain can be measured experimentally with great precision. In the $S=1$ antiferromagnetic Ni chain $[Ni(C_2H_8N_2)_2(NO_2)]ClO_4$ (NENP), electron paramagnetic resonance (EPR) measurements provide evidence for the existence of a spin state associated with the substitution of Ni by nonmagnetic Zn, Cd, or Hg atoms, consistent with the valence bond state (VBS) picture where each impurity frees two $S=\frac{1}{2}$ states (Glarum *et al.*, 1991). Specific-heat measurements confirm the existence of a spin state by detecting the corresponding Schottky anomaly (Ramirez *et al.*, 1994). While this study was first argued to give a different spin state value than EPR, the controversy was finally resolved by careful treatment of long enough spin chains (Batista *et al.*, 1998). More refined experiments were then performed in the Ni chain oxide YBa_2NiO_5, a better prototype of the spin-1 chain than NENP, with $J=280$ K (Buttrey *et al.*, 1990). When introducing nonmagnetic Zn or Mg impurities, EPR studies reveal the presence of spin states accompanied by a Curie contribution to the macroscopic susceptibility (Ramirez *et al.*, 1994; Batista *et al.*, 1998; Payen *et al.*, 2000; Das *et al.*, 2004). The Curie constant corresponds to about two $S=\frac{1}{2}$ per Zn, as expected. Note, however, that any attempt to analyze the macroscopic magnetization quantitatively is hindered by the fact that a Curie behavior is already observed in the nominally pure compound without any Zn, a feature encountered in most experimental realizations of low-dimensional systems. This native Curie term is usually due to the presence of both spurious paramagnetic phases and local defects within the crystal itself, such as vacancies or interstitials of oxygens. As anticipated, any defect which is coupled to the spin chain itself will induce in turn a local moment, i.e., a Curie law in a magnetization measurement. This limits any refined quantitative analysis of such macroscopic experiments, as well as EPR studies. To bypass this difficulty, NMR has proven to be an ideal probe, since it allows one to identify the actual effect of the Zn substitutional atom in its vicinity and moreover to resolve this effect spatially, while other techniques only give the total spin value induced by the defect. In YBa_2NiO_5, NMR of the yttrium nucleus probes the local magnetization $M(r)$ of the Ni sites, with a site by site resolution. Without impurity, the ^{89}Y NMR shift measures the pure uniform susceptibility of the Ni chain and displays the usual Haldane gap behavior (Shimizu *et al.*, 1995). When adding nonmagnetic isovalent impurities such as Mg^{2+} or Zn^{2+}, new NMR satellite lines appear, each of them due to the Y nuclei at a given distance from an impurity as shown in Fig. 14 (Tedoldi *et al.*, 1999; Das *et al.*, 2004).

Their frequency shift relative to the pure case is directly proportional to the local average spin $\langle S^z(i)\rangle$ along the external field direction z at the corresponding Ni site. Since the polarization $\langle S^z\rangle$ alternates, the shifts relative to the main line produce both positive and negative satellites, as shown. They decay exponentially from the

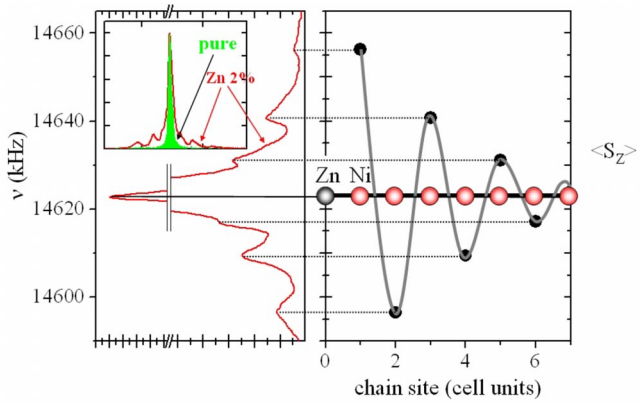

FIG. 14. (Color online) NMR reconstruction of an impurity-induced magnetization in a spin chain. The left panel displays an ^{89}Y NMR spectrum in pure and Zn-substituted YBa_2NiO_5. The various satellites which appear with Zn doping allow the reconstruction site by site of the induced staggered magnetization near the Zn atoms substituting Ni in the chain (Tedoldi *et al.* 1999; Das *et al.* 2004).

Ni first neighbor of the impurity site. Their temperature dependence is governed by that of the Ni closest to the impurity, which follows approximately a Curie law, together with the T dependence of the envelope extension ξ_{imp} plotted in Fig. 15. This spatial behavior is a consequence of the exponential decay of the spin-spin correlation functions in such Haldane gapped spin chains. Furthermore, the extension ξ_{imp} measured for different impurities appears almost identical to that of the pure spin-spin correlation function ξ_{pure} computed by QMC techniques, also shown in Fig. 15. The fact that the impurity reveals the intrinsic spin-spin correlations of the system is the key result which gives us insight into the other more complex and less controlled correlated systems such as high-T_c superconductors: a nonmagnetic

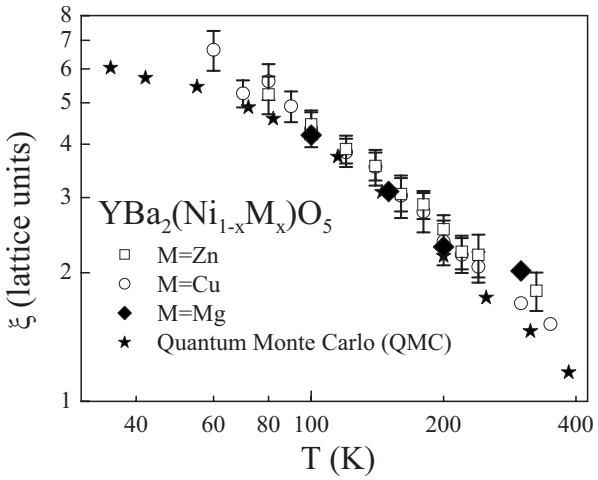

FIG. 15. Comparison of-the-extension of the staggered induced magnetism due to Mg (Tedoldi *et al.*, 1999), Zn, or Cu (Das *et al.*, 2004) impurities in YBNiO. The correlation length measured by QMC by Kim *et al.* (1998) for the pure system is shown for comparison.

impurity can be used as a probe of the intrinsic properties of a correlated system, much like a magnetic impurity in a metallic host could be used to probe the Fermi-surface properties through the RKKY oscillation.

Inelastic neutron-scattering experiments also allow one to measure the end-chain excitations, which are peaked at the antiferromagnetic wave vector along the chain, and show an alternating pattern with extension $\xi_{\rm imp}=8$ at $T=0.1$ K, consistent with the NMR studies (Kenzelmann *et al.*, 2003).

The case of a magnetic impurity in a spin-1 chain was mentioned previously: a Cu spin-$\frac{1}{2}$ substitution on a spin-1 site results in the formation of a spin-$\frac{1}{2}$ effective state as probed by EPR in NENP (Hagiwara *et al.*, 1990) (see Fig. 13). Specific-heat measurements confirm this through the observation of a Schottky anomaly as in the case of nonmagnetic Zn (Batista *et al.*, 1998). In addition, DMRG and QMC computations predict that the magnetic impurity induces an alternating magnetization close to the defect (Sørensen and Affleck, 1995; Tonegawa and Karubaki, 1995; Roos and Miyashita, 1999). In the case of YBa_2NiO_5, ^{89}Y NMR experiments similar to those reported for Zn and Mg show similar results for magnetic Cu impurities (Das *et al.*, 2004). The envelope remains exponential with the same extension $\xi_{\rm imp}$ as shown in Fig. 15. In comparison with nonmagnetic Zn defects, one sees a different shift for these satellites, i.e., a smaller amplitude of the induced polarization, by about 20%, for all Ni sites producing the polarization. A QMC computation can be performed in this specific case, which reproduces the experiment if Cu is coupled antiferromagnetically to its neighboring Ni with a coupling $J'\simeq 0.1-0.2J$ (Das *et al.*, 2004), a result qualitatively similar to that found in NENP (Hagiwara *et al.*, 1990).

3. Ladder systems

In Sec. III.C.4, we argued that the low-energy physics of an even-n-leg spin-$\frac{1}{2}$ ladder could be mapped onto an integer spin-$\frac{n}{2}$ chain and that of an odd-leg ladder to a spin-$\frac{1}{2}$ chain. Thus the influence of an impurity in the ladder follows from the considerations pertaining to the spin-1 and spin-$\frac{1}{2}$ cases. For instance, for a two-leg ladder, we conclude that when a nonmagnetic impurity is located on one of the legs, a spin-$\frac{1}{2}$ state should appear on the opposite leg, with an amplitude centered around the site across from where the impurity sits. We emphasize once again (see Sec. III.C.4) that it is important to keep in mind the particular topology of the ladder that the mapping involves, when discussing end states. For instance, a spin-$\frac{1}{2}$ state is localized near the edge of an open spin-1 chain whereas no such state is found at the open end of the two-leg ladder shown in the left panel of Fig. 7.

Numerical studies of the spin-$\frac{1}{2}$ ladder with impurities find a magnetic polarization which oscillates from site to site along the leg of the ladder, with an amplitude which decays exponentially with a characteristic length $\xi_{\rm imp}$ (Martins *et al.*, 1996, 1997; Mikeska *et al.*, 1997; Miyazaki *et al.*, 1997; Sandvik *et al.*, 1997; Laukamp *et al.*, 1998; Laeuchli *et al.*, 2002). But whether or not the value of $\xi_{\rm imp}$ is equal to the coherence length of the pure system (equal to three to four lattice spacings) is still unclear.

These polarized states either produce a Curie law for the susceptibility or may even lead to an antiferromagnetic transition (Greven and Birgeneau, 1998). For the three-leg ladder the physics seems consistent with that of the spin-$\frac{1}{2}$ chain with a nonmagnetic impurity (Sandvik *et al.*, 1997). Experimentally, nonmagnetic Zn can be substituted in the two-leg ladder $SrCu_2O_3$. Macroscopic susceptibility measurements reveal the appearance of a Curie law at high temperature, which corresponds to one spin-$\frac{1}{2}$ per Zn in the dilute limit (Azuma *et al.*, 1997). A concomitant $1/T$ broadening of the Cu NMR line is observed, proportional to the number of impurities, which provides evidence for the existence of an alternating induced magnetization which extends over the ladder (Fujiwara *et al.*, 1998; Ohsugi *et al.*, 1999). No satellites could be resolved, in contrast with the case of YBa_2NiO_5. This limits any quantitative evaluation of the magnetization shape and extension. Magnetic $S=1$ Ni substitution leads to similar effects.

4. Summary of impurities in spin chains

Impurities create edges in spin chains. For strictly 1D systems, pairs of edges divide the system into even-or odd-length segments. The magnetic response to such defects contains two parts, which mirror the two contributions to the spin-density operator of the pure system: (i) the uniform contribution—the gradient of the phase—is essentially identical to that of the impurity free system, except close to the boundaries, and (ii) the umklapp contribution near the antiferromagnetic wave vector, by contrast, is qualitatively affected by the boundary; this is because the RVB parameter (for spin-1 chains and for ladders) or the staggered magnetization (for spin-$\frac{1}{2}$ chains) show long-range or quasi-long-range order at this wave vector for the pure system. Since impurities break translational invariance, momentum is no longer a good quantum number so that a uniform perturbation can give rise to a spatially oscillating magnetization and, conversely, an alternating perturbation can contribute to the uniform response. This is precisely what is seen in chain segments. The ground state of odd chains is a spin-$\frac{1}{2}$ doublet. An infinitesimal magnetic field will give a uniform Curie contribution which, in turn, will promote an alternating magnetization. For even chains, one also gets the same effect at finite temperature when transitions to the excited (triplet) state are allowed. The reverse effect is observed (at least numerically) in the case of a single edge, in the presence of a magnetic field. In this case, the induced uniform spin polarization causes an alternating magnetization to develop near the boundary. Its spatial extension is of the order of the coherence length of the pure system and this mode contributes to the uniform magnetic response. These features are hallmarks of strongly correlated systems where

several length scales are simultaneously relevant (Anfuso and Eggert, 2006). We show later that similar effects occur in two dimensions, when nonmagnetic defects are introduced in the copper-oxide planes.

5. Impurities and long-range order

There cannot be true long-range order at finite temperature for purely 1D systems, but addition of a small interchain coupling $J_\perp$ between spin chains will drive the quasi-1D system antiferromagnetic. The Néel temperature T_N can be determined from the exact expression of the staggered susceptibility of the chain, using the RPA (Eggert *et al.*, 2002, 2003). One finds that $T_N \sim J_\perp$. Nonmagnetic impurities do cut the chains into segments, but LRO is not destroyed since two segments belonging to a given chain can still be magnetically connected through the interchain $J_\perp$. In fact, $T_N/J_\perp$ is a function of the scaling variable $[(1/p)-1]J_\perp$. As the concentration p of impurities is increased, T_N falls. However, in some situations, the magnitude of the staggered moment and the Néel temperature may increase with p (Eggert and Affleck, 2004). Similar effects can be obtained for a large enough single-ion anisotropy (Sakai and Takahashi, 1990; Zheludev *et al.*, 2000).

In other words, the introduction of impurities enhances long-range order. This is one of the various routes to get "order from disorder" (Villain *et al.*, 1980; Shender and Kivelson, 1991). For example, in two-leg spin-$\frac{1}{2}$ ladders compound $SrCu_2O_3$, specific-heat and susceptibility measurements show that a concentration $x=1\%$ of Zn at a Cu site leads to antiferromagnetic behavior at $T<T_N=3$ K (Azuma *et al.*, 1997). When the number of impurities is increased, T_N increases to 8 K at 4%, and then decreases again. Concentrations as small as $x=0.1\%$ still lead to antiferromagnetic order (Manabe *et al.*, 1998). In the spin-Peierls chains compounds $CuGeO_3$ as well, either magnetic (Ni, Co) or nonmagnetic (Mg, Zn), defects at a Cu site simultaneously reduce the spin-Peierls transition temperature T_{SP} and induce a long-range AF order whose frozen moment is spatially inhomogeneous (Hase *et al.*, 1993; Oseroff *et al.*, 1995; Regnault *et al.*, 1995; Renard *et al.*, 1995; Anderson *et al.*, 1997; Kadano, 1997; Kojima *et al.*, 1997). Similar effects are also observed in some $S=1$ spin chains like $PbNi_2V_2O_5$ (Uchiyama *et al.*, 1999) or $S=\frac{1}{2}$ chains like Sr_2CuO_3 (Kojima *et al.*, 2004). Even though the physics exhibited in these various substituted systems is rich, it is not directly relevant here, as it is governed by subtle deviations from a purely one-dimensional Heisenberg situation.

IV. EXPERIMENTS ON POINT DEFECTS IN 2D SYSTEMS: THE METALLIC CUPRATES

A. Overview

The work discussed on 1D or quasi-1D systems has been devoted mostly to insulating spin systems, as the major available experimental systems are nonmetallic. The most direct extension to two dimensions of the work sketched above for spin chains would be to study the response to impurities in the case of a spin-$\frac{1}{2}$ Heisenberg plane, for which theoretical computations along similar lines are available (see Sec. II). This situation might be encountered in the case of undoped cuprates, e.g., La_2CuO_4 and $YBa_2Cu_3O_6$, which are good Mott-Hubbard insulators. We explain in Sec. IV.C why this simple experimental extension has not been successfully performed so far. On the other hand, in cuprates, hole or electron doping is easy to achieve and allows one to span the phase diagram of Fig. 2. The most important work done so far using defects or impurities to probe 2D systems has been focused on the doped layered cuprates, among which are the HTSC phases.

Before giving a detailed description of the experiments, it is essential to recall here important features that characterize the different phases of Fig. 2. Here the loss of AF order does not give way immediately to a metallic and superconducting ground state, but rather to an intermediate regime in which a disordered magnetic ground state, usually described as a spin-glass (SG) phase, separates the AF domain from a superconducting region which takes the form of a dome. One denotes, respectively, the left and right of the dome as the underdoped and overdoped regimes, and refers to the doping at which the maximum T_c occurs as optimal. An essential feature that has been demonstrated experimentally is that the superconducting state does not have a uniform gap amplitude in $\mathbf{k}$ space but is rather d wave, i.e., it has a maximum gap in the CuO bond axis directions and nodes in the diagonal directions (Tsuei and Kirtley, 2000). Now this would be simple if the metallic state above the superconducting regime were a simple metal describable within a Fermi-liquid theory. In fact this limit seems to be achieved only for large doping, on the far right of the phase diagram, i.e., as far away from the Mott AF state as possible. Directly above the superconducting dome the transport properties, e.g., a T linear dependence of the resistivity with large scattering rates $\tau^{-1} \approx k_B T/h$ at optimal doping, appear to be at odds with a simple Fermi-liquid description; hence the designation "strange metal" (Varma *et al.*, 1989). Most importantly, in the underdoped regime the magnetic properties exhibit unusual behavior, with a spin susceptibility revealed by NMR Knight-shift data which exhibits a large drop at low T, and is nearly suppressed before the superconducting singlet state is even established (Alloul *et al.*, 1989). This drop in the susceptibility occurs as if a gap were opening in the excitation spectrum of the system, justifying the "pseudogap" designation introduced since 1989, as a small density of states still remains at T_c. The corresponding gap in the spin excitations has been detected by spin lattice relaxation data (Yasuoka *et al.*, 1989) and neutron-scattering experiments (Rossat-Mignod *et al.*, 1991). This pseudogap, which was observed later by specific-heat measurements, STM, ARPES, etc. (see Timusk and Statt, 1999, for a review on the pseudogap) opens at a temperature T^* which

drops sharply with increasing doping, defining a crossover line in the phase diagram of Fig. 2. This pseudogap is most probably intimately linked with the correlated nature of these systems, and its actual physical origin is still intensely debated. One class of interpretations could be the establishment of a hidden order disconnected from superconductivity such as a spin ordering [resonating valence bond (RVB) (Anderson, 1997) or *d*-density wave (DDW) (Chakravarty *et al.*, 2001)], involving orbital currents (Varma, 2006), or a charge segregation into stripe order (Carlson *et al.*, 2002). Another interpretation is a precursor pairing state, the superconducting phase being only established at T_c when pairs achieve long-range phase coherence (Emery and Kivelson, 1995a, 1995b). Currently the understanding of the pseudogap state remains unresolved.

In this section we describe experiments on point defects performed in the normal state of the HTSC systems, which cover many phases of the above phase diagram. We start with a discussion of the defects which can be used (Sec. IV.B). Experiments which allowed one to probe the magnetic response of the CuO_2 planes both on a local scale and on the macroscopic scale will be reviewed in Sec. IV.C. Since the systems in question are metallic, defects also cause significant modifications of the transport properties, which differ dramatically in the various parts of the phase diagram, as discussed in Sec. IV.D. Overall, these data have some profound implications for the normal state properties of the cuprates. The prominent qualitative features will be discussed in Sec. IV.E, while comparison with theoretical approaches will be postponed to Sec. V.

B. Controlled defects in and out of the CuO_2 planes

Impurity substitutions are *a priori* the simplest defects allowing one to induce well-defined perturbations and to "tune" the nature (spin or/and charge) of the perturbing potential. The ideal experimental situation would be to choose both the impurity and the atomic substitution site in the synthesis process. Furthermore, one would like to achieve this for any doping level in the planes, in order to compare the impurity properties in the various phases of the phase diagram. Unfortunately, physical chemistry considerations play a large role since competing solid-state phases combining the impurity atom and constituents of the cuprate may exist. Even in the absence of such phenomena, various substitution sites may occur depending on the charge reservoir layers of the cuprate material, and interference between the intended substitution and ions responsible for the doping of the CuO_2 planes may be present. Efforts have been made to control both the doping process and the associated disorder effects in the pure cuprates, as well as the impurity substitutions and/or defect content.

1. Hole doping of the cuprates

Doping the parent insulating cuprates to span the phase diagram is usually done by a modification of the layers separating the CuO_2 planes, either by a heterovalent substitution or by changing their oxygen content. In both cases, ions introduced into the structure create a modification of the Coulomb potential which disrupts the lattice periodicity and which will be felt as a scattering potential by the carriers in the CuO_2 layers. The influence of this source of disorder on the properties of the cuprates was neglected in the early cuprate studies.

It is clear that dopant disorder is particularly strong if the ionic dopant is in the separating layer of multilayer cuprates or in the reservoir layer near neighbor of the CuO_2 planes. For example, Sr^{2+}/La^{3+} in La_2CuO_4 and Ca^{2+}/Y^{3+} substitutions in $YBCO_6$ induce hole doping of the CuO_2 planes. These heterovalent substitutions are easily achieved, as no other substitution site seems to be available, and enable one to span the phase diagram, which is found to be similar for the above two families, but with rather low optimal $T_c \approx 40$ K. For $Y_{1-y}Ca_yBa_2Cu_3O_6$, the solubility limit is apparently smaller than $y \approx 0.35$ required to reach the optimum T_c (Casalta *et al.*, 1993). These systems are important to study the electronic properties of the lightly doped AF charge-transfer insulator.

In other families of cuprates, the doping is produced by introduction of extra oxygens atoms in the charge reservoirs, on sites located far from the CuO_2 planes. The optimal T_c's found in such cases, i.e., in single-layer Hg-1201, Tl-2201, or bilayer $YBCO_{6+x}$ and Bi-2212, are higher ($\gtrsim 90$ K) than those found for the heterovalent substitutions mentioned above. So it has been understood for some time that the dopant disorder certainly plays a role in limiting T_c over the superconducting dome. This source of disorder is revealed in NMR experiments on the NMR widths either as a distribution of magnetic hyperfine effects (Bobroff, Alloul, Mendels, *et al.*, 1997) or as a distribution of T_1 relaxation times (Singer *et al.*, 2002). Recent experiments in which the various substitution sites have been systematically used to dope Bi-2212 have confirmed this correlation between the optimum T_c and the proximity of the substitution site to the CuO_2 plane (Eisaki *et al.*, 2004). The existence of dopant disorder in Bi-2212 and its influence on the local superconducting properties were revealed by STM experiments (McElroy *et al.*, 2005).

Finally, we point out that the disorder of chemical dopants is a well identified source of disorder, but that other sources of disorder do occur in the cuprate families. For instance, the structural modulations due to the misfit between the lattice parameters of the CuO_2 plane and BiO plane in $Bi_2Sr_2CaCu_2O_8$ (BSCCO), or the tilt of the oxygen pyramids and the stripe structure around $x = 0.12$ in the Ba-doped lanthanum compound $La_{2-x}Ba_xCuO_4$ (LBCO). This type of "disorder" is even less controllable and dependent on the family. Because we are dealing with specific impurity effects, we are forced to consider these aspects and also to select systems in which "intrinsic disorder" is minimal. Here we include in the definition of intrinsic disorder both any structural disorder arising in the charge reservoir or

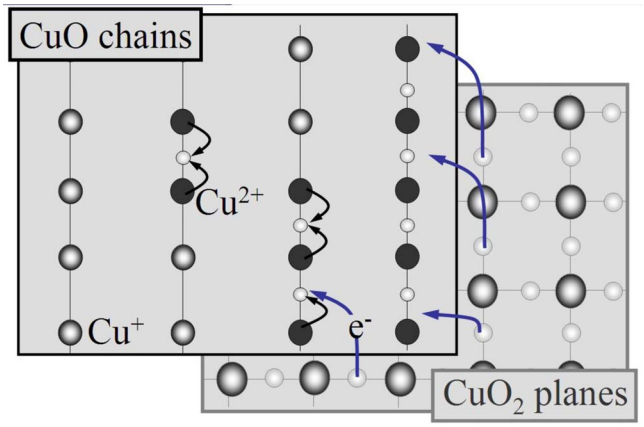

FIG. 16. (Color online) An oxygen inserted between two copper sites in a vacant chain row only changes the (initially) Cu^+ into Cu^{2+}. This does not transfer any charge to the CuO_2 plane. When a chain segment with at least two oxygen atoms is formed, charge transfer to the plane occurs. Full chains like that shown on the right might then form an ordered pattern, with specific values of the hole content in the planes, and minimal disorder.

CuO_2 layers as well as that due to the random distribution of the dopant atoms.

We highlight here the particular case of $YBCO_{6+x}$ for which the hole doping of the parent compound $YBCO_6$, which has no oxygen in the intermediate pure Cu(1) layer, is obtained by inserting oxygen in this layer. As shown in Fig. 16, the charge transfer is only initiated when x is large enough to give near neighbor oxygens. With the growth of chain segments the hole content n_h of the planes increases, but does not scale with x. Thus the phase diagram versus x differs markedly in appearance from that obtained by heterovalent substitutions for which n_h is controlled directly by the atomic substitution. At fixed values of x, ordered oxygen structures are formed, the most prominent for $x=1$, with filled Cu-O chains, which corresponds to slight overdoping of the plane (with T_c about 1 K lower than optimal). For $x=0.5$ the ortho-II phase with alternating filled and empty chains can be formed and corresponds to a good underdoped situation with a well-defined large pseudogap. But again for $x>0.5$ the added oxygen between chains (see Fig. 16) does not dope the planes as long as two oxygen sites are not near neighbors, that is, ideally in an ordered structure up to $x=0.75$, which explains the T_c plateau at 60 K around $x\simeq 0.6$. For these reasons, $x=1$ and $x\simeq 0.6$ are important compositions characteristic of the near-optimal and pseudogap phases, which can be easily reproduced. Furthermore, at $x\simeq 0.6$, the ordering of the chains, and the reduced effect of the Coulomb potential from the Cu^{2+}-O^{2-}-Cu^{2+} units, with an overall charge equivalent to 2 Cu^+, promotes a situation where intrinsic disorder is less important than in most other cuprate systems, as highlighted by NMR measurements (Bobroff *et al.*, 2002). The fact that the ordered chain phases are important fixed points of the phase diagram has been investigated by (Liang *et al.*, 2000). YBCO is therefore an interesting family for impurity substitution studies, since once a substitution has been performed, the undoped AF, the pseudogap phase, and the near optimal phase are accessible with simple heat treatments and correspond to phases with weak intrinsic disorder. Y-1248 (Karpinski *et al.*, 1988), a variant of YBCO with a well-ordered two-chain layer, is also an interesting case of underdoped pseudogap compound with little disorder.

2. Impurity substitutions in the cuprates

Since the early 1990s, impurity substitutions have been studied in the two preferred cuprate families YBCO and LSCO, and later, after the development of ARPES and STM experiments, data on substituted BSCCO have been taken as well. The easiest path to ensure that an impurity substitutes on a given site is to assume a substitution in the ceramic synthesis and check by x rays the absence of impurity phases which definitely occur if the substituent does not enter in phase, or substitutes on an alternate site. This allows one to perform Rietveld analysis of the powder patterns (see, for instance, Maeda *et al.*, 1989), to measure the variation of lattice parameters and to determine the solubility limit in solid state. Synthesis of single crystals does not allow similar checks but can be calibrated with respect to results on ceramic samples.

It is important to note that the physical chemistry complications linked with substitutions raise serious problems if one deals with a system which has some intrinsic disorder, as correlation between the impurity locations and the intrinsic disorder occur naturally, and therefore these effects are not additive. So studying impurity effects directly will be easier in families of cuprates with minimal intrinsic disorder.

a. Homovalent substitutions in the separating layer of multilayer cuprates

Substitution on the Y^{3+} sites by rare earths, allowing magnetic probes in the blocking layers, have been performed in the YBCO family. Most rare-earth moments interact very weakly with the CuO_2 planes, however, since superconductivity is nearly unaffected even for the pure compounds such as DyBaCuO or GdBaCuO (Hor *et al.*, 1987). Apart from applications purposes, the main interest of these substitutions is to provide new spin probes for the experimental study of the magnetic properties of the CuO_2 layers. A few percent of Gd substituted allowed thorough studies by Gd^{3+} ESR (Janossy *et al.*, 1994), while Yb substitutions allows one to use Yb^{3+} as a Mössbauer effect probe (Hodges *et al.*, 1995). These techniques provide hyperfine probes similar to the ^{89}Y nuclear spin probe, but allow the exploration of different T ranges as well as different electron spin relaxation time windows.

Pr acts differently from the other rare earths as it reduces the charge carrier content so that $PrBaCuO_7$ is antiferromagnetic and resembles the parent compound $YBCO_6$. At small Pr content, it has been demonstrated

that Pr hybridizes more with the O of the CuO_2 planes than the other rare earths, and that its effect is then to reduce the hole content in planes by filling holes on the neighboring oxygen (MacFarlane *et al.*, 2002). In this picture, the effective charge of Pr is then closer to +4. However, the corresponding perturbation in the plane is found to display a magnetic character as well.

b. Substitutions on the copper sites

The most important substitutions are the Zn and Ni substitutions on the Cu(2) sites of the CuO_2 planes which allows one to replace the Cu $3d^9$ $S=1/2$ site by nominal $S=0$ and 1 impurities, respectively. These substitutions have been performed in LSCO as they only take place on the single Cu site of the structure. But as this system contains significant intrinsic disorder due to Sr^{2+}-La^{3+} substitution, correlated disorder effects may severely modify the influence of the impurities.

In YBCO, the difficulty comes from possible substitutions on either the chain or plane Cu sites. It is easy to ensure that an impurity substitutes for Cu, by checking with x rays the absence of impurity phases. But once it is ensured that up to 4% Zn and 3% Ni substitute for Cu, thorough studies are required to determine on which site this substitution occurs. Various experimental investigations using EXAFS (Maeda *et al.*, 1989) or XANES (Yang *et al.*, 1990) suggest that Zn substitution preferentially occurs on Cu(2) in the CuO_2 planes while Ni substitutes on both the chain Cu(1) and planar Cu(2) sites. In the case of Zn the observation by NMR of the ^{89}Y near neighbors of Zn allowed one to ensure, from the integrated intensity of this line, that more than 90% of the nominal Zn content substitute on the Cu(2) site, within experimental accuracy (Mahajan *et al.*, 1994). Since such an experiment is impossible in the case of Ni, the equal probability of atomic substitutions on the Cu(1) and Cu(2) sites given by structural studies could not be controlled independently. Finally, Li has also been found to substitute solely on the Cu(2) site (Sauv *et al.*, 1996) in YBCO, with the actual Li content determined from ^{89}Y near-neighbor intensity measurements (Bobroff *et al.*, 1999).

Many impurities have been found to substitute preferentially on the chain Cu(1) site, such as Co^{3+}, Fe^{3+}, or Ga^{3+} (see Bridges *et al.*, 1989, and references therein). The impurities on the chain site donate their extra electrons to the planes and also interrupt the chains, which further reduces the charge transfer to the planes (Miceli *et al.*, 1989). These 3+ impurities often do not like the square oxygen coordination of the chain site and accommodate extra oxygen sites, which partly compensate the reduction of hole doping and maintains a tetragonal structure of the compound whatever the oxygen content, as, for instance, for Ga^{3+} (Xiao *et al.*, 1988). The dominant overall effect of such substitutions on the chain site is a reduction of the hole doping of the CuO_2 plane, making the optimally doped composition impossible to reach. In many cases, even for Ni (Adachi *et al.*, 2000), it has been found that heat treatments in controlled atmosphere do allow partial transfers of impurities between the Cu(2) and Cu(1) sites.

c. Defects induced by electron irradiation

To control defect creation in a solid, one may use irradiation by energetic particles, preferably light ones which have a large enough penetration length to damage bulk samples.

Ions or even protons produce a large density of defects which recombine into clusters of defects. In particular, energetic heavy ions yield linear tracks of heavily damaged material which can be used to pin vortices in the SC state (Civale *et al.*, 1991; Konczykowski *et al.*, 1991). To produce isolated point defects, the most suitable method is to irradiate with high-energy (MeV) electrons at low T, optimally in liquid H_2 at 20 K, which avoids recombination of the point defects created. In cuprates, this allows the production of Cu and O vacancies in the planes, with the ejected Cu and O trapped in interstitial locations out of the CuO_2 planes. Upon heating the sample, some of the created defects recombine, the oxygen atoms first as their mobility is larger (Legris *et al.*, 1993; Giapintzakis *et al.*, 1994; Tolpygo, 1994). The complete set of studies performed so far indicate that the damage is homogeneous on samples of thickness <50 μm, and that the vacancies in the CuO_2 planes primarily modify the transport and superconducting properties, yielding effects quantitatively identical to those produced by Zn substitutions (Rullier-Albenque *et al.*, 2000). If this method is ideal for transport studies in single crystals of small thickness, it unfortunately requires too much electron beam time for the large amount of sample required for bulk or NMR experiments.

C. Magnetic properties induced by in-plane impurities

1. Impurities in AF phases

The parent compounds of the cuprates appear to be good Mott insulators, with a very large Heisenberg exchange interaction $J \simeq 1500$ K (Lyons *et al.*, 1988). This is revealed by neutron-scattering experiments which display an inelastic scattering peak at the AF wave vector (π,π). The q width of this peak gives a quantitative estimate of the dynamic AF correlation length $\xi(T)$, which fits perfectly at high T in La_2CuO_4 the $\exp(J/k_BT)$ variation expected for the Heisenberg 2D square lattice (Birgenau and Shirane, 1989). However, while a spin-$\frac{1}{2}$ Heisenberg 2D system should only order magnetically at $T=0$, the undoped cuprates display a well-established 3D AF order with Néel temperatures T_N, which should be largely dependent on the magnitude $J_\perp$ of the interplanar couplings. As this is not the case (Alloul *et al.*, 1990; Mendels *et al.*, 1991) it has become clear that the ordering is governed instead by a deviation of the plane Hamiltonian from the ideal Heisenberg situation. Indeed, a very small XY anisotropy of the exchange interaction drives a Kosterlitz-Thouless transition in the 2D

system at a temperature T_{KT} which is slightly modified by 3D interactions (Alloul, 1991; Keimer *et al.*, 1992).

a. Substitution effects in the undoped phase

What happens when a Cu is substituted by a nonmagnetic or magnetic impurity? In $YBCO_6$, magnetic impurities substituted on the Cu(1) sites are only found to change the coupling between bilayers in such a way that planes of neighboring bilayers switch from an AF ordering to a ferromagnetic ordering, still retaining the bilayer AF order (Lutgemeier, 1988; Dooglav *et al.*, 1996). But T_N, which is fixed mainly by T_{KT}, is not modified significantly by this change of 3D magnetic structure of the ground state. For a nonmagnetic impurity such as Zn, which substitutes on the planes, the dominant effect is the dilution of the magnetic lattice, which was studied (Vajk *et al.*, 2002) and found to reduce T_N moderately at low concentration as a result of the reduction of ground-state energy and of T_{KT}. Overall, the influence of substituted impurities on the macroscopic properties of the ground state do not tell us much about the single-plane physics.

In this AF state, local measurements of the modifications induced by a nonmagnetic defect are somewhat difficult. The main observation has been the reduction of intensity of the ^{63}Cu NMR signal detected in the internal magnetic field without external applied field (zero field NMR: ZFNMR) (Mendels and Alloul, 1988). This gives an indication of the spatial range over which the impurity induces a sizable modification of the AF order (Mendels *et al.*, 1990). So far these experiments did not enable a detailed study of the local modifications of the magnetic order, as their analysis depends on the modifications of the various parameters and are not solely associated with the single plane physics and its spin-liquid state. Experiments above T_N in the paramagnetic state allowed one to detect modifications of the spin dynamics from NMR spin lattice relaxation data (Carretta *et al.*, 1997), but again no local study of the magnetic properties around impurities could be achieved.

b. Impurities in the doped antiferromagnetic state

We first recall the effect of small hole dopings (below 10%) in the "pure" systems. One important fact learned early on from studies on LSCO is that carriers abruptly reduce T_N, less for electron doping than for hole doping (Birgenau and Shirane, 1989), but much more than for spinless homovalent substitutions, such as Zn^{2+}. A similar decrease of T_N occurs for hole doping by Ca in $Y_{1-y}Ca_yBa_2Cu_3O_6$ (Casalta *et al.*, 1993). In any case these carriers are mobile at high T as the planar resistivity increases above room temperature as in a metal (Ando *et al.*, 2004). They should localize at low T in the Coulomb potential of the dopant, so that nongeneric modifications of the AF state are expected. Although detailed studies have not been performed so far, T_N suppression is, however, achieved for a comparable doping of $n_h \simeq 0.03$ for Sr and Li, which correspond, respectively, to out-of-plane and in-plane Coulomb potentials (Suh *et al.*, 1998). It has been generally seen that a new "phase" appears below T_N, which contains some amount of static disorder, and which has some characteristics of a mixed AF–spin-glass phase (Chou *et al.*, 1993).

For hole dopings larger than $n_h \simeq 0.03$, the ordered magnetic state disappears and gives way to a static disordered magnetic phase detected by magnetization measurements, muon spin rotation (μSR), or NMR (Cho *et al.*, 1992; Chou *et al.*, 1995; Niedermayer *et al.*, 1998). This latter phase has many characteristics of a true spin-glass (SG) phase. In some systems like the lanthanum family it extends over a large doping range, between 0.03 and 0.07, but still exists far into the SC state nearly up to optimal doping $x=n_h=0.15$, albeit with a low spin-glass temperature T_g (Niedermayer *et al.*, 1998). Whether the tendency to stripe formation at $x=0.12$ in the Ba doped case favors a coexistence of the SG and SC phases on a microscopic scale or leads to a phase separation is not fully clarified. In $YBCO_{6+x}$ the SG phase has been occasionally detected for intermediate oxygen contents $x \simeq 0.45$ but has totally disappeared for $x \simeq 0.6$, that is, $n_h \simeq 0.10$. So it is clear that the SG phase is not generic in the phase diagram of the "pure systems," but is linked with the intrinsic disorder present in the systems. In a specific family of bilayer cuprates CaBaLaCuO, systematic studies reveal a clear relation between the T_g and T_c values in the phase diagram, which suggests that the influence of the intrinsic disorder in these systems affects these temperatures similarly (Keren and Kanigel, 2003).

The introduction of spinless impurities adds to the existing disorder in these phases. It is remarkable that Zn substitution in YBCO extends significantly the SG phase range in this system (Mendels, Alloul, Brewer, *et al.*, 1994) (see Fig. 17), so that the phase diagram of $YBCO:Zn_{0.04}$ resembles that observed in nominally pure LSCO, or in $Y_{1-y}Ca_yBCO_6$. This suggests again that extrinsic or intrinsic disorder may have similar influences on the properties of these systems at least in the low-hole-doping range.

Regarding the influence of controlled impurities in the intermediate doping range, we again emphasize that we are not dealing with single-impurity effects, and that the interferences with the intrinsic disorder of the pure systems complicate the situation markedly. As shown in Sec. VI.E, Zn impurities in LSCO around $n_h=0.10$ obviously nucleate a long-range magnetic order detected by neutron-scattering experiments which is not present in the pure system. This kind of order induced by disorder bears some analogy to the situation in spin chains for which magnetic order can be enhanced by impurities (see Sec. III.D.5). Although many qualitative and materials aspects are revealed by experiments involving impurity substitutions, such observations are even harder to analyze theoretically than those done in the undoped AF case (see, however, Sec. V).

2. Impurities in the pseudogap phase above T_c

When the doping is large enough to destroy the static AF phase and to establish a metallic and superconduct-

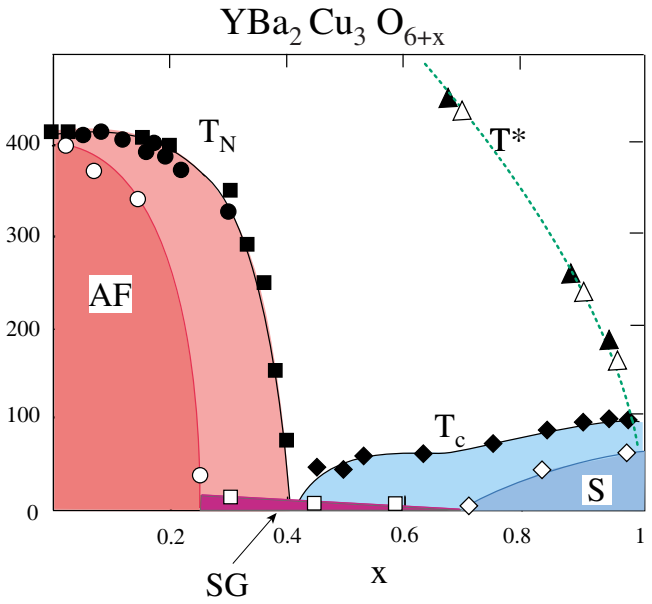

FIG. 17. (Color online) Phase diagram of pure and Zn-substituted $YBCO_{6+x}$. Note that the phase diagram of pure $YBCO_{6+x}$ (full symbols) only exhibits a small range of oxygen contents, near the tetragonal-to-orthorhombic transition at $x=0.4$, for which disordered static magnetism occurs at low T. With Zn substitution, at a concentration of 4% (open symbols), the superconducting range is highly suppressed; the local magnetism induced by Zn drives the appearance of a large spin-glass (SG) regime. The phase diagram becomes then similar to that of Fig. 2. Note that the onset of pseudogap opening T^* is not modified by Zn substitution. Figure from Alloul *et al.*, 2000.

ing state, the magnetic properties display, in the underdoped regime, a "pseudogap" (see Fig. 2). The pseudogap opens up at a very high temperature T^* ($\approx$350 K in $YBCO_{6.6}$) and is signalled by a decrease in the spin susceptibility (see Fig. 18). Here we are in an interesting doping range where the system is a metal with magnetic correlations, which is a difficult theoretical problem. This is the regime for which the use of impurities to probe the physical properties was expected to be the most fruitful. Such an approach was started in the early 1990s and provided first basic qualitative information. Improvement of the samples and experimental techniques have since allowed one to obtain more refined quantitative information on the perturbations introduced by the impurities. A major effort has been devoted to the case of Zn, Ni, and Li impurities substituted for Cu in the $YBaCuO_{6+x}$ system specifically for $x \simeq 0.6$ for which the intrinsic disorder is minimal.

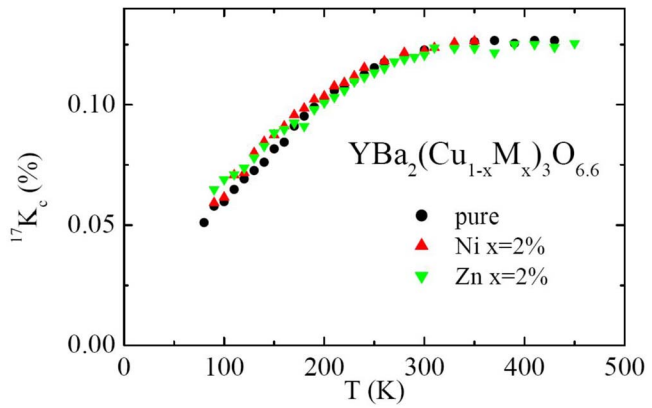

FIG. 18. (Color online) ^{17}O NMR shift vs T for $YBCO_{6.6}$ pure and substituted with 2% Zn and 2% Ni. The NMR shift for the sites far from the Zn is found to be totally independent of the substitution, with the onset of opening of the pseudogap remaining at $\approx$350 K for all samples.

a. Influence of impurities on the pseudogap

The first point that was investigated in the early experiments was the influence of the substituted impurities on the temperature T^* at which the pseudogap opens. As shown in Fig. 18, the NMR shift of nuclei located far from the impurities is not affected by the impurities Zn or Ni, even when the impurity content is large enough to completely suppress superconductivity (Alloul *et al.*, 1991; Riseman *et al.*, 1994; Bobroff, Alloul, Yoshinari, *et al.*, 1997).

Most probes sensitive to the normal-state pseudogap far from the defects confirmed these findings later on, and showed that they applied to any kind of disorder, such as irradiation defects or Li impurities. Some early inelastic neutron-scattering (INS) (Kakurai *et al.*, 1993) and ^{63}Cu T_1 experiments (Zheng *et al.*, 1993) claimed a filling of the pseudogap in the spin excitations at the wave vector (π,π), in the presence of impurities. However, later data have confirmed that the Zn impurities create low-energy midgap excitations (Harashina *et al.*, 1993; Bourges *et al.*, 1996). These excitations, described in Sec. IV.C.4, are associated with the fluctuations of the local moment AF staggered response spatially localized near the Zn. They partially fill in the pseudogap which characterizes the behavior far from the Zn; this is apparent in both the ^{63}Cu T_1 data and the INS, as shown in Fig. 19. Indeed, NQR investigations (Itoh *et al.*, 2003), in which the resonances of the sites far from the impurity could be singled out, reveal the persistence of the pseudogap for the T_1 data of these sites (see Fig. 20).

This body of experiments gives consistent evidence that the pseudogap is not modified far from the Zn site, while the local magnetic properties are strongly modified near the Zn location. This is also confirmed by other experiments which allow one to detect the onset of the pseudogap from macroscopic data, such as specific heat (Loram *et al.*, 1994), transport for Zn substitutions (Mizuhashi *et al.*, 1995; Walker *et al.*, 1995), and irradiation defects (Rullier-Albenque *et al.*, 2003).

b. Local moments induced by Zn

The first question that arises is whether a nonmagnetic site induces a free paramagnetic moment in a *metallic* correlated system, as shown in the case of undoped spin chains and ladders. Ideally, this might be probed by macroscopic susceptibility measurements, or by electron spin resonance (ESR) experiments. A theoretical pro-

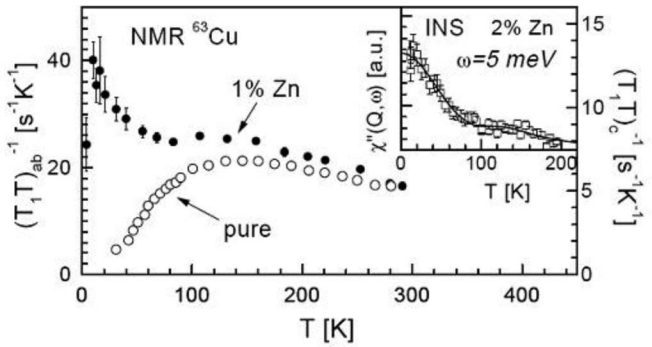

FIG. 19. ^{63}Cu NMR $(T_1T)^{-1}$ data taken in Zn-substituted $YBCO_{6.6}$ display a large increase at low T, which is also seen in the inelastic neutron-scattering data taken at the AF wave vector (π,π) shown in the inset. Both data are dominated at low T by the contribution of sites near the Zn, but display evidence for the onset of the pseudogap as a high-T maximum of the dynamic susceptibility around 150 K, seen in the pure samples. From Julien *et al.*, 2000.

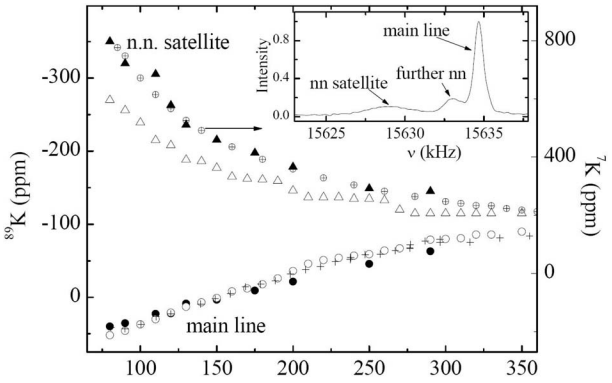

FIG. 21. ^{89}Y NMR spectrum of $YBCO_{6.6}$:Zn (or equivalently $YBCO_{6.6}$:Li) exhibits a main line and two satellite resonances as shown in the inset. Their shifts ^{89}K are plotted vs T as empty and full symbols, respectively, for Zn and Li substitution. While the main line shifts (circles) retain the characteristic pseudogap T variation of the pure sample (crosses), the NN satellite shifts depart markedly at low T, the difference of shift with the main line displaying a Curie T^{-1} variation. This results from the large Curie-like spin polarization which appears on the four Cu sites around the Zn or Li, two of them being directly sensed by the ^{89}Y NN to the Zn (see Fig. 22). The ^{7}Li NMR shift (cross in a circle, right scale) directly probes as well this Curie polarization of its four Cu neighbors. Figure from Bobroff *et al.*, 1999.

posal for the occurrence of a local moment with an ESR experiment in LSCO:Zn to support this view was given by Finkelstein *et al.* (1990). Although the theoretical idea was valuable, the detected signal could not be associated with isolated Zn impurities, as shown in Sec. IV.C.4. Indeed, the early experiments were plagued by materials problems. For instance, ESR signals detected in YBCO samples were exclusively due to the so-called "green phase" Y_2CuO_5, which also induced Curie terms in the susceptibility of pure samples. Although some initial susceptibility data on Zn-substituted YBCO samples did suggest evidence of Curie contributions, they could not be considered as proofs for the existence of impurity induced paramagnetism (Cooper, 1991). The actual contribution of substituted impurities to the magnetic susceptibility has only been determined since, in carefully controlled samples, as shown below.

The first indirect but unambiguous evidence that Zn induces a dynamic paramagnetic moment in an underdoped cuprate was obtained by monitoring the ^{89}Y NMR linewidth in $YBCO_{6.6}$:Zn_y (Alloul *et al.*, 1991). A nonmagnetic impurity in a metallic host yields only a T independent broadening of the unshifted host NMR signal due to Friedel oscillations of the density of states. By contrast, the unshifted ^{89}Y NMR has a linewidth that is found to increase markedly at low T, while the susceptibility of the host decreases due to the pseudogap. This reveals that the spatially dependent spin susceptibility induced by the Zn impurities displays a T-dependent paramagnetism which increases at low T and is therefore "Curie-like," as illustrated in the case of a spin chain (see Fig. 14). The only difference is that the signals of the different near-neighbor shells of the impurity are overlapping and yield a broadening of the line. The actual T dependence of the susceptibility could not be ascertained by such a measurement, since the relationship between the magnitude of the induced spin polarization and the magnetic susceptibility is not straightforward, as described below. That a Curie-like moment developed in the vicinity of the Zn was confirmed by resolving with dilute samples the satellite NMR signal of the ^{89}Y near-neighbor (NN) sites of the substituted Zn (Mahajan *et al.*, 1994) (see Fig. 21). This provided the first local detection of the field induced paramagnetism near the Zn, well before the equivalent information could be monitored in the case of spin chains. These data imply that the spin polarization of the Cu NN to Zn is, already at 100 K, more than ten times larger than that of the pure host, so this is not a minor modification of the host density of states, but a strong effect of the electronic correlations of the system, similar to that observed in spin

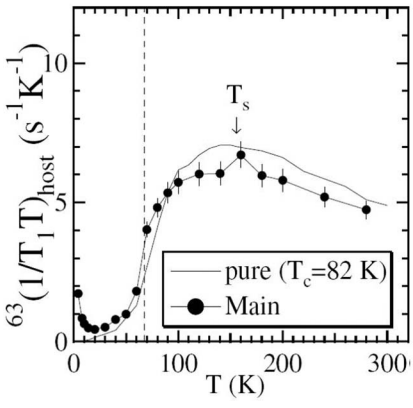

FIG. 20. ^{63}Cu nuclei far from the Zn impurities display in YBCO-1248 the same reduction of $(T_1T)^{-1}$ as that found in the pure compound below the pseudogap temperature. From Itoh *et al.*, 2003.

chains. The very short spin lattice relaxation T_1 of the ^{89}Y NN NMR at low T is further evidence which establishes the occurrence of a local moment induced by the spinless Zn impurity. Analogous ^{89}Y NN NMR data were obtained later on Zn substituted YBCO-1248, which is also a low disorder underdoped cuprate, thus confirming the generality of these observations (Williams *et al.*, 1998).

This Zn-induced paramagnetic contribution to the macroscopic susceptibility χ_c can be determined from superconducting quantum interference device (SQUID) magnetization data taken on samples in which the fraction of parasitic impurity phases could be minimized and remained only as traces (Mendels, Alloul, Collin, *et al.*, 1994; Zagoulaev *et al.*, 1995). For $x=0.66$, a Curie-Weiss law $\chi_c=\mu_{\rm eff}^2/3k_B(T+\Theta)$ could be associated with Zn-induced magnetism down to $T\approx 10$ K, with a small value $\Theta\lesssim 4$ K for $x=4\%$ and an effective moment $\mu_{\rm eff}=1.0\mu_B$ (Mendels *et al.*, 1999).

With the known hyperfine couplings for the ^{89}Y nucleus, the spin polarization on the 4 Cu NN to the Zn corresponds to a total susceptibility of the same magnitude as χ_c. This was initially taken as an indication that the moment was mainly localized on the 4 Cu first NN to the Zn (Mahajan *et al.*, 1994). But the data allow one to conclude only that the sum of the staggered magnetic susceptibility on more distant sites roughly cancel out and contribute little to χ_c (Mahajan *et al.*, 2000).

The ^{63}Cu nuclear spin itself, which is more sensitive to the on-site magnetization, allows one to probe this long-distance staggered magnetism (Walstedt *et al.*, 1993; Julien *et al.*, 2000). The large increase of the ^{63}Cu linewidth induced by Zn established the existence of long-distance spin-polarization effects but did not provide enough quantitative information to correlate them with the short-distance information gained from ^{89}Y NMR data.

In Fig. 22, we summarize the sensitivity of various nuclei used in cuprate NMR to the Cu sites of different symmetry relative to planar impurities.

c. The Ni impurity: A weakly coupled local moment and the first evidence for a large $\xi_{\rm imp}$

The Ni impurity, which is in a $3d^8$ state, was expected to display significantly different magnetic properties owing to its on-site local moment. In this case, the macroscopic spin susceptibility χ_c per Ni site was found to be larger than for Zn, with $\mu_{\rm eff}=1.7\mu_B$ for $x=0.66$ nearer that expected for a spin $S=\frac{1}{2}$ than for a spin $S=1$, so that the local moment is somewhat reduced with respect to that expected for a free ion (Mendels *et al.*, 1999). A crude explanation is that the $3d_{x^2-y^2}$ component of the Ni moment couples to the CuO_2 band and roughly replaces the Cu spin, while the $3d_{z^2-r^2}$ orbital contributes to a spin-$\frac{1}{2}$ local moment weakly coupled with the CuO_2 band. This conjecture is supported by the evidence that the broadening of the ^{89}Y NMR (Riseman *et al.*, 1994) is dominated by the dipole field of the Ni local moment, and is only slightly affected by the staggered magnetism on the Cu sites, with no NN ^{89}Y line detected in that case.

On this basis, it was clear that data on the ^{17}O NMR, which has larger hyperfine couplings with the Cu(2) magnetization, would be less sensitive to the direct dipolar local fields induced by the local moment and would give more information on the staggered paramagnetism. The result obtained was that the ^{17}O linewidth did not increase at low T as the Curie $1/T$ behavior displayed by χ_c but much faster (see Fig. 23). This was considered a proof that in contrast with expectations for RKKY oscillations in a noncorrelated electron host (Bobroff, Alloul, Yoshinari, *et al.*, 1997), the T variation of the linewidth is not solely due to that of the magnitude of the staggered susceptibility but also that its decay length $\xi_{\rm imp}$ around the impurity has a large T variation (Bobroff *et al.*, 1998; Morr *et al.*, 1998). This occurs as well for Zn impurities as shown in Fig. 23, so that it appears more specific to the host than to the impurity response. To obtain quantitative determinations of $\xi_{\rm imp}$, the Li impurity which is a spinless impurity, as Zn, appeared more practical technically, as shown below.

d. The Li spinless impurity: Comparison with Zn

Li has been found to substitute on the Cu(2) sites (Sauv *et al.*, 1996) in YBCO, but detailed comparisons with Zn could only be performed when it was established that the ^{89}Y and ^{17}O NMR data in $YBCO_{6.6}$:Li samples were nearly identical to those found for $YBCO_{6.6}$:Zn, as shown in Fig. 21 (Bobroff *et al.*, 1999). This allowed one to understand that a Li^+ spinless impurity which introduces a hole in the plane induces the same local magnetic properties as the spinless isovalent substitution of a Zn^{2+} on a Cu^{2+} site. The fact that the ^{89}Y NN sites of the Li and Zn isolated impurities display almost the same shift is evidence that the charge difference is not screened on the atomic scale. The hole donated by Li to the band is rather delocalized, and of course changes the doping slightly, but this is experimentally a negligible effect as long as one considers dilute concentrations of Li. So the magnetic response of the CuO_2 plane to the local perturbation is dominated by the *spinless character of the impurity* which disrupts the AF interactions with the neighboring sites, while the extra Coulomb potential of the Li impurity is negligible in that respect.

The advantage in using Li as an impurity is that the large gyromagnetic ratio of the ^{7}Li nuclear spin and its small quadrupole moment allows one to detect its NMR signal, its shift, as shown in Fig. 21. This quantity is a direct measure of the magnetization of its four Cu NN sites. This then allowed three important technical advantages beyond what was permitted by the study of the NN ^{89}Y NMR:

- The high sensitivity of the ^{7}Li NMR permitted accurate measurements of $\chi(T)$ of the Cu NN of the spin-

less impurity. In the underdoped samples, this variation displays a perfect Curie T dependence (see Fig. 21), which confirmed the ^{89}Y NMR observation that the impurity-induced state behaves as a nearly free paramagnetic moment (Bobroff *et al.*, 1999).

- The dynamics of the local moment can be studied through the ^{7}Li nuclear spin relaxation time T_1 data (MacFarlane *et al.*, 2000).
- The possibility to use in the same sample the ^{7}Li, ^{89}Y, ^{17}O, and ^{63}Cu nuclear spin probes has enabled the quantitative determination of the spatial structure of the induced polarization, that is, its magnitude and $\xi_{\rm imp}(T)$ (Ouazi *et al.*, 2004).

This last point will be now discussed, in both the underdoped and optimally doped parts of the cuprate phase diagram.

e. Spatial extent of the staggered spin polarization

While ideally one would like to measure directly the local magnetization on the nuclear spins of the magnetic sites themselves, i.e., Ni sites in the $S=1$ chains or Cu in 1D or 2D systems, in most cases this is hampered by technical limitations linked with the large hyperfine couplings on those sites. We have shown that other neighboring nuclear probes such as ^{89}Y can help to extract information in a less direct way. While in 1D YBaNiO chains the ^{89}Y nuclei probe the magnetization of a single Ni moment in a chain, the information is not as straightforward with a nucleus which has many different Cu neighbors, such as ^{17}O which experiences the response of two nearest-neighbor Cu sites in YBCO. This results in a form factor which connects the field induced on a nuclear site to the local magnetization in its vicinity. Although this appears as a complication at first sight, it is on the contrary an advantage since the availability of different nuclear spins allows one to probe various spatial ranges of the induced spin polarization. In particular, when the magnetization has a staggered spatial dependence it is clear that, for nuclei which have z Cu near neighbors in a plane, the cancellation of the local field sensed is more efficient for larger z (see Fig. 22). One can then understand that the range of the spin polarization sensed is larger for ^{63}Cu, which is affected by the on-site polarization, as compared to ^{17}O ($z=2$), and further compared to ^{89}Y ($z=4$).

The data given by the NMR shifts of ^{7}Li, of the NN satellite resonances of ^{89}Y, and the line shapes of the ^{89}Y and ^{17}O NMR main lines can be compared with numerical simulations made for model spin polarization radial dependences (Ouazi *et al.*, 2004). This analysis showed that the staggered spin density decays exponentially a few lattice constants away from the impurity, and that the induced spin magnetism is not singularly high on the near neighbors of the Li (or Zn) impurities. Similar to the chain case, the local moment perturbation has a spatial extent which is characterized by a single range parameter $\xi_{\rm imp}$ and the macroscopic moment appears as

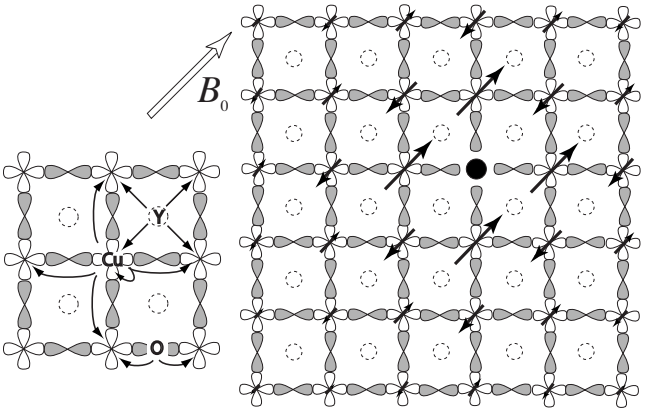

FIG. 22. Cu $3d_{x^2-y^2}$ and O $2p_x$, O $2p_y$ orbitals of the CuO_2 plane, with a Li or Zn impurity substituted on one Cu site. The magnetization induced on each Cu site by the applied field is staggered and decreases in magnitude to reach the very small uniform value found in the pure compound. Inset: The hyperfine coupling paths linking the different nuclear-spin sites with their near-neighbor Cu orbitals (also with the on site orbitals for Cu). The Y sites are below the CuO_2 plane (and above the other CuO_2 plane of the bilayer).

the sum of this oscillating polarization. Performing such a data analysis at different T allowed one to confirm that $\xi_{\rm imp}$ and the magnitude of the spin polarization have large T variations, as shown in Fig. 24.

3. From the underdoped to the optimally doped case

The same approach can in principle be applied for increasing hole doping in the CuO_2 plane. In pure compounds, the pseudogap temperature decreases and approaches T_c. What happens then to the magnetic response? Does it change drastically above T^*? This question has of course a direct relationship with the im-

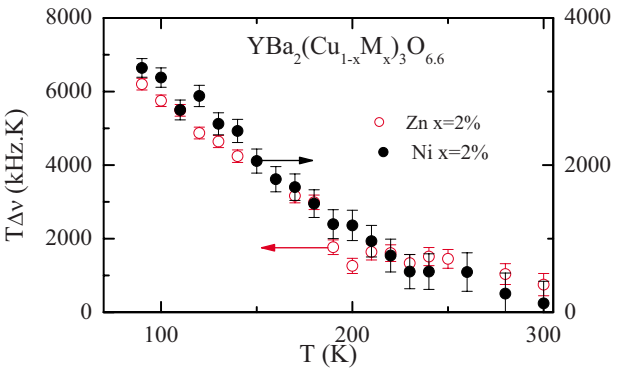

FIG. 23. (Color online) Difference $\Delta\nu$ of the ^{17}O NMR linewidth between the substituted and pure $YBCO_{6.6}$ samples gives a measure of the histogram width of local fields induced by Zn or Ni on ^{17}O nuclei. The product $T\Delta\nu$ increases markedly at low T, while it should remain constant if the spin polarization had a mere Curie $1/T$ variation. This is evidence that both the magnitude of the local fields and the width of their histogram, that is, the decay length $\xi_{\rm imp}$ of the spin polarization, increase sizably at low T. Data from Bobroff, Alloul, Yoshinari *et al.*, 1997 and Ouazi *et al.*, 2004.

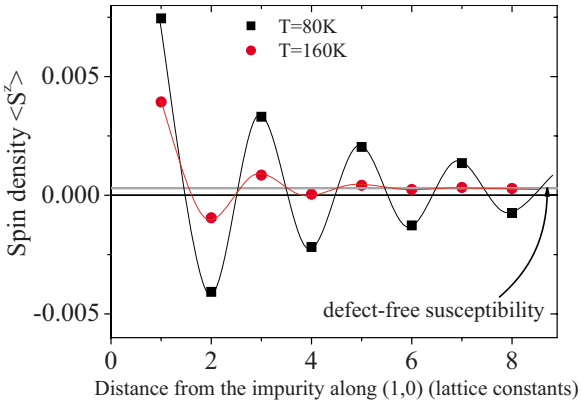

FIG. 24. (Color online) Spatial variation of the model spin densities which fit the NMR data on ^{7}Li, ^{89}Y, and ^{17}O nuclei in $YBCO_{6.6}$, as a function of distance to the impurity site along the (10) direction in the CuO_2 plane. It can be seen that the local magnetization magnitude and decay length ξ_{imp} both decrease with increasing T. For a large number of sites, the local magnetization is much larger than that of the pure sample, which is the limiting large-r value at 160 K, and which is even smaller at 80 K. From Ouazi *et al.* 2004.

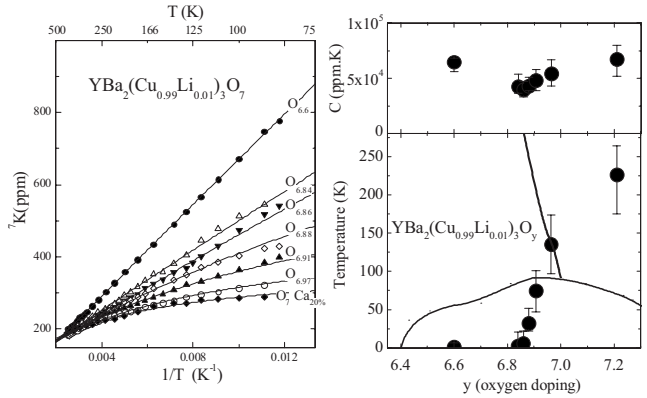

FIG. 25. Doping dependence of ^{7}Li NMR shift. Left: ^{7}Li NMR shift vs T^{-1} for a series of $YBCO_y$ samples as well as for an overdoped Ca^{2+}/Y^{3+}-substituted sample for $y=7$. The data are fitted with Curie-Weiss laws. Right bottom: The corresponding Weiss Θ values vs oxygen content y are seen to increase sharply near optimal doping. The full curve represents the variation of T_c in the pure samples. Right top: Effective moment parameter μ_{eff}^2 of the Curie-Weiss fit (Bobroff *et al.*, 1999).

portant question still pending regarding the phase diagram of the cuprates: does the pseudogap line cross the T_c line, giving rise to a quantum critical point near optimal doping, or does it merge with the T_c line? We examine this point first.

a. Pseudogap line and QCP

Experimentally, the pseudogap temperature T^* drops sharply with increasing doping and approaches the superconducting dome around optimal doping. As shown above, the introduction of impurities reduces T_c and allows one to probe the normal-state properties at temperatures below T_c of the pure compound. As impurities do not modify the pseudogap in the underdoped part of the phase diagram, a reduction of T_c induced by impurities should open a window allowing the study of the continuation of the T^* line in the optimally doped regime. NMR studies performed on substituted samples of $YBCO_7$ do not show any evidence for a discontinuous change of the NMR shift of any nuclear-spin species of the material between the T_c of the pure compound and that of the substituted one. Even with 4% Zn, the ^{59}Y NMR shift is found to remain constant when T_c has been reduced to 55 K (Alloul *et al.*, 1991). The existing experiments do not allow one to conclude whether the pseudogap line crosses the T_c line, although some report data points in their phase diagram which would suggest otherwise (Williams *et al.*, 1997).

b. Spinless impurity magnetism

Experimentally, although no nearest-neighbor ^{89}Y NMR resonance could be resolved in $YBCO_7$:Zn, the early NMR data (Alloul *et al.*, 1991) provided evidence for a low-T increase of the ^{89}Y NMR linewidth which could not be associated with impurity phases. In view of the above analysis, this was already evidence that magnetic correlations persist, since in a nonmagnetic metallic system one would expect a T independent linewidth when the spin susceptibility is Pauli-like as in $YBCO_7$. Indeed, the non-Korringa T dependence of the Cu(2) T_1 was also a direct proof that magnetic correlations remain important (Takigawa *et al.*, 1991). Most evidence in the SC state discussed in Sec. VI also indicates that below T_c some paramagnetic moment character appears. But this qualitative evidence cannot be connected easily to the more quantitative analysis done above in the underdoped normal state. The first more quantitative point came from SQUID data on clean samples of $YBCO_7$:Zn in which the impurity-induced χ_c was found much smaller at low T than in the underdoped compound, which indicated a weaker magnetism, and certainly not a free $S=\frac{1}{2}$ moment (Mendels *et al.*, 1999).

Subsequently, ^{7}Li NMR data allowed one to measure $\chi(T)$ directly on the four NN Cu atoms, which is shown in the left panel of Fig. 25 to deviate from a Curie law. The Curie-Weiss behavior found in $YBCO_7$ with a sizable Θ only weakly dependent on Li content ensures that this results from the isolated impurity response (Bobroff *et al.*, 1999). Again, comparison of the ^{17}O and ^{89}Y NMR shapes and widths data leads one to conclude that there is no appreciable difference between the Li- and Zn-induced magnetism, while Ni has a larger magnetic susceptibility χ_c but, as in the underdoped case, induces a comparatively smaller in-plane perturbation (Riseman *et al.*, 1994). Study of the T dependence of the ^{7}Li NMR shift vs hole doping shown in Fig. 25 provides evidence that the Curie-Weiss temperature Θ varies abruptly with hole doping and becomes nearly zero in the underdoped regime. As the effective moment found appears independent of doping, one can conclude that the low-T reduction of susceptibility in the optimally doped case is

due to the onset of the energy scale $k_B\Theta$, in analogy with the Kondo reduction of local moments in classical metallic systems. We show later, after performing an analysis of $\xi_{\rm imp}(T)$, that this analogy also applies to the dynamic properties of the local moment.

The occurrence of a local moment induced by substitution of Cu^{2+} by nonmagnetic Al^{3+} has been established as well. Ishida *et al.* (1996) showed that Al^{3+} exhibits a local moment behavior in optimally doped $La_{2-x}Sr_xCuO_4$. The ^{27}Al NMR shift exhibits a Curie-Weiss T dependence, with a sizable Weiss temperature ($\Theta \approx 50$ K). It is not clear whether this value of Θ could be reduced with respect to the single impurity limit by the large impurity concentration (3%) used in this experiment.

c. Magnetic correlations and $\xi_{\rm imp}(T)$

The weakness of the induced susceptibility, that is, the large value of Θ measured for optimal doping, is compatible with the absence of detectable ^{89}Y NMR nearest-neighbor resonances within the experimental resolution (limited by the ^{89}Y linewidth) for Li or Zn in $YBCO_7$. This does not prevent multinuclei analysis of the staggered magnetism, as the hyperfine couplings determined for the NN ^{89}Y in the underdoped case can still be used. Indeed, it was shown that the hyperfine couplings, which are based on atomic orbital physics (Mila and Rice, 1989), do not depend on the hole content in the cuprates (Alloul *et al.*, 1989; Pennington and Slichter, 1990).

Analysis (Ouazi *et al.*, 2004) of the T dependences of the ^{7}Li shift and ^{89}Y and ^{17}O NMR spectral shapes suggest that the magnitude of the staggered magnetism decays exponentially a few lattice constants away from the impurity. The local susceptibility is about four times larger at 100 K on the Cu NN to Zn than that of the pure optimally doped compound. This establishes the similarity with the staggered magnetism induced in the underdoped case, despite claims to the contrary (Tallon *et al.*, 2002); also see reply by Bobroff *et al.* (2002). Although $\xi_{\rm imp}$ has a similar magnitude at room temperature in the normal and underdoped cases, $\xi_{\rm imp}(T)$ increases much less at lower T in the former situation, as shown in Fig. 26. These results demonstrated that the local moment susceptibility and $\xi_{\rm imp}$ have much weaker T variations in the optimally doped case than in the underdoped one. The energy scale Θ may control the T variations of both quantities, however. Since overdoping corresponds to an increase of Θ well beyond the value found for optimal doping (Fig. 25), such a scheme allows a smooth crossover towards the Fermi-liquid limit for large overdoping.

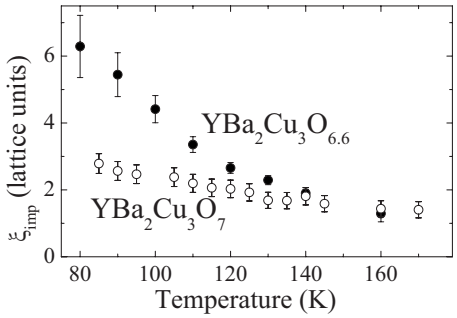

FIG. 26. Temperature dependence of the spatial extension $\xi_{\rm imp}$ of the polarization induced by Zn or Li impurities in underdoped $YBaCuO_{6.6}$ and optimally doped $YBaCuO_7$. The T variation is larger for the underdoped case (Ouazi *et al.*, 2004).

4. Spin dynamics

We have considered so far only the static response of the electronic states to a magnetic field. We might wonder what the microscopic process is that drives the dynamics of the local moment induced by spinless impurities. In undoped spin systems, the local moment fluctuations should be driven by the magnetic excitations of the system, if not by a different degree of freedom such as a spin-phonon coupling. In a 2D metallic system, charge degrees of freedom will play a role as well.

The nuclear spin lattice relaxation T_1 of the nuclear spins is governed by local fields fluctuations induced by the dynamic susceptibility (Pennington and Slichter, 1990). Modifications to the T_1 rates of the pure system due to local moment fluctuations are seen on nuclei even at large distances from the local moment, but are usually hard to analyze due to the distribution of coupling constants (Alloul and Bernier, 1973). The most reliable experimental situation is that for which a well-defined nuclear spin site with respect to the impurity can be singled out (Alloul, 1977). For instance, the resolution of a shell of ^{63}Cu neighbors of Zn by NQR (Itoh *et al.*, 2003) showed that nuclei near the impurity display the fastest relaxation rates, as expected in the local moment picture, contrary to previous claims (Ishida *et al.*, 1993).

This is the case as well for the ^{89}Y NNs of the impurity (Mahajan *et al.*, 2000), or for the impurity ^{7}Li NMR itself in the case of Li substitution (MacFarlane *et al.*, 2000). In these cases the contribution to $1/T_1$ of the local moment fluctuations overwhelms that of the pure system (Mahajan *et al.*, 2000), and it was studied for the Li case (MacFarlane *et al.*, 2000).

In a simple relaxational model for which the local moment is assumed to fluctuate as a single entity at a rate τ_s^{-1}, the nuclear spin lattice relaxation rate is related to τ_s^{-1} and the local moment susceptibility χ_c by

$$1/T_1T = 2k_B(\mu_n A/\hbar\mu_B)^2\chi_c\tau_s, \tag{29}$$

where μ_n and μ_B are the nuclear and electronic magnetic moments. Here A is the effective hyperfine coupling of the nuclear spin to the local moment obtained from the shift of the nucleus by $K = A\chi_c/\mu_B$. Therefore $(T_1TK)^{-1}$ is a direct measure of τ_s as shown for the ^{7}Li nuclei in Fig. 27. They are fully compatible with those obtained from the ^{89}Y NN T_1 data which were found identical for Li and Zn substitutions.

The low-energy excitations detected by inelastic neutron scattering at (π,π) in the normal state of under-

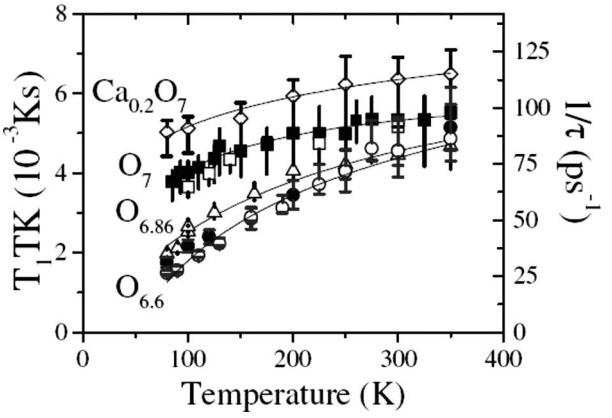

FIG. 27. Electronic relaxation rate τ^{-1} obtained from T_1TK, as measured for the ^{7}Li NMR for different hole dopings and Li contents (empty symbols, 1%; full symbols, 2%) in YBaCuO. From MacFarlane *et al.*, 2000.

doped YBCO:Zn have energy widths which agree with h/τ_s (Sidis *et al.*, 1996, 2000). This quantitative consistency confirms that the dynamics is not that of a purely atomic local moment, but concerns the extended staggered AF state, which is the assumption made in Eq. (29).

The τ_s values are so short that the expected ESR linewidths are too large to be observable with standard 10 GHz ESR, which explains the absence of any such direct observation in cuprates and implies that the ESR signals detected in the early LSCO:Zn experiments (Finkelstein *et al.*, 1990) were not linked with the Zn-induced local moments (Mahajan *et al.*, 2000).

Additional evidence which can be drawn from the data of Fig. 27 is that $1/\tau_s$ has behavior similar to that found for $1/\chi_c$, as both increase quasilinearly with T for the underdoped cases and are less T dependent for the optimally doped case. In fact, a nearly perfect linear variation of $(T_1TK)^{-1}$ versus K applies, with a slope S corresponding to the universal Korringa constant $S=(4\pi k_B/\hbar)(\mu_n/\mu_e)^2$. This provides direct evidence that χ_c and τ_s^{-1} are governed by the same energy scale. In other words, the applicability of a Curie-Weiss law for χ_c with a Weiss temperature Θ is associated with limiting low-T behavior $\tau_s^{-1}=k_B\Theta/h$ for the local moment fluctuation rate. This is reminiscent of the Kondo effect for a local moment in a noble metal host, the Kondo energy being the width of the resonant state which governs at low T the fluctuations in the Kondo state. These results are discussed in Sec. V.

D. Transport properties

Transport properties are among the most unusual properties of the cuprates, and may be influenced by the disorder-induced magnetic phenomena as discussed. Scattering of the charge carriers from inelastic magnetic fluctuations is often assumed to be responsible for the strange metal behavior exemplified by the linear T dependence of the resistivity above T_c, although there is no complete theory available. The influence of impurities and defects on the transport properties provides information on the properties of the carriers themselves, and the coupling between charge and spin degrees of freedom.

In contrast with simple metals, where experiments probing impurity effects can be performed down to low T, there are severe limitations in the present case, owing to the onset of superconductivity at a high T_c. On the other hand, the suppression of T_c by defects is an additional element of characterization available which serves as a reference in the experiments although it is not solely linked to the properties of the normal metallic state.

We recall, first, that reliable in-plane transport data require small high-quality single crystals, and that the synthesis of impurity-substituted single crystals does not necessarily benefit from the experience gained with ceramics, which are reacted in different thermal conditions. Thus the impurity content, fractional site occupancies, and actual carrier content of single crystals quoted in the literature are not always accurately determined. As pointed out in Sec. IV.B.2, electron irradiations are helpful, as one can span a series of defect concentrations using only one single crystal by increasing the irradiation dose progressively.

We first discuss the basic transport measurements which allow one to demonstrate the simple characteristics of the scattering induced by specific defects: residual resistivities, Hall effect, and thermopower, which will be correlated with the induced reduction of T_c. This will then allow us to discuss more sophisticated effects such as low-T resistivity upturns and magnetoresistance.

1. High-T in-plane transport and scattering rates

An important question in transport processes is the applicability of Mathiessen's rule, which in classical metals states that the impurity scattering rate adds incoherently with the inelastic scattering rate in the pure material, usually due to phonons. In the cuprates, the approximate additivity of the impurity scattering and that by magnetic excitations of the pure samples was pointed out for Zn substitutions in $YBCO_7$ as shown in Fig. 28 (Chien *et al.*, 1991).

Data taken later with electron irradiation on a single crystal with increasing defect content are even more convincing, as shown in Fig. 29. At high T, well above T_c, the $\rho(T)$ curves parallel each other, which establishes that the hole content is not modified by defects introduced by electron irradiation and that a residual resistivity term simply adds to the T-dependent part of the scattering. However, at low T and for high enough defect content, low-T upturns of the resistivity appear. This phenomenon has often been interpreted in terms of a metal-insulator transition (MIT).

An estimation of the residual resistivity due to the impurities can be obtained either by extrapolation of the high-T behavior to $T=0$ or in the best cases like that shown in Fig. 29 by measuring the parallel shift of the

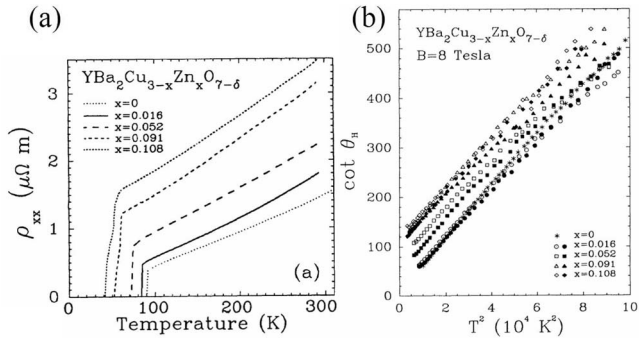

FIG. 28. Effect of Zn on the transport properties of YBCO crystals. (a) Temperature dependence of the in-plane resistivity averaged over a and b for a pure single crystal of $YBCO_7$ and for various Zn concentrations in substituted single crystals; (b) T variation of cot θ_H, where θ_H is the Hall angle, for the same samples (Chien *et al.*, 1991).

$\rho(T)$ curves at high T. The residual resistivity per plane $\Delta\rho_{2D}$ is a measure of the scattering rate of the conduction electrons by the impurity potential. In classical metals, the scattering analysis is done in terms of phase shifts. Such analyses are successful as long as the scatterers are atomic scale defects and if one takes into account a decomposition of the Bloch wave functions into partial waves of different symmetries s, p, d, which undergo different phase shifts. In particular cases, as for transition-metal impurities, one scattering channel dominates and a single phase shift is sufficient to characterize the scattering. While such a simple limiting situation has no *a priori* reason to be valid for impurities in correlated electrons systems, the data have been analyzed in cuprates by assuming an s-wave scattering with a unique phase shift δ which corresponds to

$$\Delta\rho_{2D} = (4\hbar n_d/e^2 n)\sin^2\delta, \tag{30}$$

where n_d and n are, respectively, the impurity and hole concentrations.

In the case of Zn substitutions the residual resistivity associated with the Zn scatterers yields a large value of the scattering rate, with $\sin^2\delta \approx 1/3$ if Eq. (30) above is applied (Chien *et al.*, 1991). This is more than two orders of magnitude larger than that of the Zn impurity in copper. This unexpected large scattering by a homovalent impurity is an illustration of the strange metal properties of the cuprates, which may only be explained by the correlated nature of the electron states. The residual resistivity associated with Cu and O vacancies in irradiated samples is large as well (Legris *et al.*, 1993).

The Hall effect was also found to display an anomalously large T dependence in the cuprates, as was pointed out by Chien *et al.* (1991). By comparing pure and Zn-substituted samples, it was found that the cotangent of the Hall angle varies as

$$\cot\theta_H \equiv \rho_{xx}/\rho_{xy} = \alpha n_d + \beta T^2, \tag{31}$$

as seen in Fig. 28. This supports the idea by Anderson (1991) that cot θ_H reflects a second scattering rate τ_H^{-1}, with a T^2 variation in the pure samples, which is independent of the resistivity scattering rate τ^{-1}. The first term in Eq. (31) implies that the Zn impurities contribute independently to the two scattering channels.

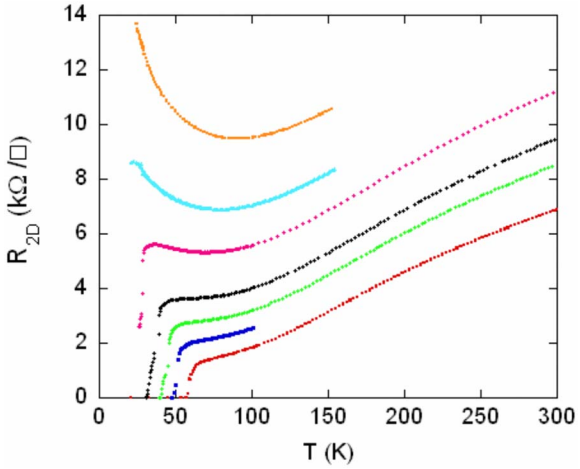

FIG. 29. (Color online) Resistivity vs T for a single crystal of $YBCO_{6.6}$ irradiated at 20 K by 2.5-MeV electrons for increasing irradiation doses. The resistivity curves display at high T a parallel vertical shift associated with the increase of the impurity induced residual resistivity. Therefore the defect content does not modify the high-T inflection point, linked with the pseudogap T^*. For high defect contents, when T_c is sufficiently reduced, low-T upturns are evident, and ultimately the resistivity curve diverges exponentially (Rullier-Albenque *et al.*, 2001).

2. Variation of the high-T transport properties with hole doping

These experiments have been extended to the underdoped regime in order to quantify the variation of the scattering rates with hole doping. As shown in Fig. 29 the in-plane resistivity of underdoped pure samples acquires a nonlinear T variation which signals a suppression of the scattering when the pseudogap opens at T^*. Experiments on substituted YBCO or LSCO single crystals with Zn (Mizuhashi *et al.*, 1995; Fukuzumi *et al.* 1996), or on electron irradiated samples (Rullier-Albenque *et al.*, 2000) demonstrate that this T dependence is not altered by disorder, as shown in Fig. 29, which indicates that hole doping and T^* are not modified by these defects.

a. Residual resistivity

The applicability of Eq. (30) for different hole dopings has also been checked. As shown above, determinations of $\Delta\rho_{2D}$, n_d, and n are done with an accuracy hardly better than 20%, so that estimates of $\sin^2\delta$ are possible only within a factor of 2. However, Fukuzumi *et al.* (1996) assumed that, within the approach described above, the scattering rate is large enough to correspond to unitary scattering ($\delta \approx \pi/2$) whatever the hole doping. They suggested that one should identify the number of carriers n with the number of doped holes n_h for the

underdoped samples and with $1-n_h$ for overdoped ones, to get a consistent explanation of the data.

Alternatively, experiments using point defects created by electron irradiation allow more accurate determinations of $\Delta\rho_{2D}$, as shown in Fig. 29. Furthermore, in $YBCO_{6+x}$ samples, the concentration n_d of defects created *in situ* at low T is independent of oxygen content and solely determined by the electron fluence. Accurate comparisons of $\Delta\rho_{2D}$ for different hole contents show then that unitary scattering cannot apply for both $YBCO_{6.6}$ and $YBCO_7$ (Rullier-Albenque *et al.*, 2000). Rather, keeping $n=n_h$, one finds that the scattering is stronger for the underdoped case, which suggests that the scattering rate has some relation with the range ξ_{imp} of the magnetic perturbation induced by spinless impurities.

b. ΔT_c and residual resistivity

As accurate determinations of the scattering rate are not easy to obtain directly from resistivity data, an alternative approach is to seek information from the decrease of T_c induced by the scattering centers. Although this is rather a measure of the pair-breaking effect associated with the defects, it gives us information on the scattering rates within a d-wave scenario for the superconducting state, which is supported by many experiments in cuprates, as discussed in Sec. VI. In such a case, within a BCS theory of a d-wave superconductor the initial reduction of T_c is determined solely by the normal-state scattering rate (see Sec. VI.C),

$$\Delta T_c = -\pi\hbar/4k_B\tau. \tag{32}$$

Here the scattering rate is given by the residual resistivity as $\tau^{-1}=ne^2\Delta\rho_{2D}/m^*$. Thus, as long as the effective mass of the carriers is not sample dependent, ΔT_c and $n\Delta\rho_{2D}$ should be independent measures of the scattering rate, and therefore scale with one another, regardless of the concentration and microscopic structure of the point defects. This universal scaling has been found to apply perfectly for Zn and electron irradiation defects in many cuprates (Rullier-Albenque *et al.*, 2000) (see Fig. 30) provided that the number of carriers is taken as $n=n_h$.

The fact that dT_c/dn_d generally decreases with increasing n_h is mainly due to a reduction of τ^{-1} when electron correlations become less relevant. In that sense, one expects to eventually recover a weak scattering for Zn impurities in the overdoped Fermi-liquid limit. This is qualitatively supported by T_c data taken on Bi-2212 for various Zn and doping contents (Kluge *et al.*, 1995) but has not been studied quantitatively in the far overdoped regime, because Zn substitutions in overdoped systems like Tl-2201 have not been successfully performed so far to our knowledge. Direct determination of the scattering rate in such systems cannot be done by electron irradiation as the actual number of defects cannot be determined accurately either.

Finally, this universal scaling of ΔT_c and $n\Delta\rho_{2D}$ does not apply for the LSCO system. This is particularly clear for Zn substitutions for which the scaling is not valid

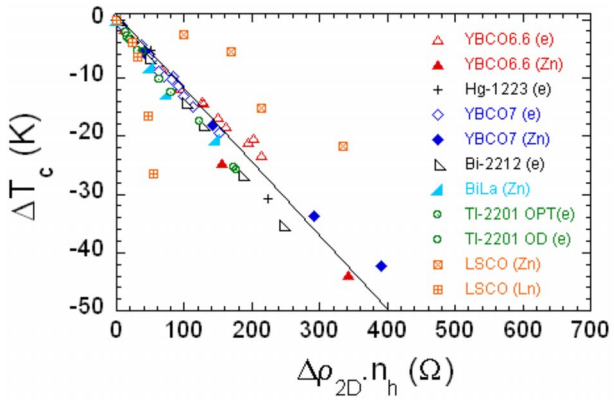

FIG. 30. (Color online) Decrease of T_c vs $n_h\Delta\rho_{2D}$ for various families of cuprates, for Zn impurities or electron irradiation defects. The universal relation which applies whatever the hole doping n_h, except for the LSCO family, establishes that the T_c depression is governed by the scattering rate τ^{-1} (Rullier-Albenque *et al.*, 2000).

even at optimal doping. Fractional homovalent substitution of Nd on the La sites at optimal doping also yields drastic reductions of T_c (Fujita *et al.*, 2005). But this specific system is well known to favor stripe ordering in the CuO_2 plane [the $La_{1.6}Nd_{0.40}$-substituted samples exhibiting a fully ordered stripe structure even at optimal doping (Tranquada *et al.*, 1997)]. So, quite generally, point defects appear to favor the existence of structural and/or electronic instabilities in LSCO, which may explain why this compound behaves differently from other HTSC materials.

There are several aspects of the observed T_c suppression that are currently poorly understood. At optimal doping, the measured initial suppression has been compared to Abrikosov-Gorkov (AG) pair-breaking theory and deviations explained by anisotropic scattering effects (Balatsky *et al.*, 2006) (see, however, Graser *et al.*, 2007). In electron irradiation experiments the concentration of metastable defects created is not limited by the equilibrium thermodynamics, which governs the solubility limits of impurities in a high-T solid-state synthesis. This allows one to follow the suppression of T_c until it vanishes, and the initial linear slope continues and eventually curves up, in contrast to the AG theory for which it would curve down (Rullier-Albenque *et al.*, 2003). This suggests the importance of including phase fluctuations when the superfluid stiffness becomes small.

Finally, we recall that, as emphasized in Sec. IV.B.1, the dopant and intrinsic structural disorders play a large role in controlling the actual observed T_c values in many "lower-T_c cuprate families" (Bobroff, Alloul, Mendels, *et al.*, 1997; Eisaki *et al.*, 2004; Fujita *et al.*, 2005). If the situation for in-plane disorder seems under experimental control, the influence of other types of disorders such as those discussed above in the case of LSCO are only qualitatively understood (Graser *et al.*, 2007). Quantifying the correlation between the decrease of T_c induced by various types of disorder, the associated residual resistivities, and other physical properties demands further

experimental studies, which requires overcoming difficult materials challenges.

c. Hall effect and thermoelectric power

Hall effect measurements have been extended to the overdoped and underdoped regimes (Abe *et al.*, 1999) and the analysis performed for optimal doping seems to apply as well, which highlights the existence of two scattering rates. However, quantitative comparisons between samples are even harder to perform than for the residual resistivity, so that the data did not allow the determination of the physical origin of the actual difference between the two scattering rates. Modifications of the specific heat induced by Zn or Ni substitutions has been investigated, but the normal-state electronic contributions of Zn or Ni could not be separated from the dominant phonon contribution (Loram *et al.*, 1990a; Mirza *et al.*, 1994). Tallon *et al.* (1995) found that the electronic thermoelectric power (TEP) is independent of Zn content at room temperature, which is an independent indication that hole doping is not modified, as the TEP value at room temperature is found to vary with hole doping in pure cuprates (Obertelli *et al.*, 1992).

3. Low-*T* upturns of the resistivity

Since the parent AF state of the cuprates is insulating, a generic phase diagram of the cuprates should display a MIT with decreasing hole or electron doping. Of course, the introduction of in-plane impurities in a metallic state of these 2D systems is also expected to yield a MIT associated with localization effects which should occur in any case if the residual resistivity exceeds the Mott-Ioffe-Regel limit. In both pure and substituted cuprates, low-T upturns of the resistivity as T is decreased have been observed and usually been associated with the occurrence of a MIT.

Due to the occurrence of the SC state, the most effective way to explore these effects is to suppress SC in large applied fields. It has, for instance, been found that LSCO exhibits at optimal doping a $-\ln T$ increase of ρ_{2D} in a 60 T applied field (Ando *et al.*, 1995). This was initially taken as an indication that the MIT already occurs for optimally doped cuprates, but it has been shown since that resistivity upturns only occur in the underdoped regime in BiLa-2201 (Ono *et al.*, 2000), suggesting that the location of the MIT is influenced by the intrinsic disorder of the family considered as shown by Rullier-Albenque, Alloul, Balakirev, *et al.* (2008).

In the cleanest cuprates such as $YBCO_{6.6}$ or Tl-2201, the influence of controlled defects on the conductivity can be studied more directly. The possibility of inducing a MIT by introducing enough Zn in the CuO_2 planes of YBCO was also noted in early experiments (Fukuzumi *et al.*, 1996). As shown in Fig. 29, resistivity upturns are also detected for electron irradiation defects. In the overdoped regime of Tl-2201, the upturns of ρ_{2D} only appear for large defect content, and the magnitude of the $-\ln T$ terms scale with n_d^2, as expected for weak localization contributions (Rullier-Albenque *et al.*, 2001), which probe coherence effects in multiple impurity scattering (Lee and Ramakrishnan, 1985), in good metallic Fermi liquids. Therefore these experiments are consistent with the expectation that the overdoped cuprates are good Fermi-liquid metals.

For Zn-substituted $YBCO_{6.6}$ the upturns of ρ_{2D} were also detected by partly suppressing SC with an applied field (Segawa and Ando, 1999) and it was concluded that they could not be attributed to weak localization effects. The data accuracy for electron irradiation defects in $YBCO_{6.6}$ allowed the detection of upturns in ρ_{2D} above T_c, even in zero field. A subtraction of the sample resistivity before irradiation allowed one to demonstrate that the resistivity upturns scale initially linearly with n_d so that these upturns are associated with single impurity scattering (Rullier-Albenque *et al.*, 2001). It is therefore tempting to correlate these experimental evidences with the Kondo-like behavior observed for the impurity induced magnetism.

If these resistivity upturns were solely explained in terms of spin-flip scattering, they should be suppressed by a field. However, prior to any conclusion on the normal-state properties in presence of impurities, one needs to ensure that SC is fully suppressed by the field. Indeed, a large SC fluctuation regime above T_c has been initially detected by Nernst and diamagnetic measurements (Wang *et al.*, 2006). In the presence of disorder, this regime has been shown to survive even after a large reduction of the 3D T_c (Rullier-Albenque *et al.*, 2006; Rullier-Albenque, Alloul, Balakirev, *et al.*, 2008), a fact which remains to be understood. This difficulty to separate out the various contributions to the normal-state scattering properties constitutes a serious complication when one studies the dilute impurity limit.

For instance, a positive "magnetoresitance" has been reported initially in Zn-substituted YBCO (Segawa and Ando, 1999). The survival of the SC fluctuation contribution to the conductivity which saturates only at large applied fields, could explain this behavior (Rullier-Albenque, Alloul, Proust, *et al.*, 2007). By contrast, in underdoped Zn-substituted BiLa-2201, for which T_c could be reduced to zero, a negative magnetoresistance has been detected (Hanaki *et al.*, 2001). Recent experiments for irradiation defects, where high fields suppress superconductivity, show evidence that the upturns saturate at low T (Rullier-Albenque, Alloul, Balakirev, *et al.*, 2008), also consistent with the Kondo analogy.

Theoretical arguments allowing us to establish the occurrence of the local moment and to reproduce at least partly the observed behavior are given in Sec. V. The arguments for and against this analogy with Kondo effect will be discussed there.

For increasing defect content $\rho_{2D}(T)$ becomes more singular than $-\ln T$ and diverges at low T, signalling a real MIT in which carrier localization occurs. Optical experiments on Zn-substituted cuprates reveal a reduction of the Drude contribution to the conductivity and the appearance of a high-frequency absorption mode for large Zn content which have been attributed to such

localized carriers (Basov *et al.*, 1998). However, this type of experiment does not give information on the length scale of these localized states.

E. Significance for normal-state physics

We have described the available experimental information on the influence of impurities on the magnetic and transport properties in the normal state of the cuprates. In this section we collect them and present the main conclusions which can be drawn from the qualitative aspects of the data. We focus on the implications for the physical properties of the pure system, and on the questions which arise then for the theory of this normal state.

1. What about the phase diagram?

We first return to the properties of the pure cuprates and summarize the implications of the impurity investigations on the phase diagram. In the low-doping range we have shown that the controlled disorder associated with impurity substitutions or irradiation defects affects the phase diagram and expands the SG regime. So in this range the phase diagram might be dependent as well on the existing intrinsic disorder in the lower-T_c cuprate families. On the other hand, the pseudogap crossover temperature T^* is unaffected by disorder, which explains why T^* is nearly identical for most families of cuprates whatever their optimum T_c (Williams *et al.*, 1997). However, we have recalled why the impurity experiments do not allow one so far to extrapolate the behavior of T^* at, and above, optimal doping.

The magnetic behavior of correlated systems with impurities changes abruptly near optimal doping (Fig. 25). It is then tempting to associate this evolution with a crossover line between the strange metal and correlated Fermi-liquid regimes. NMR experiments yield a characteristic energy scale Θ for the magnetic susceptibility which is associated with such a crossover. Θ increases as one overdopes the system and, for temperatures far below Θ/k_B, it appears that ξ_{imp} becomes T independent. Better experimental accuracy is required before a generic phase diagram can been drawn using the above criteria, but the overall trend of the data is not inconsistent with this picture. The fate of Θ in the highly overdoped limit when the system should evolve toward a standard Fermi liquid is still an open question.

2. Importance of electronic correlations

Another point that has been established is that, as in spin chains, a nonmagnetic impurity induces a local moment in its vicinity. This moment results from summing the staggered response of the near-neighbor Cu sites which extends over a distance that can be characterized by a single spatial length scale ξ_{imp}. This antiferromagnetically correlated object is not static but highly dynamic, and a macroscopic magnetization can only be detected in an applied field, or with a probe with a higher time resolution than the fluctuation rate of the correlated cloud. These isolated local moments cannot be detected by zero-field μSR experiments, which probe only static moments.

These observations of magnetic responses of a metallic state to a nonmagnetic impurity can only occur in (and are therefore indisputable evidence for) the presence of electronic correlations in the cuprates. Similarly, the large scattering cross section of conduction electrons by nonmagnetic impurities cannot occur in a simple broad *s-p* band. It results from the inability of the Cu_{3d}–O_{2p} hybridized quasiparticles to penetrate the Zn or Li sites which translates into an extended scattering potential caused by correlations. This effect is also completely driven by magnetic correlations in this narrow band.

Although the importance of magnetic correlations is revealed by some properties of the pure systems such as the peak of the dynamic susceptibility at the AF wave vector, these experiments on impurities allow one to better follow the evolution with hole doping of the magnetic correlations and to measure both the magnitude and the range ξ_{imp} of the induced staggered magnetization. In addition, they provide evidence that the correlated state is still present in optimal and lightly overdoped systems, although with a ξ_{imp} which only exceeds slightly the unit-cell length, and with a weak susceptibility.

Finally, static moments are seen only for large enough defect content, when interactions between moments pins a disordered spin-glass-like state at low T. Also, in the specific LSCO system for which the intrinsic order can yield the formation of stripes, impurities and stripe structures may interact and then yield frozen magnetic states. But such a situation is not encountered in cleaner cuprates.

3. Influence of the charge degrees of freedom on the magnetic effects

In regular metallic systems, such as noble metals, a charged impurity induces an oscillatory Friedel charge oscillation which constitutes the response of the system, and combines the screening of the charge and the associated spin-density oscillations. In cuprates, where spin and charge might be distinct degrees of freedom, one might imagine that different length scales would characterize the screening and the staggered magnetism. It is sometimes considered that charge depletion might occur in the vicinity of the Zn^{2+} with a corresponding increase of the magnetic correlation in this range. Conversely if Li^+ were to bind a hole on its NN oxygen sites, that would prevent a Zhang-Rice singlet from visiting the Cu sites' NN to Li^+ and would yield different magnetic effects on these sites than near Zn^{2+}. However, the absence of microscopic difference over several lattice spacings for Li^+ and Zn^{2+} is a strong evidence that such effects are unimportant, and that the spinless character of the impurities in the correlated host is the major per-

turbation which yields the appearance of a local moment.

The carrier scattering does not depend significantly on the impurity charge, as seen from the analogous T_c reductions by Li^+ and Zn^{2+}. Although the occurrence of superconductivity severely limits the analysis of the transport data, we have seen that the scattering by spinless impurities is not always unitary, but that the scattering cross section increases from the overdoped to the underdoped regime.

4. Quantitative information on the physical properties of the pure compounds

The length scale ξ_{imp} is a signature of the response of the system, which is weakly connected to the properties of the impurity itself, as even a magnetic Ni induces a staggered magnetism which has a similar spatial extent. However, the magnitude of the magnetic response depends on the nature of the perturbation. Then ξ_{imp} is likely related to the magnetic correlation length ξ of the pure cuprate, reflecting the $\mathbf{q}$ dependence of $\chi(\mathbf{q},\omega)$. In the spin-1 chains, the occurrence of a single degree of freedom (the spin) left no other alternative than $\xi_{imp}=\xi$, as confirmed by theory and experiment. As the impurity charge has little influence on ξ_{imp} in the cuprates, it is natural to consider that ξ_{imp} is at least a lower estimate of ξ.

The determination of ξ in pure cuprates has been a long-standing controversy. Inelastic neutron-scattering (INS) experiments reveal that peak widths of $\chi(\mathbf{q},\omega)$ at the AF wave vector $\mathbf{q}_{AF}$ are T independent and, if interpreted as a measure of ξ^{-1}, would correspond to $\xi \approx 2.5a$ and $\xi \approx a$, respectively, in the underdoped and optimally doped YBCO. In the slightly overdoped $YBCO_7$, no INS peak has been detected (Bourges 1998). However, the INS experimental $\mathbf{q}$ width might be broadened by incommensurability effects. Also, taking into account the actual band structure could yield a different shape of the $\mathbf{q}$ dependence of $\chi(\mathbf{q},\omega)$, thereby increasing the $\mathbf{q}$ width of the AF peak with respect to ξ^{-1} (Markiewicz, 2003, 2006). Another approach to determine ξ has been to analyze the longitudinal and transverse relaxation times T_1 and T_{2G} of the ^{63}Cu NMR within a phenomenological approach, assuming that $\chi(\mathbf{q},\omega)$ has a Lorentzian shape peaked at $\mathbf{q}_{AF}$ (Millis *et al.*, 1990). For $YBCO_7$ this analysis gives $\xi \approx 2a$ at room T, with a slight increase down to T_c. The extension of such a phenomenological analysis to underdoped compounds in presence of the pseudogap is inconclusive (Goto *et al.*, 2002).

In summary, the length scale $\xi_{imp}(T)$ deduced from impurity experiments agrees quantitatively with $\xi(T)$ obtained from the analysis of the T_1 and T_{2G} ^{63}Cu NMR data in the optimally doped compound, and is always *larger* than determinations done by INS experiments. This suggests that ξ_{imp}, which increases at low T, and in the pseudogap phase, might be the best estimate of ξ of the pure system.

We have also shown that the effect of impurity scattering on transport properties gives information on the properties of the pure material. For instance, the universality of the relation between ΔT_c and $\hbar/\tau$ induced by impurities can be taken as an evidence that the carrier density in the pure compound is indeed that of the doped holes. Furthermore, the Hall effect data in cuprates with impurity substitutions have allowed one to ascertain that two independent relaxation rates characterize the transport in these 2D electronic systems and that impurities contribute independently to both.

Impurity experiments have revealed many important aspects of these correlated magnetic systems, including the importance of the electronic correlations and magnetic effects in the perturbations induced by in-plane point defects in these systems. We have stressed the need to produce systems free of intrinsic disorder to avoid nongeneric conclusions about the phase diagram. The actual properties of the specific response to isolated spinless impurities have also been found to reveal quantities which are specific to the pure systems. Any theory aiming to describe the physical properties of the high-T_c superconductors should be able to explain the existence of the local moments induced by spinless defects, the residual resistivities associated with these, the magnitude of the correlation length ξ_{imp}, the energy scale Θ, and the occurrence of the Kondo-like behavior in magnetic and transport properties.

V. THEORIES OF IMPURITIES IN CORRELATED HOSTS

The theory of moment formation in uncorrelated metals was begun by Friedel (1958) and Anderson (1961), who pointed out that a sufficiently strong *local* Coulomb interaction U could effectively project out of the Hilbert space corresponding to a weakly hybridized atomic level the state with double (spin-up and spin-down) occupation. This leaves in the effective low-energy Hamiltonian for a metal with a single impurity an essentially localized spin-$\frac{1}{2}$ magnetic degree of freedom. The subsequent screening of this moment by the surrounding *noninteracting* electron gas as temperatures or energies are further reduced is a many-body phenomenon known as the Kondo effect, the subject of intense theoretical activity in the 1960s and 1970s. This has been reviewed by Hewson (1993).

While we will not discuss the Kondo problem in a noninteracting metal in detail here, it is important to note that the energy scales for the processes of magnetic moment formation and moment screening by the electron gas are typically different by orders of magnitude, and may be discussed independently. By contrast, the physics of vacancies and other impurity states in strongly interacting chains and ladders, as discussed in Sec. III, suggests that the two phenomena of "moment formation" (impurity-induced magnetization) and screening inevitably occur together, even for weak interactions in the 1D or quasi-1D host material. This naturally raises the question of the effect of a nominally nonmagnetic

potential in an interacting host in two or higher dimensions. In these cases, exact analytical methods available to treat the single-impurity Kondo problem, or nonmagnetic impurities in interacting chains or ladders, are not applicable. However, many have attempted to treat the homogeneous strongly correlated electron host system using the approximate methods from Sec. II, and subsequently added an impurity-type perturbation. In this section we identify the ingredients of a minimal tractable model which can be used to study the impurity in a correlated host.

A. Early results

Early interest in the problem of impurity-induced magnetic moments in interacting systems arose in the context of studies of transition metal alloys such as Pd:Ni. In the dilute Ni limit, the appropriate problem is to study a single Ni embedded in the nearly ferromagnetic Pd host metal. A good deal of progress was obtained using so-called "local paramagnon theories" (Lederer and Mills, 1968), in which the nearly magnetic host was treated within Stoner theory, whereby the uniform susceptibility was enhanced by $(1-U_0\rho_0)^{-1}$, where U_0 is the Hubbard interaction on Pd sites and ρ_0 is the bare density of d-band states at the pure Pd Fermi level. The Ni site is assumed to have its own, larger Hubbard interaction for doubly occupied sites, $U_0+\Delta U$, which is above the threshold to create a magnetic state according to the Stoner model. The spatial extent or character of the local magnetic state was not studied extensively, as the concern was primarily to account for bulk thermodynamic and transport properties.

Questions regarding interaction-induced magnetic moments arose again in studies of the metal-insulator transition in P-doped Si and similar systems (for a review, see Lee and Ramakrishnan, 1985). Scaling treatments of the disordered interacting metal (Finkel'shtein, 1983) near the transition included interactions effectively to all orders, but disorder only perturbatively, to leading order in $(\epsilon_F\tau)^{-1}$. Within such theories, the spin susceptibility was renormalized near the transition (Castellani *et al.*, 1986), suggesting the formation of clusters of magnetic moments with anomalously slow dynamics. This notion was confirmed generally by experiment (Paalanen *et al.*, 1986; Alloul and Dellouve, 1987), but results on the metallic side were consistent with a picture of weakly interacting diffusive quasiparticles and random local moments. First-principles theories of moment formation in such random systems were then investigated, in which interactions were treated perturbatively (Paalanen *et al.*, 1988; Milovanović *et al.*, 1989; Sachdev, 1989), and disorder treated exactly, within numerical finite-size studies. A Hartree-Fock factorization of the interaction term, equivalent to that performed by Anderson (1961) for the single-impurity model, leads to an effective single-particle problem with random hopping. For sufficiently large on-site Coulomb interaction U, it was found that some magnetic susceptibility eigenvalues turned negative, signaling an instability toward local moment formation. Lakner *et al.* (1994) then pointed out that qualitatively similar results could be obtained by studying the isolated scattering potential in an otherwise homogeneous interacting medium. These early works on the Si:P problem were also not concerned with the details of the magnetic state thereby created.

B. Weak-coupling approaches

In these early studies, correlations in the host material were modeled with a Hubbard Hamiltonian [Eq. (1)], and moment formation was found to be enhanced with increasing repulsive U. The basic physics can be obtained via the usual mean-field factorization:

$$H = -\sum_{i,j,\sigma} t_{ij} c_{i\sigma}^{\dagger} c_{j\sigma} + \sum_{i,\sigma} (U n_{i\bar{\sigma}} + \epsilon_\sigma \delta_{i_m,i} - \mu) c_{i\sigma}^{\dagger} c_{i\sigma}, \quad (33)$$

where ϵ_σ is the on-site impurity strength, i_m is the impurity site, μ is the chemical potential, and $n_{i\sigma} \equiv \langle c_{i\sigma}^{\dagger} c_{i\sigma} \rangle$. The local magnetization in this decoupling where spin rotation invariance has been explicitly broken is $M_i = \langle c_{i\uparrow}^{\dagger} c_{i\uparrow} - c_{i\downarrow}^{\dagger} c_{i\downarrow} \rangle$. If the impurity potential on site i_m is proportional to the local occupation of opposite spin $\bar{\sigma}$, $\epsilon_\sigma = \epsilon n_{i\bar{\sigma}}$, this model is identical to the local paramagnon models at the mean-field level, and can be used to describe a magnetic impurity. On the other hand, if $\epsilon_\sigma = \epsilon$ independent of spin, the model describes a short-ranged screened Coulomb potential which may be more appropriate for an impurity like Zn, which has a closed shell. This latter case manifests no magnetic moment in zero applied magnetic field if U is below the critical value for long-ranged "background" antiferromagnetic order, consistent with the experiments described in Sec. IV. This is the approach adopted by Bulut (2000, 2001) and Ohashi (2001, 2002) to model Zn impurities, and which we outline here. Note also that Bulut analyzed Hamiltonian (33) for t_{ij} limited to nearest-neighbor hoppings, while Ohashi included next-nearest-neighbor hoppings.

The goal of such calculations is to calculate the spin susceptibility $\chi(\mathbf{q}=\mathbf{0},\mathbf{R})$ which determines the response of the *inhomogeneous* system in the presence of the impurity to an applied homogeneous magnetic field, and compare its temperature dependence to that of experiment [here the Fourier transform is with respect to the relative electron coordinate $\mathbf{r}-\mathbf{r}'$, leaving the dependence on the center-of-mass coordinate $\mathbf{R}=(\mathbf{r}+\mathbf{r}')/2$]. Once this quantity is known, the Knight-shift and, in principle, the distribution of local fields around the impurity as probed by NMR can be obtained. The physical idea is that the metallic state in which the impurity is embedded manifests strong but noncritical antiferromagnetic spin correlations maximized near $\mathbf{q}=(\pi,\pi)$, which are enhanced locally by the impurity. The related problem at criticality was studied by Millis *et al.* (2001).

The impurity potential couples the enhanced response of the system at (π,π) and that near $\mathbf{q}=\mathbf{0}$ which is then

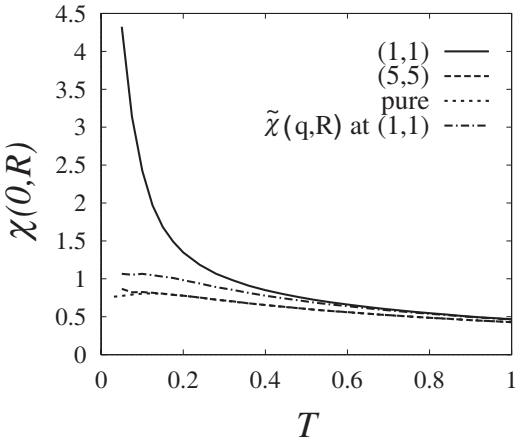

FIG. 31. Temperature dependence of magnetic susceptibility in the RPA at $\mathbf{q}=\mathbf{0}$ for different sites $\mathbf{R}$ in the presence of a strong scattering potential $V_1=100t$ at (0,0) and a weaker one $V_2=10t$ on nearest-neighbor sites. $\tilde{\chi}$ is a weighted average of χ to account for the fact that $\mathbf{R}$ may coincide with a lattice site, the center of a bond, or of a plaquette. $\tilde{\chi}(\mathbf{q}',\mathbf{R}')$ is the same quantity neglecting the mode-mode coupling effect described in the text. From Ohashi, 2001.

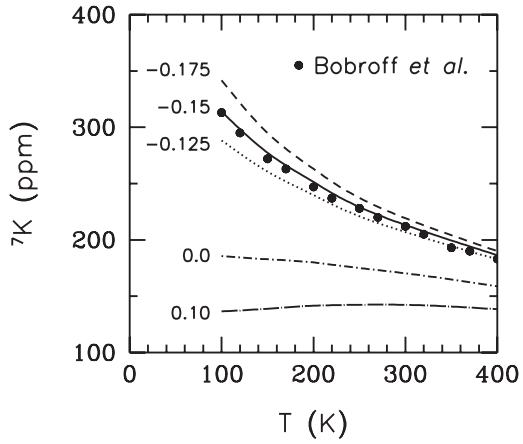

FIG. 32. Temperature dependence of Knight shift (Bobroff *et al.*, 1999) for Li impurities in YBCO within the RPA approach in the presence of a strong potential at $V_1=-100t$ at (0,0) and a weaker one on nearest-neighbor sites of strength given. From Bulut, 2001.

measured in the NMR experiment. This can be seen by examining the susceptibility determined within the random-phase approximation (RPA),

$$\chi(\mathbf{r},\mathbf{r}') = \chi_0(\mathbf{r},\mathbf{r}') + U\sum_{\mathbf{r}''} \chi_0(\mathbf{r},\mathbf{r}'')\chi(\mathbf{r}'',\mathbf{r}'), \tag{34}$$

where χ_0 is the susceptibility determined in the noninteracting system $U=0$, given by the noninteracting Green's function $G_0(\mathbf{r},\mathbf{r}')$ in the presence of a single short-range impurity described by a single-impurity T matrix. In the homogeneous case $\chi(\mathbf{r},\mathbf{r}')=\chi(\mathbf{r}-\mathbf{r}')$, the result in Fourier space is $\chi(\mathbf{q})=\chi_0(\mathbf{q})[1-U\chi_0(\mathbf{q})]^{-1}$, i.e., all momentum components are decoupled. On the other hand, in the general case (34), Fourier transforming with respect to the relative coordinate cannot disentangle the various momentum components, leading to a general integral equation relating $\chi(\mathbf{q},\mathbf{R})$ to $\chi(\mathbf{q}',\mathbf{R}')$. Similar results for the numerical evaluation of these equations were obtained by Bulut (2000, 2001) and Ohashi (2001, 2002), and are plotted in Fig. 31 as a function of temperature. While the enhancements at $\mathbf{q}=\mathbf{0}$ are smaller than at (π,π) as expected, they are significant at low temperatures and appear to follow a $\sim 1/T$ form down to the lowest temperatures on the next-nearest-neighbor sites (1,1) when the extended impurity potential on the nearest-neighbor sites is large. For smaller nearest-neighbor potential, the enhancement at $\mathbf{q}=\mathbf{0}$ weakens. At intermediate values of the extended potential strength, the susceptibility T dependence resembles the experimental NMR results discussed in Sec. IV where in the metallic phase this temperature dependence is found to follow a behavior $\chi\sim(T+\Theta)^{-1}$. Note that the mean-field form of the Hamiltonian solved, whereby the spin rotation invariance is explicitly broken, precludes these theoretical results originating from Kondo-type physics. Indeed, to describe Kondo physics one needs to allow spin-flip processes yielding transitions between the two spin eigenstates locally, and these large-amplitude fluctuations are not included within RPA.

Using an essentially identical formalism, Bulut explicitly fit the Knight-shift data on Li and Zn impurities in optimally doped YBCO samples (Bulut, 2001). In his work, however, the potential on nearest-neighbor sites is taken to be attractive, leading to a magnetic moment residing primarily on these sites. Hyperfine parameters, band parameters, and the Coulomb repulsion U were chosen from fits to NMR data on the pure system. In Fig. 32 we reproduce the Knight-shift data of Bobroff *et al.* (1999) on Li together with Bulut's calculation. It is interesting to note that similar quality fits to data on a different impurity, Zn, were obtained with nearly identical values of the nearest-neighbor impurity potential, suggesting a universality of the magnetic response to spinless in-plane defects as discussed in Sec. IV. The same model also reproduces the staggered magnetization pattern seen by experiment on sites near the impurity (although a quantitative comparison was not attempted).

The physical meaning of the nearest-neighbor potential which appears to explain the impurity-induced enhanced magnetic correlations is not completely transparent. Band calculations, in fact, suggest that such impurity potentials have a range of 1 Å or less (Wang *et al.*, 2005). This term may therefore play the phenomenological role of a different impurity-induced correlation effect in a more complete theory. The on-site impurity potential breaks translational invariance, such that the response to a uniform magnetic field contains a contribution related to the staggered susceptibility of the pure system. This quantity is quite large, but its weight in $\mathbf{q}$ space is small. Adding a nearest-neighbor potential V_2 boosts the weight at the antiferromagnetic momentum. In addition, Monte Carlo calculations (Bulut, 2003) begin with an on-site potential only, and find that an effective

nearest-neighbor potential of roughly the right order to fit the Knight-shift data in the RPA approach is dynamically generated. This phenomenon of creating dynamical extended potentials by nonmagnetic pointlike perturbations in the presence of Coulomb correlations had been pointed out earlier (Poilblanc *et al.*, 1994a) and discussed in the weak-coupling context (Ziegler, Poilblanc, *et al.*, 1996). A similarly enhanced range of the effective impurity potential due to renormalized electron-phonon coupling was predicted by Kulic and Oudovenko (1997). So in this sense, a vacancy or strong potential in a Hubbard model may provide a minimal model to describe a Cu substituent in the CuO_2 plane of cuprates around optimal doping, if the extended effective potential is generated systematically. However, the RPA theory given by Ohashi and Bulut requires a phenomenological finite range potential. Furthermore, it is not systematically extendable to the underdoped side of the phase diagram, although plausible results can be obtained by putting in the pseudogap in an *ad hoc* way (Bulut, 2001).

C. Strong-coupling approaches

The transition to the Mott antiferromagnet at low doping in the cuprates can be described theoretically only with models which invoke local Coulomb interactions in the strong-coupling limit. The problem of a nonmagnetic defect in a correlated system was first proposed in the cuprate context by Finkelstein *et al.* (1990) to account for the depression of superconductivity in La-based compounds (see the next section). For the normal-state case, Poilblanc *et al.* (1994a, 1994b) were the first to calculate the electronic structure of the *t-J* model [Eq. (2)] when a single spin was frozen, i.e., all exchange couplings and hoppings connected to a given site 0 on a square lattice were removed. They found that the rest of the system had a net magnetic moment corresponding to net spin $\frac{1}{2}$ distributed over sites near the impurity. A hole added to the system was found to bind to the impurity site in one of four symmetry channels *s*, $p_{x,y}$, and *d* corresponding to the irreducible representations of the tetragonal group. These bound states occurred for couplings above a critical value of *J* of order $\sim 0.1t$, and it was speculated that for a thermodynamically finite density of holes the critical exchange would be enhanced due to the additional allowed decay channels for the bound states. Further-finite size numerical calculations on *t-J* impurities using Hubbard operator techniques (Odashima and Matsumoto, 1997; Odashima *et al.*, 2000) showed the weakening of bound states at finite doping, but did not investigate the transition to spontaneous local magnetization.

While the numerical calculations of Poilblanc *et al.* (1994a, 1994b) indicated a tendency to spontaneous moment formation around a nonmagnetic potential in a strongly correlated host, they left open many questions regarding the physical origin of the phenomenon, as well as its dependence on doping and correlation strength. Along with the experiments on Zn-doped cuprates reviewed in Sec. IV, this stimulated interest in the search for tractable analytical approaches to the problem. It is worth recalling that there are many schemes to obtain results of the strong-coupling regime in two dimensions, none of which are fully controlled. Gabay (1994) studied the doping dependence of an impurity moment in a slave-boson approach to the *t-J* model, as discussed in Sec. II, and related the size of the moment associated with Zn in different cuprate materials and for different dopings to the screening length of the spinon fields, particularly in the spin gap phase. He also predicted a local destructive effect of the impurity-induced magnetism on the spin-gap itself. Nagaosa and Ng (1995) considered an impurity in a π-flux phase of the Heisenberg model using a slave-boson representation and predicted the existence of a spin-$\frac{1}{2}$ bound state. Similar results were obtained using a slave-fermion representation. These authors noted explicitly the analogy with 1D end-chain defects, and pointed out that although the effective potential for the spin was weaker in two dimensions, a Curie-Weiss term in the susceptibility would be the likely result.

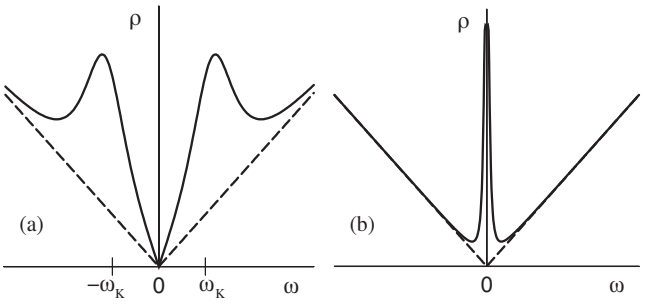

FIG. 33. Schematic plot of spinon density of states for (a) spin-1 impurity; (b) spin-0 impurity in model of Kilian *et al.* (1999). Dashed line, density of states for pure flux phase. Solid line, density of states with impurity.

Khaliullin *et al.* (1997) and Kilian *et al.* (1999) produced calculations which resulted in specific analytical predictions for impurity properties in the spin-gap state. The spin-gap or pseudogap homogeneous state was modeled by a "drone" fermion (Khaliullin *et al.*, 1997) or more conventional slave-boson approach (Kilian *et al.*, 1999) which yielded similar results. In both cases auxiliary bond field phases were chosen within a homogeneous mean-field description to give a linear "pseudogap" in the spinon sector of the theory, with density of states $\rho^0(\omega) = |\omega|/D^2$, where *D* is the spinon half bandwidth; see Fig. 33(b). Formally, this choice of mean-field parameters corresponds to the flux phase of Affleck and Marston (1988). To model a nonmagnetic impurity in the pseudogap state, a site is removed from the system by means of a local potential term $\lambda_0 f_0^\dagger f_0$, with $\lambda_0 \to \infty$, and calculation of the impurity *T* matrix then yields a spinon bound state at zero energy $\rho_{\mathrm{imp}}(\omega) = \delta(\omega)$. The local susceptibility due to the bound state varies as

$$\delta\chi(\mathbf{R},T) = \frac{1}{2\pi}\frac{\phi(\mathbf{R})}{R^2}\frac{1}{T\ln(D/T)}, \tag{35}$$

where the phase factor $\Phi(\mathbf{R})$ gives the spatial dependence of the spin polarization in a magnetic field,

$$\Phi(\mathbf{R}) = \tfrac{1}{4}|\tilde{R}^{+}e^{i\pi R^{+}/2} + \tilde{R}^{-}e^{i\pi R^{-}/2}|^2, \tag{36}$$

with $R^{\pm}=R_x+R_y$ and $\tilde{R}^{\pm}=(R_x\pm iR_y)/R$. This is a staggered pattern of spins on one sublattice only, in contradiction with the results of the weak-coupling calculations described above. It was considered by Kilian *et al.* (1999) as an artifact of the mean-field theory which underestimates long-range antiferromagnetic correlations, as evidenced by the fact that the antiferromagnetic correlation length is absent from the Eq. (35). To improve the accuracy of the calculation and include these effects, a phenomenological RPA summation was performed along the lines of Morr *et al.* (1998), $\tilde{\chi}(\mathbf{q})=\chi^0(\mathbf{q})/[1+J_{\mathbf{q}}\chi^0(\mathbf{q})]$, where χ_0 is the homogeneous susceptibility and $J_{\mathbf{q}}=2J(\cos q_x+\cos q_y)$, as in the theory of the nearly antiferromagnetic Fermi liquid (NAFL) (Monthoux and Pines, 1994). For the inhomogeneous susceptibility, approximate analytical expressions can be obtained for the long-distance behavior,

$$\delta\tilde{\chi}(\mathbf{R},T) \simeq -\cos(\mathbf{Q}\cdot\mathbf{R})\frac{1}{8\pi}\frac{1}{R^2}\frac{\xi(T)^2}{T\ln(D/T)}, \tag{37}$$

where $\mathbf{Q}=(\pi,\pi)$, and $\xi(T)\equiv\{J\chi_0(\mathbf{Q},T)/[1-4J\chi_0(\mathbf{Q},T)]\}^{-1/2}$ is the NAFL antiferromagnetic correlation length for the pure system. The final result, Eq. (37), shows the commensurate staggered behavior of the moment as well as the $(T\ln T)^{-1}$ divergence of the susceptiblity, reflecting the marginal bound state found in the mean-field theory.

Kilian *et al.* (1999) compared their results with data from Bobroff, Alloul, Yoshinori, *et al.* (1997) on underdoped YBCO, and concluded that a good fit could be obtained if the temperature dependence of the correlation length in Eq. (37) was assumed to follow $\xi(T)\sim 1/(a+bT)$, with a and b adjustable parameters. With these parameters fixed, the theory can account for the broadening of the NMR line with increasing Zn concentration. It is seen that, while not all parameters could be computed directly from microscopic theory, a physically reasonable picture of the impurity in the pseudogap state is ultimately obtained. It should be noted, however, that the spatial decay of the local susceptibility as one moves away from the impurity has a different functional form in Ouazi *et al.* (2004) compared with Eq. (37). Indeed, NMR line shapes cannot be accounted for by using R^{-2} or R^{-3} spatial dependences for $\delta\tilde{\chi}$.

The strong-coupling approaches discussed above assumed the existence of a pseudogap in the one-particle density of states, which is required for the formation of the spinon bound state. One would therefore expect the singular magnetic response to disappear when the pseudogap does; indeed, this is consistent with the fact that no static moment is observed in zero-field experiments on clean optimally doped cuprates and that the field induced magnetic response is not a simple Curie $(1/T)$ form (see Sec. IV). However, a theory of this type should describe the field-induced paramagnetic moments observed by NMR experiments in the metallic state on an equal footing. This was accomplished by Gabay *et al.* (2008), who considered the optimally doped state of cuprates within a t-t'-J model [Eq. (8)]; the strong impurity potential implies a site from which spinons and holons are forbidden. The Hamiltonian was treated in a slave-boson mean-field approach, following Ubbens and Lee (1992). This model remains metallic at low T and is thus suitable for the study of the normal state. One introduces the local order parameters

$$\langle f^{\dagger}_{i\sigma}f_{j\sigma}\rangle = \chi^{\sigma}_{ij},$$

$$\langle b^{\dagger}_{j}b_{i}\rangle = Q_{ij},$$

$$\langle f^{\dagger}_{i\uparrow}f_{i\uparrow} - f^{\dagger}_{i\downarrow}f_{i\downarrow}\rangle = m_i, \tag{38}$$

where f_i and b_i create spinon and holon fields, respectively, and i,j are nearest neighbors. Within such a theory, the spinon bandwidth $t_f^{ij}=tQ_{ij}+(J/2)\chi_{ij}$ is suppressed close to half filling $\delta\to 0$. When the effect of the impurity is accounted for, the bandwidth is found to decrease locally as well, as shown in Fig. 34(c). Such effects are important for a quantitative treatment of local correlations and electronic structure around the impurity, and are missed in the weak-coupling approaches discussed above. A semianalytic solution of the mean-field equations reveals that the local decrease of the spinon bandwidth in the vicinity of the impurity has two effects. One is to produce an extended scattering potential which enhances the staggered Fourier component of the local magnetizations m_i. The other is to increase the magnetic response, since—in a Stoner-like picture—a larger value of $J/t_f(i)$ brings the system locally closer to a magnetic phase. In order to treat correctly the nondouble-occupancy constraint for the holons and spinons, a numerical solution of the mean-field equations is required (Gabay *et al.*, 2008). It yields results for both the spatial decay of the staggered magnetization induced in a field and the temperature dependence, which is found to correspond to a Curie-Weiss law similar to that found in experiment on overdoped samples. The results displayed in Fig. 34 are in reasonable agreement with their experimental counterparts, shown in Figs. 25 and 26. It is intriguing that the results of the slave-boson mean-field theory for the strong-coupling t-t'-J model in the spin-liquid state (optimally doped case) are qualitatively similar to the weak-coupling results in Sec. V.B. This suggests that for the optimally doped materials a Fermi-liquid approach captures the essential details of the physics. On the other hand, in the strong-coupling case there is no analog for the requirement of an extended bare impurity potential to fit experimental data as found by Bulut (2000) and Ohashi (2001). This may reflect the failure of the weak-coupling approaches to treat the renormalized band structure in the vicinity of the impurity, e.g., the spinon bandwidth shown in Fig. 34. At

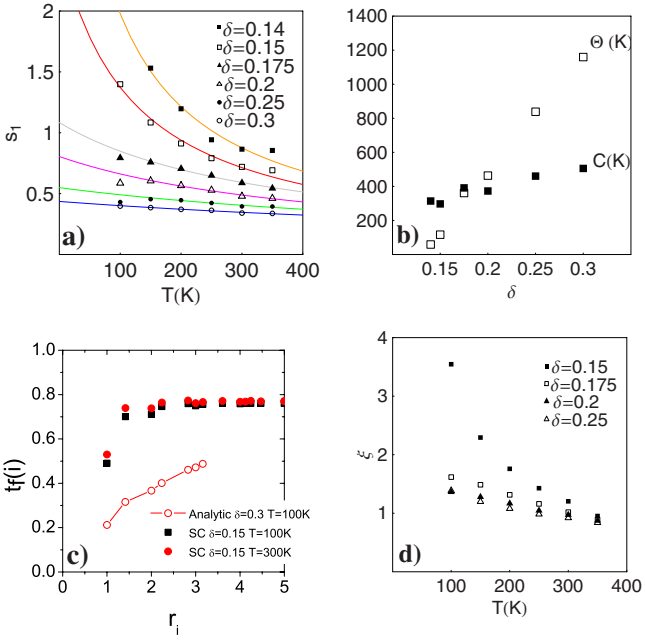

FIG. 34. (Color online) Results for fully self-consistent evaluation of magnetization from slave-boson equations (Gabay *et al.*, 2008). (a) Normalized magnetization s_1 on nearest-neighbor site as function of T for values of doping δ from 0.14 to 0.30. Solid lines show fits to $s_1=C/(T+\Theta)$. (b) Effective moment constant C (filled squares) and Curie-Weiss constant Θ (open squares) extracted from fits in (a) vs δ. (c) Spinon bandwidth in fully self-consistent evaluation as a function of distance from the impurity site at filling $\delta=0.15$ and $T=100$ K (filled squares) and 300 K (filled circles). Bandwidth from semianalytic calculation at $\delta=0.3$ and 100 K is shown (open circles) for comparison. (d) Temperature dependence of extracted theoretical correlation lengths ξ vs T (compare Fig. 26).

present, no microscopic approach to the problem of an impurity in a correlated host has been able to reproduce systematically the crossover between underdoped and optimally doped regimes observed in the cuprates and described in Sec. IV. In principle, slave-boson and similar renormalized mean-field theories are a promising avenue to pursue. In addition, a phenomenological approach by Prelovšek and Sega (2004) has suggested a way to parametrize this crossover in terms of the doping dependent correlation length ξ of the pure system. They showed that a crossover between the Curie and Curie-Weiss behavior of the local susceptibility observed in experiments as the system is doped is to be expected generically in a homogeneous doped antiferromagnet. They made the ansatz that the impurity suppresses only the spin correlations $\langle S_0^z S_j^z\rangle$ involving the impurity site 0, with all others taken to correspond to the pure system. While this seems to contradict other microscopic analyses discussed above, the results resemble experiments qualitatively and suggest that the pure ξ determines the T dependence of the system.

D. Magnetic impurities in correlated systems

One attractive feature of the Kilian *et al.* (1999) approach is that it accounts naturally for differences observed between Zn and Ni substitutions for Cu in underdoped YBCO. In Fig. 35 we show a schematic picture of a RVB-type singlet state in the presence of an impurity of various types. In the case of a nonmagnetic impurity like Zn, a spin singlet is broken while a spin $\frac{1}{2}$ is freed from a given singlet bond. By contrast, if one models the Ni perturbation as a spin-1 object, the spin $\frac{1}{2}$ on the Cu site nearest the impurity screens the Ni spin, leading to a free spin-$\frac{1}{2}$ degree of freedom. This picture is analogous to that established for impurities in 1D spin chains in Sec. III. Of course, as we have seen, more detailed calculations lead to the "free" spin-$\frac{1}{2}$ spread out over a healing length in both cases. To model a Ni spin $\mathbf{S}_0$ of magnitude 1 coupled to the surrounding Cu spins $\frac{1}{2}$, Kilian *et al.* (1999) added an impurity potential consisting of nearest-neighbor exchanges with the impurity $H_{imp}=J'\Sigma_\delta \mathbf{S}_0\cdot\sigma_\delta$ to the system. The spin 1 is decomposed as $\mathbf{S}_0=\mathbf{S}_a+\mathbf{S}_b$, where $\mathbf{S}_{a,b}$ are spin-$\frac{1}{2}$ operators, and the spin-1 algebra is retained by adding a ferromagnetic exchange term $-J_c\mathbf{S}_a\cdot\mathbf{S}_b$ to the Hamiltonian, then allowing $J_c\to\infty$. This gives

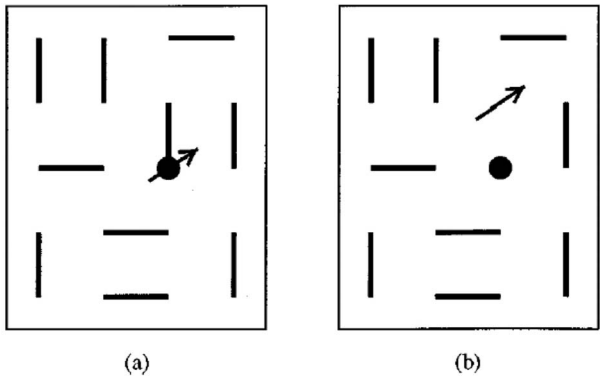

FIG. 35. Schematic picture of spin-$\frac{1}{2}$ impurity produced in case of (a) Ni and (b) Zn.

$$H_{\rm imp}=-\sum_{\delta\sigma}(\Delta'_\delta f^\dagger_{0\alpha}f_{\delta\alpha}+\text{H.c.})-J_c\mathbf{S}_{\rm eff}\sigma_0, \tag{39}$$

where $\Delta'_\delta=J'\Sigma_\sigma\langle f^\dagger_{\delta\alpha}f_{0\alpha}\rangle$ is the local flux phase amplitude on bonds near the impurity, $\mathbf{S}_{\rm eff}$ is a localized spin-$\frac{1}{2}$ operator, and σ_0 is the spinon spin density on site 0. Thus this case reduces to an impurity which locally renormalizes the spinon bandwidth and adds a local exchange with a free spin $\frac{1}{2}$ in a fermionic bath with pseudogap. Note that such a treatment neglects the transverse spin fluctuations which lead to the Kondo effect. Nevertheless, the pole in the T matrix is found to have a resonance in the pseudogap at finite energy $\omega_K=(\pi/4)J'/\ln(D/J')$, leading to a contribution to the density of states

$$\delta\rho(\omega) = \frac{1}{2}\frac{\omega_K^2}{\ln D/\omega_K}\frac{|\omega|}{(\omega^2-\omega_K^2)^2+[\pi\omega_K^2/4\ln D/\omega_K]^2}, \tag{40}$$

whose form is shown schematically in Fig. 33(a). The impurity susceptibility after performing the identical RPA analysis as above is

$$\delta\tilde{\chi}(\mathbf{R},T) \simeq \frac{J_c(0)J}{J'^2}\cos(\mathbf{Q}\cdot\mathbf{R})\frac{3}{64\pi}\frac{1}{R^3}\frac{\xi(T)^2}{T}, \tag{41}$$

where $J_c(0)$ interpolates between D for $J'=J$ and $2\omega_K$ for $J' \ll J$. This expression is similar to the nonmagnetic case (37), but decays more rapidly, as $\sim 1/R^3$, and has a more singular $1/T$ dependence. The reduction of both spin-0 and spin-1 impurity models to Hamiltonians with effective localized spin-$\frac{1}{2}$ exchange terms raises the question of the fate of the Kondo effect, the screening of a single localized spin exchange coupled to a free Fermi gas, as electronic correlations increase. This effect was neglected in the mean-field treatments above. The question was studied first by Fulde and co-workers (Schork and Fulde, 1994; Khaliullin and Fulde, 1995). These authors began with the slave-boson mean-field theory of Read and Newns (1983) for the Anderson impurity model, which is known, in the noninteracting case, to correctly reproduce the low-temperature Kondo resonance in the f-electron density of states at the correct scale T_K. Perturbative corrections in the Hubbard U were then found to renormalize the various Read-Newns parameters, including the Kondo scale T_K:

$$\tilde{T}_K/T_K = \exp\{[\alpha/\rho_0 J(1+\alpha)]\}, \tag{42}$$

where $\alpha=(3/2)\ln 2U\rho_0$, J is the exchange of the Anderson impurity with the conduction electrons in the Kondo limit, and ρ_0 is the density of conduction electron states at the Fermi level. Thus, for the usual repulsive-U case the Kondo scale is enhanced due to the suppression of the charge degrees of freedom. Similar conclusions were reached by Hofstetter *et al.* (2000) in a more sophisticated calculation combining dynamical mean-field theory with numerical renormalization-group methods. In addition to the effects of interactions on impurity properties, there are interaction-dependent renormalizations of conduction electron properties by the Kondo impurity which are predicted to be visible in thermodynamics. (Neef *et al.*, 2003).

E. Transport

There is currently little theoretical work attempting to explain the apparent close relation between the disorder-induced magnetic properties of cuprate systems and transport properties, e.g., the resistivity "upturns" at low T observed in cuprate materials when they become disordered or are subjected to high fields. Based on the general properties of gauge theory descriptions of the HTSC phase diagram, Nagaosa and Lee (1997) attempted to understand the residual resistivity measurements of Fukuzumi *et al.* (1996) in terms of a Boltzmann transport description with assumed unitarity limit scatterers and carrier concentration proportional to hole doping n_h in the underdoped cuprates, crossing over to $1-n_h$ for optimal doping. Some criticisms of this picture were mentioned in Sec. IV. Kontani and Ohno (2006) calculated the local susceptibilities in a Hubbard model with strong impurities within fluctuation-exchange (FLEX) -type approximations, and fed the resulting self-energies and vertex functions into a disorder-averaged transport calculation. The enhanced scattering due to the creation of local moments led in some cases to upturns in the residual resistivity at low temperatures similar to those seen in experiments. While some details do not correspond to observation (upturns in YBCO were found to be stronger than in LSCO, for example), this is a promising step allowing one possibly to approach the "metal-insulator transition" from the metallic side.

F. Two dimensions vs one dimension

Since there is to date no consensus on a theoretical description of the homogeneous system in the strongly correlated limit, further insight into the 2D case may be gained by considering the 1D situation. The literature devoted to the study of impurities in doped 1D systems is significant, but we discuss here only a small number of results directly relevant to the 2D case. In one dimension, a weak link, i.e., a slight local modification of the kinetic energy and of the magnetic coupling or a weak potential modeling a charge imbalance, renormalizes to a large perturbation as the temperature is reduced, in the case of repulsive interactions. As $T \to 0$, the transmission in the spin and charge channels approaches zero (Kane and Fisher, 1992a, 1992b; Furusaki and Nagaosa, 1993). Applying a uniform magnetic field H yields a local alternating magnetic polarization with an amplitude proportional to H and a spatial extension generically of the order of the correlation length of the pure system. The crossover between the weak- and strong-perturbation regimes is frequently described in Kondo language, and the characteristic temperature T_K depends exponentially on the difference between the kinetic (or potential or coupling) energy of the pure system and that of the modified link (Rommer and Eggert, 1999, 2000).

The impact of the impurity on transport and magnetism can be considered separately, because of spin-charge separation at low energies, but, in both channels backscattering is very strong at low temperature. The Luttinger-liquid parameter K varies from $\frac{1}{2}$ to 1 as the hole doping increases, showing a reduction of the enhancement of the staggered polarization as one moves toward the Fermi-liquid limit. A similar behavior is observed in numerical studies of ladder systems (White *et al.*, 2002). Calculations of transport properties also produce low-T upturns in the resistivity which reflect the pinning of charge-density waves by impurities; see, for instance, Giamarchi (2004), Chap. 9.

G. Summary

At this stage, we interpret some results described in Sec. IV in the framework of the theoretical models. Experiments reveal that a spinless impurity introduced in a correlated host produces in its vicinity a large and spatially extended alternating magnetic polarization, similar to one dimension. On the basis of NMR and μSR spectra it has been demonstrated that this magnetization is not associated with a static moment. The maximum amplitude of the staggered polarization is of the form $CH/(T+\Theta)$, where C is a constant and the extension $\xi_{\rm imp}$ of this polarization away from the defect follows a similar T dependence. For a fixed T, the (spatial) extent of the staggered state increases as one underdopes the system ($\Theta \rightarrow 0$). A finite density of impurities produces a magnetization which scales linearly with the concentration. Moving to the optimally doped and, beyond, to the overdoped regime, both the amplitude of the alternating polarization and its spatial extent decrease, bringing these gradually back in line with values expected for a Fermi-liquid metal.

Furthermore, both NMR spin lattice relaxation and inelastic neutron-scattering data suggest that this entity should be viewed in the optimally doped case as a resonant state rather than a free moment. By this we mean that, in zero field, the total spin of the system in the ground state is $S=0$ rather than $S=1/2$. The fluctuation rate $h/\tau \approx k_B\Theta$ corresponds to about 100 K or 10 meV.

For a wide range of hole dopings, the transport scattering rate in CuO_2 materials displays a $-\ln T$ upturn at low T. In the overdoped case, this behavior is explained by weak localization effects in a good metallic system. In the underdoped case, the upturns are much larger than predicted by weak localization theory, and may be due to impurity induced magnetism.

The above features are suggestive of Kondo physics, with the picture of a screened moment formed around a nonmagnetic impurity. However, as shown a number of these magnetic and transport signatures are qualitatively captured by the theoretical models reviewed here which ignore processes leading to Kondo screening. Typically, the impurity is represented as a strong or infinite nonmagnetic potential, which creates a nearby cloud of staggered polarization and net paramagnetic moment by coupling the system's antiferromagnetic correlations to a homogeneous external magnetic field. The universal magnetic response of any impurity substituting for Cu in the CuO_2 plane found by NMR is strong evidence in favor of such models. Remarkably, treatments which start either from a weak-coupled Fermi liquid or from a strong-coupling description of the host are able to reproduce the key features seen in experiments; the characteristic energy Θ, the temperature dependence of the Knight shift, the resonant nature of the staggered magnetic polarization, and general trends in the observed doping dependence are obtained roughly correctly. Weak-coupling approaches have been mostly devoted to the study of the optimally doped regime; they appear to require tuning the Hubbard U to a value close to an AF instabilility and using extended impurity potentials. In the strong-coupling limit, mean-field approximations give a qualitatively correct carrier doping dependence for Θ (and for C, which changes only slightly with the hole content). A current drawback, however, is the inability of any single model to span the entire cuprate phase diagram and make predictions for the full doping dependence of the response.

Further considerations suggest caution against taking the Kondo analogy too literally. In the Kondo-Anderson picture there are two energy scales. The upper one is related to the formation of the local spin, i.e., to a (local) bound state, and the lower is related to the screening of the moment by conduction electrons. In cuprates, moment formation and screening are driven by the same set of conduction electrons. Furthermore, it is unclear how different an extended itinerant staggered magnetization cloud with a net moment—which is obtained when a nonmagnetic impurity is introduced in a correlated system—is from the single localized impurity spin $\frac{1}{2}$ that forms at high energies, in the Kondo case. In the Kondo scenario of a magnetic impurity in a noble metal host, the characteristic energy scale is set by the carrier density and the exchange interaction through $\Theta \sim J \exp\{-[J\rho(E_F)]^{-1}\}$. For underdoped cuprates, the nonsuperconducting regime corresponds to temperatures $T \gg \Theta$, since Θ is found to approach zero; in a Kondo description, $T \gg \Theta$ corresponds to the weak-coupling limit $J\rho(E_F) \ll 1$; yet spin dynamics, seen in NMR experiments, continue to show the fluctuations of a strongly correlated extended magnetic entity around the impurity. This might be due to the existence of the pseudogap.

In the overdoped regime, as the physics gets closer to the Fermi-liquid limit, one does not expect to observe Kondo-like signatures any longer. Indeed, a nonmagnetic impurity is not expected to produce a Kondo resonance in conventional metals. Thus understanding the reduction of the amplitude of the staggered moments, the spatial extent of the polarization, and the evolution of C and Θ for large dopings may require a different description.

VI. IMPURITIES IN THE SUPERCONDUCTING STATE

A. Overview

The subject of impurities in the superconducting state of the cuprates, and the theory of impurity states in unconventional superconductors generally, is already quite vast. We benefit from recent reviews by Balatsky *et al.* (2006) on local aspects of impurity states, by Hussey (2002) on effects of disorder on bulk quasiparticle properties, by Hirschfeld and Atkinson (2002) on nonperturbative disorder effects in two dimensions, and by Flatté and Byers (1999) on general impurity properties in superconductors. Here we review aspects of the effects of nonmagnetic impurities on d-wave superconductivity before discussing theoretical approaches to the inclusion of

electronic correlations in the superconducting state impurity problem, as well as relevant experiments. We comment on the case of magnetic impurities, but ignore the case of impurities which induce low-lying crystal-field levels above the ground state, as occurs with rare-earth impurities in conventional superconductors (Fulde *et al.*, 1970).

It was recognized shortly after the publication of the BCS theory that while nonmagnetic impurities would not affect thermodynamic properties of a conventional superconductor (Anderson, 1959), they might do so in hypothetical p-wave pairing systems (Balian and Werthamer, 1963). When a high density of low-energy excitations in superconducting heavy fermion systems, such "unconventional" states were considered as possible ground states of compounds like UBe_{13} and UPt_3. Gorkov and Kalugin (1985) and, independently, Ueda and Rice (1985) pointed out that linear nodal regions of the order parameter on the 3D Fermi surface would lead to a nonzero residual density of states at zero energy, $\rho(0)$. This self-consistent perturbative treatment for weak impurities, averaged over disorder, was similar to that used by Abrikosov and Gorkov (1960) in discussing gapless superconductivity induced by magnetic potentials. Pethick and Pines (1986) observed that weak scattering models of this kind could not describe transport properties measured on heavy fermion materials, and proposed that large effective impurity potentials could be treated in a T-matrix approximation. Hirschfeld *et al.* (1986) and Schmitt-Rink *et al.* (1986) then proposed the self-consistent T-matrix approximation (SCTMA) for impurities of arbitrary strength, and predicted a disorder-induced "plateau" in $\rho(\omega)$ at low energies. This plateau consists of disorder induced "impurity band" states analogous to the midgap localized states predicted for dirty isotropic p-wave superconductors by Buchholtz and Zwicknagl (1981). The nodal quasiparticles which contribute to this impurity band give rise to thermodynamic properties similar to a normal metal with reduced DOS. Stamp (1987) then investigated the character of a local single-impurity resonance within this model.

In a similar way, when experiments on good samples of cuprate superconductors in the early 1990s began indicating the existence of low-energy excitations in the superconducting state (Hussey, 2002), the importance of understanding the effect of disorder for identifying the symmetry of the order parameter was quickly realized. The effect of disorder on T_c itself was controversial early on. For example, irradiation with heavy ions was found to suppress T_c only when the scattering rate, as deduced from resistivity, became of the order of the Fermi energy (Valles *et al.*, 1989), as expected for an isotropic s-wave superconductor. On the other hand, impurities substituting for Cu in the CuO_2 plane tended to depress T_c rapidly, as expected for an unconventional superconductor, and controlled electron irradiation experiments confirmed this (Legris *et al.*, 1993; Giapintzakis *et al.*, 1994), (see Sec. IV.B.2).

On the theoretical side, the self-consistent T-matrix approximation was employed to provide a qualitative explanation of the effects of disorder on d-wave superconductors, offering evidence for symmetry identification. These arguments belong in the same category as explicitly phase-sensitive measurements like tricrystal experiments (Tsuei and Kirtley, 2000), as pointed out by Borkowski and Hirschfeld (1994). This is because the fact that nonmagnetic impurities break pairs is directly associated with the sign change of the d-wave order parameter (see Sec. VI.B). Within the SCTMA, the strength of the impurity potential is an important parameter, and the recognition that planar impurities like Zn acted as near unitary scatterers was an important step forward. For example, observations of a crossover of the magnetic penetration depth from a T to a T^2 behavior with a small concentration of Zn impurities were not initially understood to be a natural consequence of d symmetry, because it was expected that in such experiments T_c would be strongly suppressed in a d-wave system. In the unitarity limit, however, modifications of low-energy properties occur over an energy scale γ (residual scattering rate or "impurity bandwidth") which can be much larger than the normal-state impurity scattering rate Γ which controls T_c (Hirschfeld and Goldenfeld, 1993). A similar analysis by Hotta (1993) explained the dependence of the residual $T \rightarrow 0$ Knight shift of YBCO on Zn concentration. Calculations of transport properties within this framework also provided evidence for near-unitarity scattering, and helped rule out candidate extended s-wave states (Borkowski *et al.*, 1995).

While successful in explaining the effects of strong in-plane scatterers in optimally doped cuprates, the basis of the SCTMA phenomenology was called into question by Nersesyan *et al.* (1995), who pointed out that the neglect of multiple-impurity scattering processes ("crossed diagrams"), which are of higher order in $1/k_F\ell$ or the density of impurity sites n_i in three dimensions, was not justified at asymptotically low energies in two dimensions since these diagrams have an additional $\ln E$ singularity coming from the line nodes of the $d_{x^2-y^2}$ gap. This leads to a breakdown of single-site perturbation theory and the need to resum at least a second class of crossed diagrams. This led to several attempts to solve the problem nonperturbatively (Nersesyan *et al.*, 1995; Ziegler, Hettler, and Hirschfeld, 1996; Pepin and Lee, 1998; Senthil and Fisher, 1999), each claiming to calculate *exactly* the density of states of a disordered 2D d-wave superconductor, but arriving at dramatically different results. A combination of numerical work (Atkinson, Hirschfeld, MacDonald, and Ziegler, 2000) and analytical weak localization calculations (Yashenkin *et al.*, 2001), reviewed by Hirschfeld and Atkinson (2002), led to the conclusion that the low-energy DOS of the 2D d-wave state was sensitive to the symmetries of the disorder model and the normal-state one-electron band employed in the calculations, in contrast to expectations based on standard localization calculations for normal metals. In addition, it was argued that corrections to the SCTMA were un-

likely to be relevant to experiments on real cuprates.

While the SCTMA is a successful approximation for properties of optimally to overdoped cuprate superconductors with nonmagnetic disorder, it cannot account for the magnetic states induced by potential scatterers as described in Sec. IV, nor other phenomena which must arise when pairing takes place in the underdoped phase near the Mott transition. Here we investigate how the physics of impurities in correlated metals discussed in Secs. IV and V is modified by superconductivity. To establish the groundwork, we first give a brief account of the formation of low-energy impurity resonances (Sec. VI.B) in a *d*-wave superconductor, and associated impurity bands by nonmagnetic potentials. We next discuss (Sec. VI.C) the interference of these states in the presence of finite disorder, and the formation of the impurity band in the *d*-wave superconductor. We then introduce electronic correlations, (Sec. VI.D) focusing on results from the weak-coupling theory of impurity-induced moment formation, since it can easily be extended to the superconducting state. We then compare a general picture which emerges from these treatments with experiments, both those which probe disorder-averaged properties, i.e., primarily states far from the impurities themselves (Sec. VI.E), and those which probe states near the impurity (Sec. VI.F). In Sec. VI.G we summarize ideas regarding the effects of disorder in the correlated *d*-wave state gleaned from both theory and experiment.

B. Single impurity in a *d*-wave superconductor

The BCS Hamiltonian for a pure singlet superconductor can be written as

$$H_0 = \sum_{\mathbf{k}} \Phi_{\mathbf{k}}^{\dagger}(\epsilon_{\mathbf{k}}\tau_3 + \Delta_k\tau_1)\Phi_{\mathbf{k}}, \tag{43}$$

where $\Phi_{\mathbf{k}} = (c_{\mathbf{k}\downarrow}, c_{-\mathbf{k}\uparrow}^{\dagger})$ is a Nambu spinor. Analytic results are presented for a parabolic band $\epsilon_{\mathbf{k}} = k^2/2m$, with corresponding *d*-wave order parameter $\Delta_{\mathbf{k}} = \Delta_0 \cos 2\phi$ (ϕ is the angle in momentum space that $\mathbf{k}$ makes with the 100 axis). The matrices τ_i are the Pauli matrices spanning particle-hole space. To the homogeneous superconductor we add a single impurity perturbation

$$H_{\text{int}} = \sum_{\mathbf{k}\mathbf{k}'} \Phi_{\mathbf{k}}^{\dagger}\hat{V}_{\mathbf{k}\mathbf{k}'}\Phi_{\mathbf{k}'}, \tag{44}$$

where $\hat{V}_{\mathbf{k},\mathbf{k}'} = \int d\mathbf{r}\, e^{i(\mathbf{k}-\mathbf{k}')\cdot\mathbf{r}}\hat{V}(\mathbf{r})$ is the scattering potential Fourier component. For a densitylike perturbation which couples to the chemical potential locally, the Nambu form is $\hat{V}_{\mathbf{k},\mathbf{k}'} = V_{\mathbf{k},\mathbf{k}'}\tau_3$. The full Green's function for a single impurity is

$$\begin{aligned}\hat{G}(\mathbf{k},\mathbf{k}') &= \hat{G}_0(\mathbf{k}) + \hat{G}_0(\mathbf{k})\hat{V}_{\mathbf{k},\mathbf{k}'}\hat{G}_0(\mathbf{k}') \\ &\quad + \sum_{\mathbf{k}''} \hat{G}_0(\mathbf{k})\hat{V}_{\mathbf{k},\mathbf{k}''}\hat{G}_0(\mathbf{k}'')\hat{V}_{\mathbf{k}'',\mathbf{k}'}\hat{G}_0(\mathbf{k}') + \cdots \\ &= \hat{G}_0(\mathbf{k}) + \hat{G}_0(\mathbf{k})\hat{T}_{\mathbf{k},\mathbf{k}'}\hat{G}_0(\mathbf{k}'),\end{aligned} \tag{45, 46}$$

where the T matrix is given by summing all single-site scattering processes,

$$\hat{T}_{\mathbf{k},\mathbf{k}'} = \hat{V}_{\mathbf{k},\mathbf{k}'} + \sum_{\mathbf{k}''} \hat{V}_{\mathbf{k},\mathbf{k}''}\hat{G}_0(\mathbf{k}'')\hat{V}_{\mathbf{k}'',\mathbf{k}'} + \cdots \tag{47}$$

$$= \hat{V}_{\mathbf{k},\mathbf{k}'} + \sum_{\mathbf{k}''} \hat{V}_{\mathbf{k},\mathbf{k}''}\hat{G}_0(\mathbf{k}'')\hat{T}_{\mathbf{k}'',\mathbf{k}'}, \tag{48}$$

and $\hat{A}$ are matrices in particle-hole space. If the impurity scattering is purely pointlike, $\hat{V}(\mathbf{r}) \propto \delta(\mathbf{r})$, the scattering is isotropic, $\hat{V}_{\mathbf{k},\mathbf{k}'} = \hat{V}$, and $\hat{T}$ is seen to be independent of momentum. For a pointlike nonmagnetic impurity potential with strength V_0, it is convenient to define the cotangent of the *s*-wave phase shift δ_0, with $c \equiv \cot\delta_0 \equiv (\pi V_0\rho_0)^{-1}$, with ρ_0 the density of states at the Fermi level. The Green's function including the impurity is therefore

$$\hat{G}(\mathbf{k},\mathbf{k}';\omega) = \hat{G}_0(\mathbf{k},\omega)\delta_{\mathbf{k}\mathbf{k}'} + \hat{G}_0(\mathbf{k},\omega)\hat{T}(\omega)\hat{G}_0(\mathbf{k}',\omega), \tag{49}$$

with $\hat{G}_0(\mathbf{k},\omega) = (\omega - \hat{H}_0)^{-1}$, and the T matrix takes the form

$$\begin{aligned}\hat{T} &= T_0\tau_0 + T_3\tau_3, \\ T_0 &= g_0/S_+S_-, \\ T_3 &= (c - g_3)/S_+S_-,\end{aligned} \tag{50}$$

where g_0 and g_3 are the τ_0 and τ_3 Nambu components of the integrated bare Green's function $(1/\pi\rho_0)\Sigma_{\mathbf{k}}\hat{G}_0(\mathbf{k},\omega)$. This expression has resonances when

$$S_{\pm} \equiv c - (g_3 \mp g_0) = 0. \tag{51}$$

Note that the off-diagonal components of the T matrix do not occur because $g_1 = g_2 = 0$ due to the *d*-wave symmetry. Furthermore, in the special case of a particle-hole symmetric system, $g_3 = 0$ and the resonance energy is determined entirely by g_0, which is given in the case of a circular Fermi surface by $g_0(\omega) = -i\int(d\varphi/2\pi)\omega(\omega^2 - \Delta_{\mathbf{k}}^2)^{-1/2}$. For low energies $\omega \ll \Delta_0$, this takes the form $g_0(\omega) \simeq -(\pi\omega/\Delta_0)(\ln 4\Delta_0/\omega + i)$. One may then solve $\text{Re}\, S_{\pm}(\omega + i0^+) = 0$ and estimate the resonance width Γ on the real axis. In the case of strong scattering $c \ll 1$, the resonance energy $\Omega_0^{\pm}$ and width Γ are

$$\Omega_0^{\pm} = \pm\pi c\Delta_0/2\ln(8/\pi c), \tag{52a}$$

$$\Gamma = \pi^2 c\Delta_0/4\ln^2(8/\pi c). \tag{52b}$$

This result was first obtained by Balatsky *et al.* (1995) for the *d*-wave case, following earlier work on the similar *p*-wave case by Stamp (1987). By contrast, in the *s*-wave case, a nonmagnetic impurity does not produce a midgap state due to Anderson's theorem (Anderson, 1959). In the *d*-wave superconductor, the impurity reso-

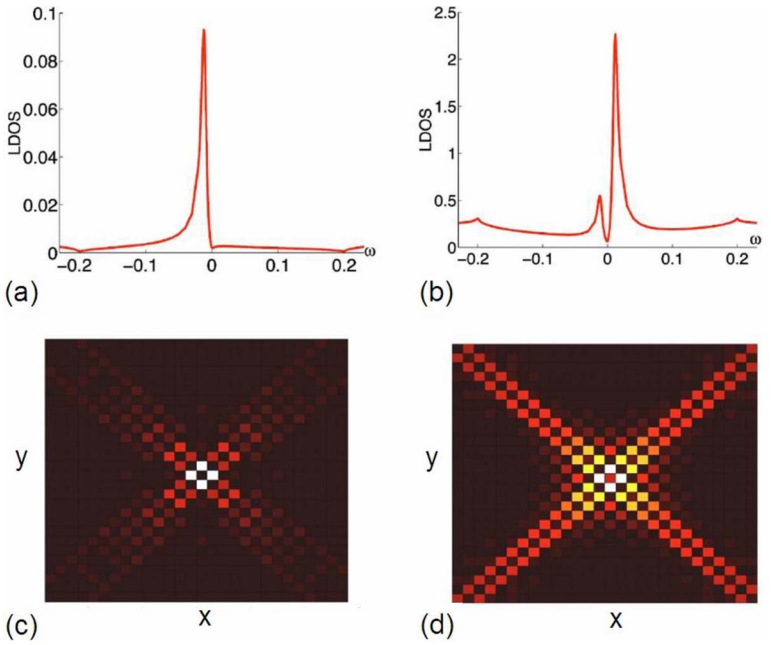

FIG. 36. (Color online) Summary of LDOS results for one-impurity problem on a tight-binding lattice, band given by Norman *et al.* (1995), bond order parameter $\Delta_d=0.1$, $\mu=0$, $V_0=10$, $|\Omega_0^{\pm}|\simeq 0.013$: (a) LDOS vs ω on the impurity site; (b) LDOS vs ω on nearest-neighbor site; (c), (d) LDOS map at resonance $\omega=\Omega_0^+$ and $\omega=\Omega_0^-$. Color scales in (c) and (d) are relative to the nearest-neighbor peak heights shown in (b). From Zhu *et al.*, 2003.

nance becomes an undamped bound state only exactly at the Fermi level $\Omega=0$, when $c=0$; for finite c there are two resonances whose energies $\Omega_0^+=-\Omega_0^-$ are symmetric about the Fermi level in this approximation. As seen from Eq. (51), in general particle-hole asymmetric systems ($g_3\neq 0$) the resonance is tuned to sit at the Fermi energy for some value of the impurity potential V_0 which is not infinite, so the term "unitarity" (as used here, $\Omega_0=0$) and "strong potential" ($V_0\to\infty$) are no longer synonymous (Joynt, 1997; Atkinson, Hirschfeld, and MacDonald, 2000).

1. Local density of states near impurity

Although the energies of the particle and hole resonant states are symmetric, their spectral weights on a given site are usually different (Balatsky *et al.*, 1995), such that locally only one resonance dominates. Define the local density of state (LDOS) as

$$\rho(\mathbf{r},\omega)=-(1/\pi)\mathrm{Im}\, G_{11}(\mathbf{r},\mathbf{r};\omega+i0^+) \tag{53}$$

with the total Green's function in the presence of the impurity $\hat{G}(\mathbf{r},\mathbf{r}';\omega)=\hat{G}_0(\mathbf{r}-\mathbf{r}',\omega)+\hat{G}_0(\mathbf{r},\omega)\hat{T}(\omega)\times\hat{G}_0(-\mathbf{r}',\omega)$, where the index 11 refers to the normal electron part of the Nambu Green's function. Now it is easy to see that any finite impurity potential acts as a local breaker of particle-hole symmetry which can lead to a pronounced peak in the LDOS. At the impurity site $\mathbf{r}=\mathbf{0}$, for a repulsive impurity potential, the resonant peak at negative energy (holelike states) is large, and the positive energy (electronlike states) peak is relatively small, as shown in Fig. 36. The situation is reversed for the nearest-neighbor site. Note, however, that for the large value of V_0 chosen, the LDOS peak at resonance is much smaller on the impurity site than on the nearest-neighbor site since the large potential excludes electrons from the impurity site.

Impurity bound states of this type have observable consequences for the local density of states, measurable by STM, and for the distributions of local magnetizations, measured by NMR. The impurity modulates the local density of states of the homogeneous system $\rho(\mathbf{r},\omega)$ by

$$\rho_{\mathrm{imp}}(\mathbf{r},\omega)=-(1/\pi)\mathrm{Im}[\hat{G}_0(\mathbf{r},\omega)\hat{T}(\omega)\hat{G}_0(-\mathbf{r},\omega)]_{11}. \tag{54}$$

The impurity-induced LDOS falls off as r^{-2} along the nodal directions, and exponentially along the antinodal ones (Balatsky *et al.*, 1995). The LDOS in the near field is more complicated; however, the nearest-neighbor sites have peaks at $\pm\Omega_0$, with the larger spectral weight at $+\Omega_0$. These spatially extended LDOS patterns are the fingerprint of the impurity-induced virtual bound states. In Fig. 36, we show the LDOS pattern expected for both particles and holes for a resonant state close to the Fermi level in this simple model.

The existence of impurity bound states in the superconductor is shown below to be related to strong T-dependent upturns in the local susceptibility, so it is of interest to establish what happens in the current model as the temperature is increased and superconductivity destroyed. If the normal state is metallic, as assumed in the current model, weak Friedel-like oscillations in the density of states remain, but the resonant character of the impurity state is destroyed. If, however, the normal state also possesses a spectral gap, resonant states may remain. This is why impurity bound states found, in models of the spin-gap phase of the cuprates (Gabay, 1994; Nagaosa and Ng, 1995; Khaliullin *et al.*, 1997), with linear density of states analogous to the d-wave superconductor, are similar to those in the superconducting state. Impurity measurements have in fact been proposed as a probe of the pseudogap state in the cuprates (Kruis *et al.*, 2001).

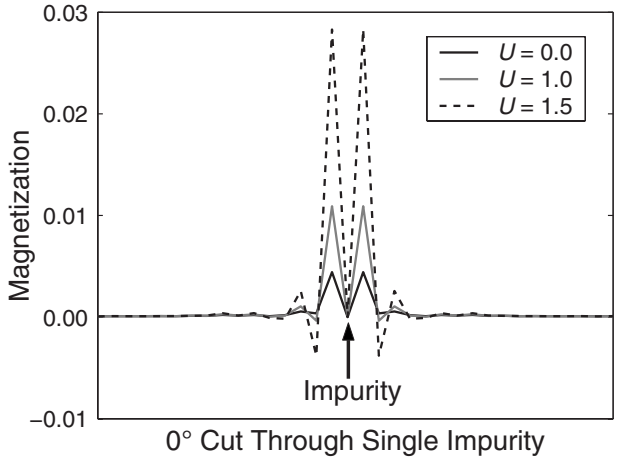

FIG. 37. Magnetization along (1,0) direction through impurity with d-wave superconductor described by tight-binding band with $t'/t=-0.2$, $V_{\mathrm{imp}}=100t$, $g\mu_B B/2=0.004t$, $U/t=0,1,1.5$. From Harter *et al.*, 2007.

Because nonmagnetic impurities are pair breaking in d-wave superconductors, the most important qualitative distinction with magnetic impurities does not exist. Nevertheless, there are some interesting phenomena associated with impurity spins in unconventional superconductors, which have been reviewed by Balatsky *et al.* (2006).

2. Effect on field-induced magnetization

In the pure d-wave state with no residual quasiparticle interactions, the paired gas has a Friedel-type response to the impurity perturbation which leads to a spatially oscillating LDOS $\rho(\mathbf{r},\omega=0)$ at the Fermi level with wavelength $2k_F$ and envelope decaying over a length scale of $\xi_0=v_F/\pi\Delta_0$. Consider a situation where the impurity is nonmagnetic; there are then no corresponding spin-density waves induced in zero field by correlation effects. However, since the local susceptibility in the superconducting state $\chi(\mathbf{r},T)$ is proportional to the density of states at the Fermi level, such oscillations translate directly into magnetization modulations in the presence of a nonzero applied field. Since the LDOS is always positive, the magnetization is always in the same direction as the applied field. This can be seen in the $U=0$ curve of Fig. 37. In the presence of electronic correlations, these modulations are enhanced, and a true alternating magnetization appears, as discussed in Sec. VI.D.

C. Effects of disorder on d-wave state

1. Quasiparticle interference of impurity bound states

As shown in Fig. 36, the strong nonmagnetic impurity in a d-wave superconductor in this approximation is characterized by a bound state with long-range tails extending along the nodal direction. If many impurities are present, these states overlap and interfere, leading to a splitting of bound-state energies and an accumulation of low-energy impurity-induced energy eigenvalues which are spread out over a so-called "impurity band" (Michaeluchi *et al.*, 2002). The formation of this band, which appears in the disorder-averaged theory, is a rather subtle phenomenon compared to, say, the analogous impurity band in disordered semiconductors, where a good deal can be understood by postulating transport via overlap of spherically symmetric hydrogenic orbitals. In the d-wave case the formation of the impurity band and the corresponding quasiparticle localization problem are influenced by the fact that significant overlaps between two impurity states can occur only if the impurities are "oriented" with respect to one another such that the nodal wave-function tails overlap (Balatsky and Salkola, 1996). In fact, analyses of the two-impurity problem show that interference effects can occur over many tens of lattice spacings between optimally oriented impurities (Morr and Stavropoulos, 2002; Andersen and Hedegaard, 2003; Zhu *et al.*, 2003). In Fig. 38, we show the local density of states due to many strong impurities using a realistic band structure, averaged over a few eigenstates within a narrow energy range abound the one-impurity resonance energy (Atkinson *et al.*, 2003). The interference tails between some impurities are visible, while others have been split outside the "observation bandwidth" due to the local disorder environment. It is this complex system that the SCTMA seeks to replace by a disorder-averaged, translationally invariant medium where the quasiparticle states of the pure system are broadened.

2. Self-consistent T-matrix approach

Since the SCTMA approach has been well described in several papers and reviews (Buchholtz and Zwick-

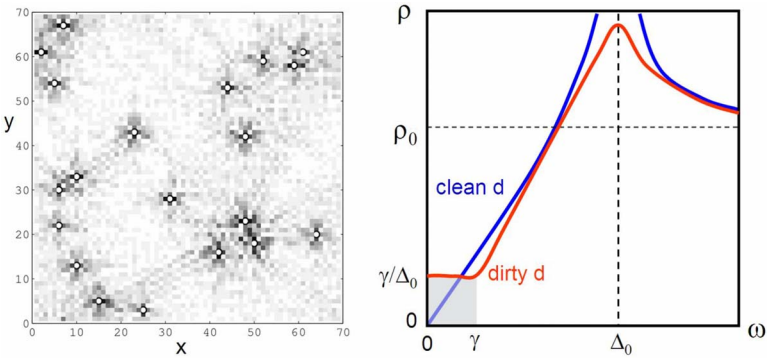

FIG. 38. (Color online) Origin of impurity band in d-wave superconductors. Left: Density of states $\rho(0)$ vs position in a 70×70 lattice, showing interference of many impurities in band with no particle-hole symmetry. White dots represent strong potential scatterers. From Atkinson, 2002. Right: Schematic density of states of a d-wave superconductor, and impurity band of width γ.

nagl, 1981; Hirschfeld *et al.*, 1986; Schmitt-Rink *et al.*, 1986; Joynt, 1997; Hussey, 2002; Balatsky *et al.*, 2006), we only briefly summarize it here. We begin with the exact equations for the single impurity T matrix (48). The self-consistent T-matrix approach now extends these equations to an approximate treatment where the disordered system is replaced by a translationally invariant dissipative medium described by a self-energy $\hat{\Sigma}(\mathbf{k},\omega)=n_{\rm imp}\hat{T}_{\mathbf{k},\mathbf{k}}$, where $\hat{T}$ is now a disorder-averaged quantity. At the same time, the full Green's function $\hat{G}(\mathbf{k},\mathbf{k}',\omega)$ is replaced by a disorder averaged $\hat{G}(\mathbf{k},\omega)$, the propagator for an electron moving in the translationally invariant effective medium, given by

$$\hat{G}^{-1}(\mathbf{k},\omega)=\hat{G}_0^{-1}(\mathbf{k},\omega)-\hat{\Sigma}(\mathbf{k},\omega), \tag{55}$$

where $\hat{\Sigma}$ is the sum of all disorder-averaged T-matrix diagrams, evaluated with the fully self-consistent disorder-averaged $\hat{G}$ on each Green's function line. The calculation is similar to the approximation of Abrikosov and Gorkov (1960), but valid for arbitrary impurity strength.

Rather than give details of the calculation of $\hat{\Sigma}$, which are reviewed elsewhere, we focus on the simplest example which displays the basic physics of a disordered d-wave superconductor, a finite density of identical strong pointlike scatterers. In this case the self-energy reduces to the analog of Eq. (50),

$$\hat{\Sigma}(\mathbf{k},\omega)=\Gamma[(c-g_3)\tau_3+g_0\tau_0]/[(c-g_3)^2-g_0^2], \tag{56}$$

where the impurity scattering rate parameter $\Gamma=n_{\rm imp}/\pi\rho_0$ and $g_{0,3}$ are now functionals of $\hat{G}$ rather than $\hat{G}_0$. Furthermore assume particle-hole symmetry and unitary limit scattering $c\to 0$. Then the self-energy reduces to the simple result $\hat{\Sigma}\to-\Gamma/g_0$. At the Fermi level, $\omega\to 0$, we assume the retarded self-energy Σ_0 reduces to a small imaginary part $-i\gamma$, so that the self-consistency equation becomes, for a circular Fermi surface and d-wave order parameter $\Delta_0\cos 2\phi$,

$$-i\gamma=-\frac{\Gamma}{g_0(0)}=\frac{-\Gamma}{-i(2/\pi)\int_0^{\pi/2}d\phi(\gamma/\sqrt{\gamma^2+\Delta_0^2\cos^2 2\phi})}. \tag{57}$$

The elliptic integral can be performed and expanded for $\gamma\ll\Delta_0$ to give the following self-consistency equation for γ:

$$\left(\frac{\gamma}{\Delta_0}\right)^2=\frac{\pi}{2}\frac{\Gamma}{\Delta_0}\Big/\ln\left(\frac{4\Delta_0}{\gamma}\right), \tag{58}$$

a transcendental equation whose solution for small Γ can be approximated to logarithmic accuracy as $\gamma\sim 0.63\sqrt{\Gamma\Delta_0}$ (Hirschfeld and Goldenfeld, 1993). The DOS at zero frequency is then given by

$$\rho(0)/\rho_0=-\,\mathrm{Im}\,g_0(0)=\Gamma/\gamma, \tag{59}$$

where the first equality is general but the second obtains only in the unitarity limit.

Thus the SCTMA generically predicts a finite density of states at the Fermi level in the presence of disorder for a d-wave superconductor. The dependence of this residual DOS on the concentration of defects ranges from the $\rho_0\sim\sqrt{n_{\rm imp}}$ behavior in the unitarity limit just exhibited to a much weaker exponential dependence, $\rho(0)\sim\exp(-\Delta_0/\Gamma_N)$, with $\Gamma_N\equiv\Gamma/(1+c^2)$ in the weak-scattering (Born, $c\gg 1$) limit. The general form for the DOS expected over the whole frequency range in the strong-scattering limit is shown in Fig. 38(b). If the scattering is weaker, the weight in the impurity band moves to higher energies as the position of the single-impurity resonance itself moves away from the Fermi level [see Eq. (52a)], and the Fermi-level DOS $\rho(0)$ decreases accordingly.

The simplest measurement showing the influence of impurities is the suppression of the critical temperature, which has been discussed in Sec. IV.D.2.b in connection with transport experiments. Within the SCTMA, the remarkable prediction is that for a d-wave superconductor with pointlike scatterers the T_c suppression follows a form identical to the prediction of Abrikosov and Gor'kov (AG) (Abrikosov and Gorkov, 1960),

$$\ln\left(\frac{T_{c0}}{T_c}\right)=\psi\left(\frac{1}{2}+\frac{1}{4\pi\tau T_c}\right)-\psi\left(\tfrac{1}{2}\right), \tag{60}$$

where T_{c0} is the transition temperature in the absence of disorder, $\psi(x)$ is the digamma function, and $1/\tau\equiv 2\Gamma_N$ is the scattering rate at the critical temperature due to impurity scattering alone, assuming that the impurity potential is nonmagnetic and of zero range, for any scattering phase shift. For small concentrations, the initial slope of the T_c suppression is then $T_c/T_{c0}\simeq 1-\pi/4\tau T_{c0}$. With increasing concentrations, superconductivity is eventually destroyed ($T_c=0$) when the scattering rate reaches the critical value

$$\tau^{-1}=\pi T_{c0}/\gamma, \tag{61}$$

where $\gamma\approx 1.78$. If Matthiessen's rule is obeyed (Sec. IV.D), the scattering rate is proportional to the change in resistivity due to disorder $\Delta\rho$ and one expects an AG-type form for T_c vs $\Delta\rho$.

3. Extended impurities

As discussed in Sec. IV.B.2, impurities which substitute for Cu in the CuO_2 planes turn out to be strong scatterers of electronic states in the plane. While the effective bare potential induced by planar impurities is expected to be on an atomic scale (Wang *et al.*, 2005), it has been suggested that the correlations could give rise to a larger effective range (Sec. V.B). This is a possible reason why the initial slope of the T_c suppression versus residual resistivity curve in the case of Zn and Ni is found to be somewhat smaller (roughly a factor of 2) than predicted by the SCTMA (see Sec. VI.E) (Franz *et*

al., 1996; Haran and Nagi, 1996, 1998; Kulic and Oudovenko, 1997; Kulic and Dolgov, 1999; Graser *et al.*, 2007).

On the other hand, there are many other defects in the cuprates, and, in fact, all cuprate materials are doped by out-of-plane ions which in most cases occupy random positions in the crystal lattice or interstitial positions. It is to be expected that these "intrinsic" impurities are poorly screened, and therefore they should have a large effective range of the scattering potential experienced by holes moving in the planes. In addition, they tend to be present in rather large concentrations, indeed of order the doping itself. With the notable exceptions of $YBa_2Cu_3O_{7+\delta}$ and $YBa_2Cu_4O_8$, cuprates at optimal doping must therefore be considered to have $O(10\%)$ concentrations of intrinsic impurities with extended potentials. Such defects will tend to scatter electrons preferentially in the forward direction. The consequences for normal-state one-electron properties were highlighted by Abrahams and Varma (2000), for the critical temperature by Kee (2001), and for quasiparticle properties in the superconducting state at low temperatures by others (Xiang and Wheatley, 1995; Kampf and Devereaux, 1997; Durst and Lee, 2000; Zhu *et al.*, 2004; Dahm, Hirschfeld, *et al.*, 2005; Dahm, Zhu, *et al.*, 2005; Nunner and Hirschfeld, 2005). Impurities of this type are assumed to be sufficiently weak such that they do not give rise to resonant effects at low energies, and are therefore not so easy to image with STM techniques. In addition, weaker potentials are not expected to induce significant local magnetism (see Sec. VI.F), but there do not appear to be theoretical investigations along these lines available.

Zhu *et al.* (2004), Dahm, Hirschfeld, *et al.* (2005), and Dahm, Zhu, *et al.* (2005) concluded that forward scatterers have a tendency to sharpen spectral features near the antinode of the *d*-wave gap, while broadening those near the node. This counterintuitive result can be understood by noting that if the scattering is sufficiently forward, scattering processes which begin with quasiparticles near the antinode cannot involve a sign change of the order parameter and are therefore not pair breaking; this is the analog of Anderson's theorem for forward scattering in the *d*-wave state. On the other hand, if a quasiparticle is sufficiently close to the node, phase space for scattering involving sign change of $\Delta_{\mathbf{k}}$ is available and spectral features will be broadened similarly to the normal state.

Forward scattering impurities might be expected to have negligible effect on transport, since they cannot relax the momentum current. On the other hand, Nunner and Hirschfeld (2005) showed that scatterers of intermediate range could produce qualitatively different temperature dependences of the superconducting state microwave conductivity, providing a possible explanation to the different results obtained for crystals of optimally doped $YBa_2Cu_3O_{7+\delta}$ and $Bi_2Sr_2CaCu_2O_8$.

4. Order-parameter suppression and pairing potential impurities

It is worth noting that the theoretical models above do not account for the local variation of the superconducting order parameter near the impurity site. The order parameter has a response to a local Coulomb potential, and the correct way to include it within a fully self-consistent Hartree-Fock theory was discussed by Fetter (1965), Rusinov (1968), and others for ordinary superconductors. In the context of unconventional superconductors, order parameter suppression around a single impurity was discussed (Choi and Muzikar, 1990; Franz *et al.*, 1996; Friesen and Muzikar, 1997; Shnirman *et al.*, 1999; Atkinson, Hirschfeld, and MacDonald, 2000). These effects were neglected early on probably because, in terms of the resonance effects on one-electron properties discussed in Sec. VI.B, the self-consistent treatment does not lead to major differences. In the disorder-averaged theory it can have important effects on transport as a new source of "off-diagonal scattering" (Hettler and Hirschfeld, 1999), however.

There is a further, more exotic possibility, which is just beginning to be taken seriously. In the self-consistent approaches above, the BCS pair interaction constant λ which appears in the gap equation is assumed to be homogeneous, and one considers the response of the order parameter to a diagonal potential with τ_3 symmetry in Nambu space, i.e., a response $\delta\Delta_{\mathbf{k}}(\mathbf{r})\tau_1$ is produced. In principle, it has been recognized that an impurity can alter the local electronic structure such that the pairing interaction itself is modified locally (Suhl *et al.*, 1962; Larkin, 1970), leading to $\lambda(\mathbf{r})$. Since coherence lengths ξ_0 of conventional superconductors are much larger than microscopic distances a, these effects are typically averaged over in observable quantities. In cuprates, however, the effects can be important, as shown by Nunner *et al.* (2005), who considered the effects of such impurities on the LDOS. Strong pairing impurities can produce resonant effects of their own with quite different characteristic LDOS patterns than conventional impurities, as shown by Chattopadhyay *et al.* (2002) and Andersen *et al.* (2006).

D. Effect of correlations

1. Single impurity

The preceding discussion relates to the simplest theory of localized potential scatterers in a *d*-wave superconductor, and to some simple generalizations within the framework of BCS theory. While the approach has had considerable success at explaining properties of disordered cuprates (see Secs. VI.E and VI.F), it is expected that strong residual quasiparticle interactions neglected in this approach are still present even in the superconducting state, and should influence the underdoped state in proximity to the antiferromagnetic insulator. Many approaches to the problem of an impurity in a correlated system discussed in Sec. V have therefore

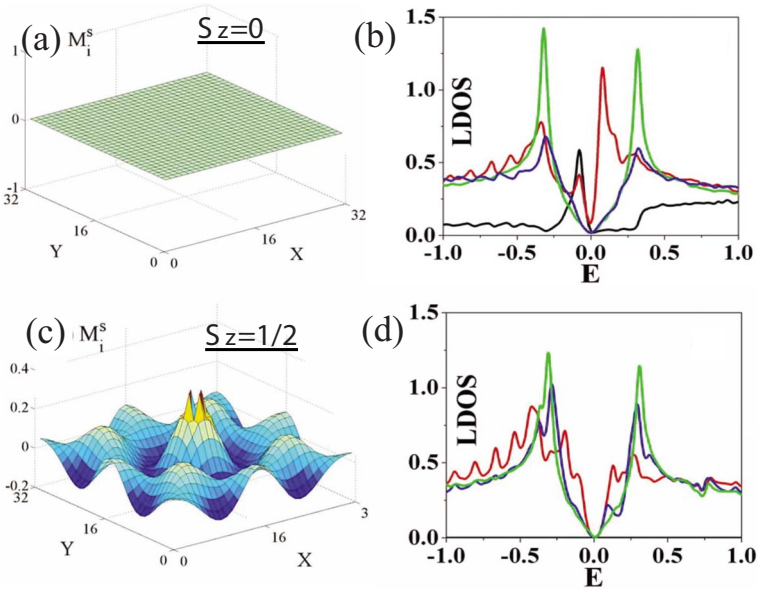

FIG. 39. (Color online) Spatial variations of the staggered magnetization M_s [(a), (c)], and LDOS spectra [(b), (d)] calculated for a 32 $\times$32 system. The impurity site is at (16,16). Solid lines in (b) and (d) are for (16,16), dashed lines for (17,16), dash-dotted lines for (17,17), and dotted lines for (16,1). The upper [(a),(b)] and the lower panels [(c),(d)] are for $(U, V_{\mathrm{imp}})=(2,3)$ and (2.35,100), respectively. From Chen and Ting, 2004.

been generalized to include pair correlations, and we present some here.

From the weak-coupling point of view, the question posed by Ohashi (2002) is, does the substantial reduction of the susceptibility in a d-wave superconductor at low temperatures ($\chi \sim \rho_0 T/\Delta_0$) prevent the enhanced magnetization near the impurity site due to the coupling of spin fluctuations at $\mathbf{q}=\mathbf{0}$ and (π,π)? In fact, the enhancement of the susceptibility by a strong impurity *relative* to the system far from the impurity site is found to be more important in the superconducting case, due to the resonant enhancement of the low-energy density of states already present even in the absence of correlations (Sec. VI.C.2). The interplay of resonant density of states enhancements and correlation-induced magnetic moments is one interesting question which arises only in the superconducting (and possibly pseudogap) states addressed here.

A phase diagram for the single-site impurity treated in the weak-coupling mean-field model was presented by Chen and Ting (2004), who related the LDOS features probed by STM to the local magnetic state around the impurity (Fig. 39). They argued that the formation of a spontaneous $S_z=\frac{1}{2}$ moment was always associated with the substantial splitting of the small-U LDOS resonance, and concluded that since the resonances observed around Zn were unsplit (Pan *et al.*, 2000b)—see Sec. VI.F.2—they were necessarily associated with the $S_z=0$ state. The "local phase transition" from the $S_z=0$ state to the $S_z=\frac{1}{2}$ state, with concomitant splitting of the LDOS resonance, is similar to the phenomenology of the singlet-doublet transition for a magnetic impurity in an s-wave superconductor (Sakurai, 1970; Sakai *et al.*, 1993; Salkola *et al.*, 1997). Chen and Ting (2004) also found in their numerical studies a $S_z=0$ phase which displayed local SDW-type order, but Harter *et al.* (2007) concluded that this phase was an artifact of the particular finite-size system studied. The simpler phase diagram presented by the latter group is shown in Fig. 40, and indicates that the tendency to form a spontaneous extended moment increases with either correlations (U) or the bare impurity potential (V_{imp}). It should be noted that mean-field treatments of this type can at best describe the tendency to form static moments. If the mean-field model indicates an $S=0$ ground state, for example, this does not preclude the existence of a fluctuating moment at low energies.

Tsuchiura *et al.* (2001) performed similar calculations in a t-J model in zero field decoupled to allow d-wave superconductivity, with a single site cut off from the system. The model was treated within the Gutzwiller approximation, amounting to assigning local bandwidth renormalizations to each bond. They found a spontaneous moment phase with alternating magnetization near the impurity site, as well as a zero moment phase similar to the weak-coupling calculations. In addition, they cal-

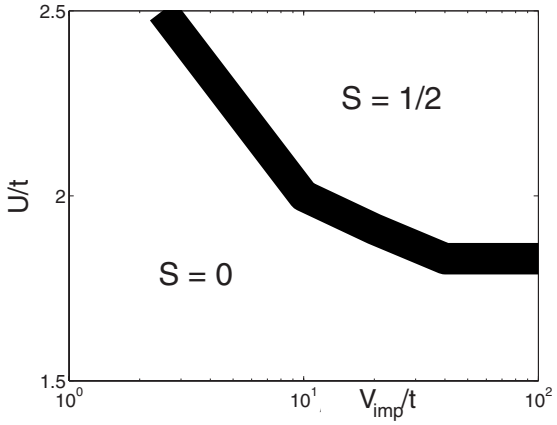

FIG. 40. Zero magnetic-field phase diagram for a single impurity of strength $\epsilon=V_{\mathrm{imp}}$ in the weak-coupling approach, with single band characterized by $t'/t=-0.2$, $n=0.85$, as a function of U. Values of S indicated are total values of S induced by an impurity in the paramagnetic state of a d-wave superconductor. From Harter *et al.*, 2007.

culated the LDOS in each case. In the magnetized state, where a net magnetization corresponding to about 58% of the full moment $S=\frac{1}{2}$ was found, they predicted a small $O(4\ \mathrm{meV})$ splitting of the resonance. Since this is not observed by STM (see Sec. VI.F.2), they also concluded that the impurity state at low T in the superconductor does not carry a static moment.

Similar conclusions were also reached by Zhang *et al.* (2002), who studied an Anderson Hamiltonian in the superconducting state with modified hybridizations connecting the impurity with the four nearest neighbor sites of a Zn. A related model was put forward earlier by Polkovnikov *et al.* (2001), who began, however, from the Kondo limit, and argued that d-wave quasiparticles effectively screen the moment. These models and the interpretation of the STM results have been reviewed by Balatsky *et al.* (2006).

Tsuchiura's work was criticized by Wang and Lee (2002), who argued that the less than full moment found was indicative of a failure of the mean-field procedure adopted. Wang and Lee also studied a vacancy in the superconducting t-J model, but used a slave-boson mean-field decomposition and spatially unrestricted Bogoliubov–de Gennes calculation of all local slave-boson amplitudes. In addition, an additional mean-field spin coupling αJ was added, so it is difficult to judge the origin of differences between the two similar calculations. In any case, the Wang and Lee (2002) result showed either a singlet $S=0$ or doublet $S=\frac{1}{2}$ ground state depending on the additional spin coupling; no singlet phase with alternating magnetization was found. The low-energy LDOS resonance was found in both cases, again slightly split in the doublet state. Wang and Lee also studied the behavior as a function of doping, and found that the static moment (doublet) state is much easier to stabilize in the underdoped phases. More recent numerical work on impurities in the superconducting t-J model by variational MC arrived at a similar qualitative picture of the local spin correlations (Liang and Lee, 2002).

We would like to remind the reader that the $S_z=0$ phase of Fig. 40, similar to the singlet phase of Wang and Lee (2002), while less interesting than the "spontaneous moment" phase is, in fact, representative of the cuprate phase diagram including the superconducting phase (the exception may be the phase labeled "spin glass" in Fig. 2). That is, as emphasized in Sec. IV, there is no experimental evidence at optimal doping for static magnetic moments around nonmagnetic impurities in zero field. In highly underdoped samples at low temperatures, a glassy response is found by μSR (see Sec. VI.E). In most cases of interest, however, we expect that the situation is like that depicted in Fig. 39(a), with zero magnetization until the field is applied. Then, as shown in Fig. 37, the presence of electronic correlations strongly enhances the natural Friedel-like response of the (paired) Fermi liquid such that the sign of the magnetism alternates from site to site. The integrated magnetization in a field of a few tesla may be less than the full spin-$\frac{1}{2}$ moment, however.

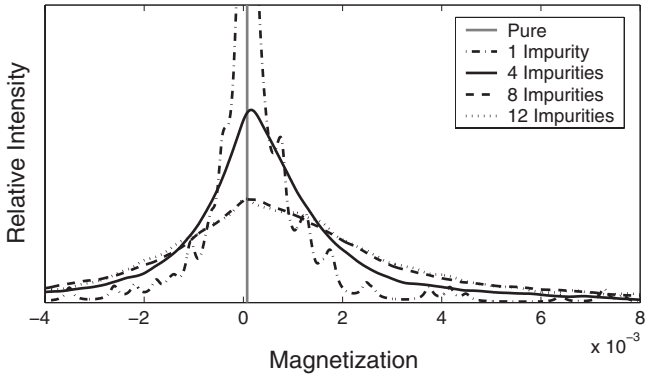

FIG. 41. Magnetization histogram for a 34×34 system with $U=1.75$, and 1, 4, 8, and 12 impurities at $T=0.013$ and $g\mu_B B/2=0.004$. From Harter *et al.*, 2007.

One may ask what the theoretical justification is for using a Fermi-liquid formalism to calculate the magnetic response in the normal state, where experimental evidence points to the absence of Landau quasiparticles. On the other hand, it is presumably justified in the superconducting state due to the collapse of the scattering rate at the transition (Basov and Timusk, 2005) and the recovery of sharp quasiparticle spectral features seen, e.g., in ARPES (Damascelli *et al.*, 2003).

2. Many-impurity interference effects

Chen and Ting (2004) investigated two-impurity interference effects in the system with correlations treated in weak coupling, finding that the magnetization on sites near an impurity in the $S_z=\frac{1}{2}$ phase could be enhanced or suppressed in the presence of a second identical impurity, depending on its orientation with respect to the first. Harter *et al.* (2007) explored this question further in the context of NMR. They looked first at the probability distribution of magnetizations for a single (field-induced) impurity, showing that sites ranging from those close to the impurity up to 12–15 lattice constants away contributed to pronounced satellite lines at certain magnetization values, but that these lines were smeared upon addition of as little as a few tenths of a percent impurities (see Fig. 41). The reason has to do with the fact that those satellites, which when broadened, determine the width of the NMR line arise from sites located in the tails of the nodal quasiparticle bound-state wave functions. As discussed in Sec. VI.C, these tail states interfere with other states when impurities are oriented close to 45° with respect to each other. This applies equally well to the spin as well as the spatial parts of these wave functions. This proposal will be discussed further in comparison to experimental data.

Several authors have discussed the effects of finite disorder on d-wave superconductivity in the presence of electronic correlations. These issues are crucial to the origin of the pseudogap, the properties of the "spin-glass phase" which coexists with superconductivity in several of the cuprates, and the origin of nanoscale gap inhomogeneity in these materials. One school begins from the

weak-coupling end, and emphasizes the competing order aspect of the phenomenon, ascribing inhomogeneity at low doping to competing superconductivity and antiferromagnetism, modulated by disorder (Atkinson, 2005, 2007; Kontani and Ohno, 2006; Mayr *et al.*, 2006; Andersen *et al.*, 2007; Harter *et al.*, 2007). Others work at strong coupling and emphasize the effects of projection (Wang and Lee, 2002; Garg *et al.*, 2008). Although these works differ depending on parameter choice, whether or not long-range interactions are treated, etc., they agree that in the presence of sufficiently strong interactions and sufficient disorder strength, "patches" of (generally incommensurate) magnetic order can be nucleated by impurities. Garg *et al.* (2008) pointed out that in their Gutzwiller approximation-based treatment of weak disorder in *d*-wave superconductors, the effect of projection seemed to be to suppress the formation of the impurity band in the density of states by screening the effective impurity potential; they proposed that the low-energy nodal states of a *d*-wave superconductor were "protected" by strong correlations. Similar effects were also found for strong impurities where correlations were treated within a weak-coupling approach (Andersen and Hirschfeld, 2008).

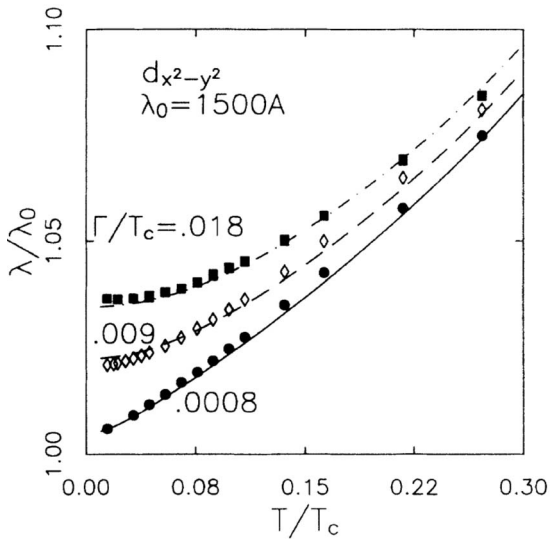

FIG. 42. Fits to penetration depth measurements of Hardy and-coworkers (Bonn *et al.*, 1994) on crystals of near optimally doped YBCO substituted with Zn concentrations 0, 0.15%, and 0.31%, using dirty *d*-wave theory (Hirschfeld *et al.*, 1994) with scattering parameters Γ as indicated.

E. Experiments probing disorder-averaged bulk properties

The SCTMA and its extensions describe the low-energy resonant enhancement of the density of states by strong impurities in dirty *d*-wave superconductor. We now explore the extent to which experiments can confirm this, and particularly those examples where the SCTMA, which neglects correlations, is insufficient. There are many fundamental experiments on bulk cuprate samples which probe the low-energy DOS in the presence of strong disorder, including specific heat, thermal conductivity, magnetic penetration depth, and microwave conductivity measurements. Many have been reviewed by Hussey (2002), who made the case for a qualitative overall agreement of the simple dirty *d*-wave ideas with experiment, but pointed out some discrepancies as well.

As discussed in Sec. IV, early T_c suppression experiments were inconclusive regarding the symmetry of the superconducting order parameter in cuprates. More decisive were penetration depth and NMR experiments which probe low-energy excitations and revealed the existence of the impurity band characteristic of gap nodes and strong potential scatterers. Figure 42 shows London penetration depth measurements reported on good quality Zn-substituted single crystals of YBCO by Bonn *et al.* (1994), together with a fit to the theory of the penetration depth in a *d*-wave superconductor with unitary scatterers (Hirschfeld and Goldenfeld, 1993; Hirschfeld *et al.*, 1994). The increase of the zero-T penetration depth and the $T \to T^2$ crossover observed reflect directly the residual density of states created by strong impurities.

In principle, the asymptotic electronic linear-T term in specific-heat experiments probes the residual DOS as well. From early days in cuprate physics, "anomalous" linear-T terms $C(T) \sim T$ for $T \ll T_c$ in the superconducting state were reported for polycrystalline and later single-crystal samples, and varying field dependences were reported as well (Hussey, 2002). These were shown to be qualitatively consistent with different levels of disorder by Kübert and Hirschfeld (1997). Systematic studies with Zn doping in single crystals were performed (Loram *et al.*, 1990b; Momono and Ido, 1996; Chang *et al.*, 2000; Sisson *et al.*, 2000), verifying the expected dependence of the residual density of states on impurity concentration.

Sisson *et al.* (2000) were the first to systematically compare the magnetic-field dependence of Zn-doped samples with the Schottky anomaly expected on the basis of the assumption of local moments of order $0.3\mu_B$, the typical order of magnitude found for these moments above T_c in optimally doped samples in early direct magnetization experiments (Mendels, Alloul, Collin, *et al.*, 1994; Zagoulaev *et al.*, 1995) on polycrystalline samples. No such effect was observed, leading to the conclusion that any moments present must be Kondo screened by *d*-wave quasiparticles (Cassanello and Fradkin, 1996, 1997; Ingersent, 1996).

We discuss now the effect of impurities on the superfluid condensate from μSR experiments. In high transverse magnetic fields, μSR experiments allow one to measure the superfluid density n_s through the muon spin relaxation rate σ due to the magnetic-field penetration in type-II superconductors. At low temperatures, the ratio $n_s(T \to 0)/m^*_{ab}$ is observed to decrease with increasing impurity concentration, as shown in LSCO, YBCO, and YCaBCO for Ni, Zn (Bucci *et al.*, 1994; Bernhard *et al.*,

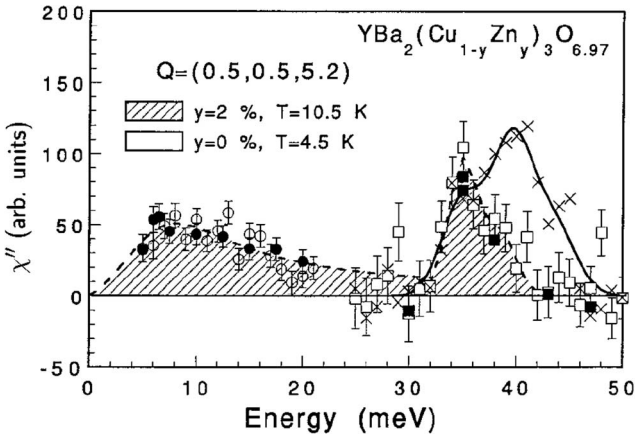

FIG. 43. Imaginary part of dynamical susceptibility χ'' ($\mathbf{q}=\pi,\pi,\omega$) on $YBCZnO_7$ extracted from neutron scattering at $T=10.5$ K. Circles and squares are independent measurements in different energy ranges; open and closed symbols correspond to different methods of determining χ'' on the same sample. Results obtained at 4.5 K in pure sample at the same O content given for comparison by crosses.

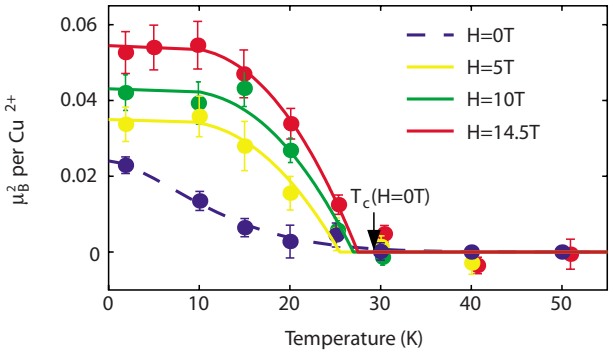

FIG. 44. (Color online) Dependence on temperature of the ordered magnetic moment squared deduced from neutron measurements on LSCO (Lake *et al.*, 2002). The zero-field signal increases gradually below T_c ($H=0$ T), and the dashed line is a guide to the eye. Also plotted is the field-induced signal (equal to the signal measured in field minus the zero-field signal) for fields of $H=5$, 10, and 14.5 T.

1996; Nachumi *et al.*, 1996) and Li impurities (Bobroff, 2005). Bernhard *et al.* (1996) observed that the impurity concentration dependence followed the expected behavior arising from pair breaking due to Zn defects considered here in the unitary limit in a *d*-wave superconductor (Bernhard *et al.*, 1996). In contrast, Uemura's group interpreted this decrease in a Bose condensate picture where T_c is proportional to n_s (Uemura, 2004). The reduction of T_c and n_s is then explained in a "Swiss cheese" model where each Zn creates a nonsuperconducting region around it with an area of $\pi\xi^2$ with ξ the superconducting coherence length (Nachumi *et al.*, 1996). Even though this interpretation seems drastic, it fits the data well with no adjustable parameters. However, local probes such as STM and NMR reveal a more complex situation with a progressive spatial evolution of the electronic properties such as density of states or local magnetism around each Zn. This contradicts the simple granular picture with normal-state islands around each Zn and superconducting condensate beyond. The Swiss cheese model is also in contradiction with the successful disorder-averaged (SCTMA) theory which predicts square-root dependences on impurity concentration, not linear.

Finally, we discuss neutron experiments. The earliest measurements on Zn-substituted YBCO crystals were performed by Sidis and co-workers (Sidis *et al.*, 1996, 2000) In the presence of Zn, they observed a pronounced increase of low-energy spectral weight $\chi(\mathbf{Q},\omega)$, where $\mathbf{Q}=\pi,\pi$, as well as a suppression and shift of the 40-meV resonance mode (Fig. 43). The spin gap at $\sim$30 meV in optimally doped $YBa_2Cu_3O_{7+\delta}$ was still present in the Zn-doped system. Sidis *et al.* (1996) speculated that sites far from the Zn contribute to the resonance mode and spin gap, while regions close to Zn are responsible for low-energy new excitations. Indeed, these excitations can be associated with the enhanced relaxation rate observed in both the normal and superconducting states in regions close to the impurity, as shown in Fig. 19. However, the distinction between the two regions is not straightforward (because of the long-range DOS effects in the superconducting state), unless one uses a local probe such as NMR. This picture is consistent with the existence of a finite DOS at the Fermi level and with NMR findings detailed below.

Lake *et al.* (2002) reported evidence of disorder induced ordered static magnetism in "pure" underdoped LSCO samples with $n_h=10\%$. No such effects were observed near optimal doping (Lake *et al.*, 2001). The basic results are summarized in Fig. 44. In zero field, weak static magnetism with an ordered moment of $\mu\sim 0.1\mu_B/\mathrm{Cu}$ was observed at a wave vector close to but not equal to (π,π). The strength of the overall moment corresponds roughly to a spin $\frac{1}{2}$ per Sr dopant, but if the moments were concentrated exclusively on the random dopant site, they would not lead to an observable signal. It therefore suggests that some fraction of the random dopants nucleate clouds of staggered polarization which then interfere to give an ordered state at low T. Note there is no evidence for such static spontaneous magnetism in any nominally pure YBCO sample except possibly at extremely low doping (Miller *et al.*, 2006).

Kimura *et al.* (2003) studied explicitly the effect of Zn substitution in a large optimally doped LSCO crystal. At zero and small Zn concentrations, no static signal was seen. However, when the Zn concentration reached 1.7%, they too found an elastic peak in the neutron response χ'' near (π,π) which increased by about 15% with decreasing temperature. This group argued that static correlations arose from the long-range antiferromagnetic coherence among the induced moments around different Zn ions. A magnetic signal was also reported in Zn-substituted optimally doped LSCO by Nachumi *et al.* (1996) at low temperatures. Thus it appears that moment formation and staggered ordering is more favored in LSCO than in YBCO, and the tendency

thereto is enhanced as one underdopes the samples. It is interesting to ask what the main difference between the two materials is. One possibility is the different way in which the two are doped, leading to an "intrinsic" Sr disorder in LSCO at the 10% level (see Sec. IV). Andersen *et al.* (2007) showed that in an increasingly random environment the probability of the local electronic structure being favorable at certain locations for induced impurity moments increases, and that when the concentration of these "active" defects is sufficient, an ordered state appears. The "order by disorder" phenomenon observed by neutrons, the distinction between YBCO and LSCO and other intrinsically doped cuprates, and the enhancement of the spin-glass behavior by the addition of Zn emerge from this analysis. More theoretical work on the magnetic properties of heavily disordered materials with out-of-plane defects is needed, however.

F. Experiments probing local properties

Local measurements such as NMR allow one to distinguish between regions close to and far from the impurity. However, in the case of Cu and O nuclear magnetic resonance, Gd electron spin resonance, or Yb Mössbauer experiments, it is not straightforward to separate the two contributions, but requires careful analysis. By contrast, STM or Li NMR measurements give direct insight into the charge and spin behavior on the nearest-neighbor sites. It is only the comparison between the former and latter types of experiments which will permit the resolution of spatially dependent effects of an impurity in a superconducting host.

1. Far from the defect

In the normal state, the existence of local paramagnetic moments around Zn, Li, and other impurities substituted at Cu site was shown by NMR (Mahajan *et al.*, 1994) and was reviewed in Sec. IV. In the superconducting state, similar experiments are not as straightforward because of the vortex lattice induced by the applied magnetic field of a few tesla. This vortex lattice results in a distribution of the local fields at the nuclei sites, which mixes with the impurity effect itself. In the case of Cu NMR, such an effect is negligible since the Cu hyperfine coupling is large, so that any impurity effect on the DOS or the magnetism dominates that of the vortex lattice. The Cu NMR shift measured in Zn and Ni substituted YBCO is reported in Fig. 45 (Ishida *et al.*, 1993).

As already demonstrated in the normal state, the NMR shift of Cu (or O or Y) probes regions far from the defects, while regions close to the defects contribute to the width and/or induce additional satellites to the main NMR line. Above T_c, in the presence of Zn or Ni, no additional shift of the main line could be observed, indicating that regions far from the defects are not affected by substitution. In contrast, below T_c in the case of Zn only, Fig. 45 shows an additional shift induced by impurities. This shift has been interpreted as due to an induced DOS close to Fermi level by Zn. Indeed, NMR

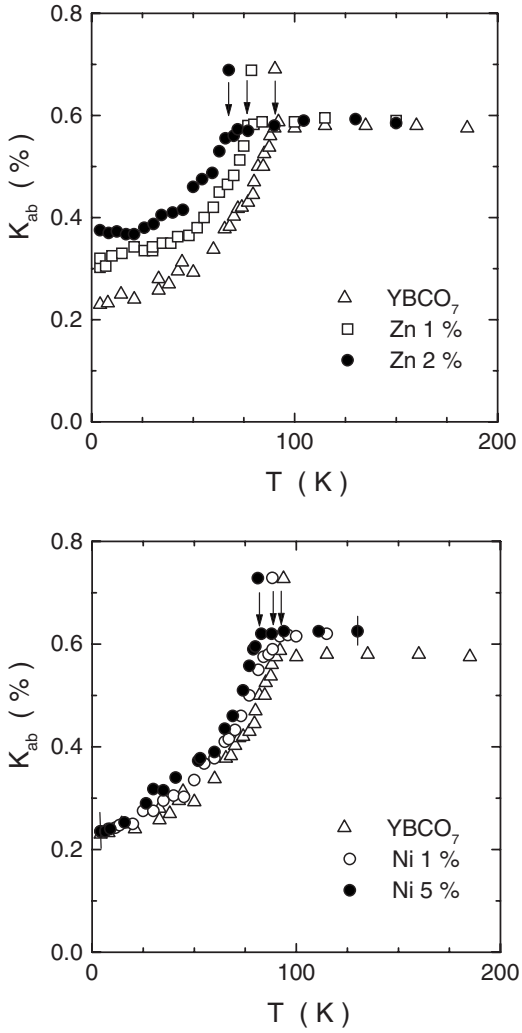

FIG. 45. T dependence of ^{63}Cu Knight shift in $YBCO_7$ with (left) Zn or (right) Ni substituted for Cu (Ishida *et al.*, 1993).

static measurements allow one to probe the DOS at the Fermi level, as demonstrated in the case of metals where the NMR shift measures the Pauli susceptibility (Slichter, 1998). In the present case, this additional shift represents the residual DOS far from impurities, which confirms that only Zn induces a sizable DOS at the Fermi level. Similar results were obtained using Gd electron-spin resonance (Janossy *et al.*, 1994). Dynamical measurements such as longitudinal nuclear relaxation T_1 which can be measured on ^{63}Cu nuclei or on the Yb nuclei by Mössbauer effect also reveal this DOS induced effect by Zn (Hotta, 1993; Ishida *et al.*, 1993; Hodges *et al.*, 1995). Ishida *et al.* (1993) analyzed T_1 as originating from two contributions, from regions either close to or far from Zn. They interpreted the T_1 variations with impurity concentration in a d-wave model where the impurities induce some residual density of states. However, as already argued in the normal state (Sec. IV.C.4) (Itoh *et al.*, 2003), the identification of the two contributions is not clear. Furthermore, an additional contribution to the relaxation may be expected from antiferromagnetic spin fluctuations enhanced in the vicinity of the impurity

even in zero applied field (Itoh *et al.*, 2001, 2003) which has the same origin as that studied on Li or Y in Sec. IV.

2. Near the defect

The most local picture we have of impurity states in cuprates is provided in principle by scanning tunneling microscopy (STM). Many aspects of the STM results were reviewed by Balatsky *et al.* (2006). The first success of the STM technique was the observation of resonant states around magnetic impurities in conventional superconductors (Yazdani *et al.*, 1997), followed by nonmagnetic defects at low temperatures in the cuprate $Bi_2Sr_2CaCu_2O_8$ (Hudson *et al.*, 1999; Yazdani *et al.*, 1999; Pan *et al.*, 2000a). The latter discovery confirmed earlier theoretical proposals that such states should be reflected in the LDOS of *d*-wave superconductors (Byers *et al.*, 1993; Balatsky *et al.*, 1995). The HTS compound Bi-2212 has been used for most STM studies because of its high quality surfaces when cleaved between BiO layers. Scanning spectroscopy measurements were performed on Zn and Ni impurities (Pan *et al.*, 2000b; Hudson *et al.*, 2001), as well as on native defects (Hudson *et al.*, 1999, 2003) which apparently occur naturally in as-grown crystals. These results are summarized in Fig. 46, where it is shown that different defects have different resonant energies within the superconducting gap, and in the case of Ni a double-peak structure is observed. In addition, the spatial patterns when the surface is scanned at the resonant energy appear to differ from impurity to impurity, and in the case of Ni show a striking rotation between positive and negative bias.

^{7}Li NMR experiments allow further insight into the defect's immediate neighborhood. Li substituted at the Cu site is identical to Zn in the sense that it induces similar T_c reduction and local induced magnetism above T_c (Bobroff *et al.*, 1999); see Sec. IV. The Li NMR shift has been demonstrated to probe only the local spin density on its four neighboring Cu, in both the underdoped and optimally doped regimes. The shift displays a Curie-Weiss-like behavior which signals the appearance of the induced staggered magnetism around the nonmagnetic impurity. In the superconducting state of underdoped YBCO, the Curie behavior observed above T_c indicating the presence of such local moments on nearest-neighbor Cu persists below T_c with no change, as shown in Fig. 47 (Bobroff *et al.*, 2001). This is evidence that induced magnetism on the nearest-neighbor site is not affected in the underdoped case by superconductivity. By contrast, a dramatic increase of the Li shift is observed below T_c in an optimally doped sample (see Fig. 47). This was originally interpreted as a reduced Kondo screening of the moment in the superconducting state since it can be fitted with the same Curie-Weiss behavior as above T_c but with a reduced Curie-Weiss temperature (Bobroff *et al.*, 2001). As shown below, the LDOS peak detected by STM experiments can contribute as well to the induced local susceptibility near the defect.

The LDOS pattern predicted for a strong impurity in a *d*-wave superconductor with noninteracting quasiparticles was shown in Fig. 36. The crucial qualitative difference between the effect predicted and observed is the existence of an intensity maximum on the central site of the impurity pattern in the case of Zn, which is impossible for potentials V_{imp} larger than the bandwidth, since electrons are effectively excluded from this site. Theoretical efforts to understand this paradox have fallen into three categories. The first is specific to the STM technique and relies on the fact that the impurity states are localized in the CuO_2 plane, two layers below the BiO surface; the intervening layers are then argued to provide a primary tunneling path which samples not the Cu below the tip, but preferentially the four nearest neighbors (Zhu *et al.*, 2000; Martin *et al.*, 2002). Some indirect support for this point of view has been provided by density-functional theory (Wang *et al.*, 2005). A second class of approaches (Polkovnikov *et al.*, 2001) attributes the redistribution of spatial spectral weight to

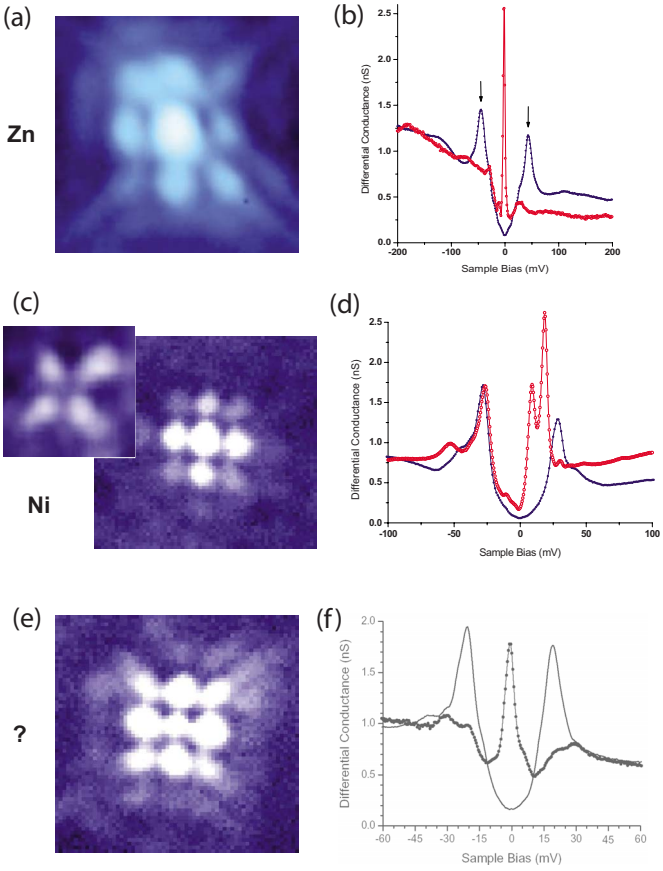

FIG. 46. (Color online) Experimental STM impurity spatial patterns at resonance and associated spectra. (a) Observed differential conductance around Zn impurity at −1.2 mV. (b) Comparison of spectra directly above Zn impurity site and at site far from impurity. (c) Observed STM intensity around Ni impurity site at 9 mV (inset: pattern at −9 mV). (d) Comparison of spectra directly above Ni impurity site and away from Ni. (e) Observed STM intensity around native defect, possibly Cu vacancy at −0.5 mV. (f) Comparison of spectra directly above native defect (thick solid line) and away from defect (thin solid line). Note that in the images (a), (c), and (f) the Cu-O bond is at 45° with respect to the horizontal.

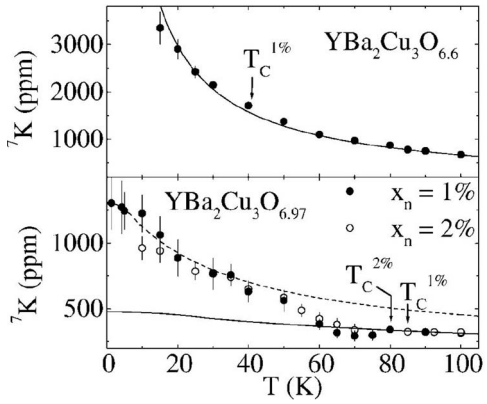

FIG. 47. T variation of the ^{7}Li NMR shift ^7K in YBCO (Bobroff *et al.*, 2001). Top: Underdoped O6.6 sample, with Curie-Weiss fit (solid line). Bottom: Optimally doped O6.97 samples, Kondo model susceptibility fit to data above (solid line) and below T_c (dashed line).

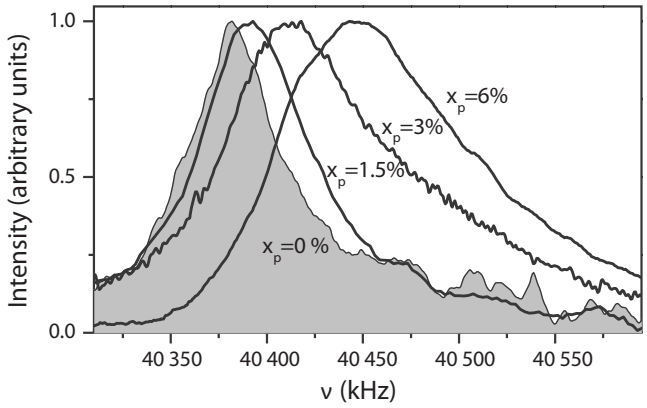

FIG. 48. ^{17}O NMR lines in $YBCO_7$ at T=15 K for three different in-plane concentrations of Zn x_p=1.5, 3, and 6 % shown relative to the pure case (in gray). From Ouazi *et al.* 2006.

nonlocal Kondo screening, an effect neglected in the calculations described in Sec. VI.D. Balatsky *et al.* (2006) argued that these models require unphysically small nonmagnetic compared to magnetic interactions to explain STM spectra. Finally, one can obtain LDOS patterns similar to experiment for both Zn and Ni by assuming a distribution of site potentials to tune the weights of on-site and nearest-neighbor LDOS (Flatté, 2000; Tang and Flatté, 2002, 2004). While the bare impurity potential is much shorter range, it may be that the phenomenological parameters used in these models are approximations to dynamically generated ones in a more complete theory; see Sec. V. There is currently no consensus as to which of these explanations, if any, is appropriate to describe both NMR and STM impurity results. Resolution of this "paradox" is crucial to the interpretation of STM images and the exploitation of their potential to provide local information on cuprates and other strongly correlated materials.

In order to resolve the impurity effect beyond the nearest-neighbor Cu sites, one has to use ^{89}Y, ^{63}Cu, or ^{17}O NMR as demonstrated in the normal state (see Sec. IV) (Ouazi *et al.*, 2006). In the superconducting case, only a ^{17}O NMR study has been performed, leading to typical spectra displayed in Fig. 48. They showed that a nonmagnetic impurity such as Zn or Li induces an asymmetric broadening of the line together with a shift toward higher frequencies (Ouazi *et al.*, 2006). The latter effect is similar to that measured with Cu NMR and is related to the residual DOS close to E_F induced by defects sitting far from the measured nuclei. On the other hand, the Zn-induced broadening is due to the induced magnetism and LDOS closer to the defect. For a more quantitative analysis, the vortex lattice effects have to be separated from the impurity effects by carrying out the experiment at different applied fields. Indeed, the field distribution due to the vortex lattice leads to a roughly field-independent broadening of the line, while both impurity-induced LDOS and paramagnetic effects lead to a broadening linear in field. The fact that Zn or Li broaden the line on both high- and low-frequency sides is evidence for the alternating behavior of the induced cloud, similarly to the normal state. However, the broadening is not symmetric anymore as in the normal state, but asymmetric toward high frequencies. This can be understood as due to the additional LDOS contributions which leads to a positive shift. This is confirmed by the fact that the Ni-induced broadening does not show such an asymmetry, as expected since it does not induce any LDOS close to Fermi level, in contrast with Zn [see Fig. 46(d)]. In summary, Cu, O, and Li NMR experiments imply that a nonmagnetic impurity induces simultaneously a staggered magnetization similar to that observed in the normal state, with typical extension of a few cell units, together with a spatially decaying LDOS contribution which is still sizable far from the impurity.

The experiments presented above in both the superconducting and normal states require an explanation in terms of a combination of LDOS enhancement of the spin susceptibility and an induced magnetic moment around the impurity sites. While it is clear that, due to the resonant nature of the LDOS effects in the superconducting state, these effects will be more important below T_c, attempts to explain the superconducting state data without invoking induced moments must encounter difficulties. For example, Williams *et al.* (2000) proposed that quasiparticle resonant states, corresponding to those imaged by STM experiments around Zn atoms in BSCCO-2212 (Pan *et al.*, 2000b), are responsible for the enhanced magnetic response near Zn seen in NMR. Chang *et al.* (2004) then argued that, for a single nonmagnetic impurity, the temperature dependence of the observed spin-lattice relaxation time and Knight shift can be qualitatively understood in terms of LDOS enhancement due to impurity bound states alone. First, significant T-dependent enhancements of local susceptibilities near nonmagnetic impurities occur in the normal state of optimally doped cuprates as well. A "LDOS-only" approach cannot account for this since impurities do not produce LDOS resonances in the normal (metallic) state. Second, the NMR experiments on these materials clearly show that the magnetization near a Zn al-

ternates in sign in both the superconducting and normal states, as discussed above. At low T, where the homogeneous polarization of the d-wave superconductor is negligible, the Friedel oscillation in the LDOS induced by an impurity must perforce be entirely positive, i.e., it cannot give rise to the observed broadening on the negative side of the line. Finally, the "Knight shift" calculated by Chang *et al.* (2004) is defined to be a local susceptibility enhancement near the impurity; in fact, the measured Knight shift in experiments where the nucleus is distinct from the impurity itself is the shift of the *total* NMR line, determined by sites far from the impurities.

These two effects can be understood in a unified picture in terms of the enhanced local susceptibility due to the effect of correlations on the resonant impurity state (Harter *et al.*, 2007). In this study, from the magnetization histogram computed and shown in Fig. 41, oxygen NMR lines could be computed for various impurity concentrations including the effect of vortices. A quantitative agreement is found with the experimental results shown in Fig. 48, tending to confirm the validity of this picture.

G. Summary

We have reviewed the simple theory of nonmagnetic impurities in d-wave superconductors, discussed attempts which have been made to include electronic correlations beyond BCS pairing in this framework, and compared the results with experiments. The important difference between the superconducting state and the normal state of optimally to overdoped cuprates is the existence of low-energy states of a quasiparticle virtually bound to nonmagnetic potentials as, e.g., Zn impurities. These bound states should exist even in the d-wave superconductor without additional correlations, and have weak paramagnetic character to the extent that they enhance the LDOS locally around the impurity sites. Such LDOS enhancements have been observed by STM experiments near impurities (although the spatial distribution of LDOS weight is not completely understood). NMR experiments find, however, that the induced spin polarizations near these sites are much larger than expected according to any calculation relying on BCS-type models alone, and we are forced to the conclusion that the usual "dirty d-wave theory" must be supplemented by interactions which lead to paramagnetic moment formation around the impurity. As discussed in Sec. IV for the normal state as well, electronic correlations of antiferromagnetic character are essential for the observations.

For optimally doped cuprates, the moments are relatively weak and well screened, but as the superconducting state is entered NMR measurements of the local susceptibility show that the opening of the superconducting gap reduces this screening, as expected. This behavior is reminiscent of Kondo screening, but has also been reproduced by theories which neglect processes which lead to the usual Kondo effect. It appears, furthermore, that a description beyond the single-impurity picture, accounting for interference of individual impurity states, is necessary to understand experiments with impurities at percent level or higher. Experiments such as specific heat, NMR Knight shift, and penetration depth which probe the average density of states primarily far from the impurity sites are sensitive to this interference and the formation of an impurity band in the superconducting state. These appear to be in close agreement with each other and with the predictions of the SCTMA.

On the other hand, at low doping it is to be expected that discrepancies will increase in underdoped samples as the magnetic character of the disorder is enhanced. In this case, strong moment formation has already occurred by the time the superconducting transition is reached, and the local susceptibility is found to be Curie-like down to the lowest temperatures, by NMR measurements. Fewer experimental data are available to support this premise, however. In disordered cuprates such as LSCO and BSCCO, a range of experiments including NMR and μSR have observed the freezing of spins in an extension of the spin-glass phase into the superconducting states. These appear to be due to disorder-induced magnetic centers which at sufficient concentration or correlation strength (underdoping) interfere coherently to create long-range magnetic order visible to neutrons. The magnetic disorder should scatter quasiparticles efficiently as in the normal state, and lead to a modification of 'dirty d-wave' predictions of superconducting transport at low T, as observed for thermal conductivity measurements (Andersen and Hirschfeld, 2008).

VII. CONCLUSIONS

The study of strongly correlated electron systems is quite challenging and requires the most sophisticated experimental and theoretical techniques. The primary approach emphasized here has been the investigation of the response of such systems to the perturbation introduced by point defect impurities. As in the classic case of Friedel oscillations in normal metals, the study of defects is valuable because they have the potential to probe aspects of the underlying pure system, e.g., magnetic and charge correlation lengths, sometimes difficult to do in situations when the fundamental nature of the states being probed is not always understood. Thus one of our primary motivations to study defects in such systems has been to try to understand what impurities tell us about the pure materials. This has consequently led us to show how extrinsic properties can be "subtracted" from an analysis of experiments on "pure" samples, in order to reveal the generic features.

Impurity states in strongly interacting materials are most unusual, and manifest a variety of phenomena depending on dimensionality, strength of correlations, carrier doping, temperature, and magnetic field. The quantum impurity problem of a spinless potential in a correlated host has attracted a great deal of theoretical attention, and promises to pose as much of a challenge as the Kondo problem. The largest effects of such a defect are naturally found in its immediate neighborhood,

within a correlation length of order a few lattice spacings, such that local probes such as NMR, NQR, μSR, or STM are valuable tools to investigate the fingerprints of correlations at small length scales. On the other hand, impurities also influence magnetic and transport properties of bulk materials, and therefore to a lesser extent we also considered techniques which measure global responses of these systems (neutron scattering, photoemission, resistivity, Hall and optical conductivities, and Raman scattering).

In a strongly correlated electron system, new length scales appear which reflect the interactions present, and which can be probed by impurities. For example, the magnetic response of an impurity in an interacting 1D system is not only much larger than the usual Friedel response to an impurity in a free Fermi gas, but also manifests a spatial decay which reflects directly the magnetic correlation length ξ of the pure system. To gain insight into the physics of correlated 2D systems, we considered the low-energy states of 1D systems, where many models are exactly soluble (Sec. III). There, a small change in a single hopping amplitude, magnetic coupling, or local potential is enough to produce total backscattering in the spin or charge channels at $T=0$ (the two situations can be discussed separately because of spin-charge separation). Application of a uniform magnetic field H to a spin chain or ladder containing a nonmagnetic site yields a local alternating magnetic polarization with an amplitude proportional to H and a spatial extent generically of the order of ξ.

Turning to the 2D (cuprate) case, experiments performed above T_c show that spinless defects substituting for Cu atoms in the planes produce a large alternating magnetic polarization on the sites surrounding the impurity. The size of the moment is orders of magnitude larger than that observed in conventional 3D metals with isovalent spinless impurities, where the effect is attributable to simple Friedel-type oscillations in the LDOS (Sec. IV). With the exception of the so-called spin-glass phase, NMR experiments indicate that the moments are strictly paramagnetic, i.e., not frozen at zero field. The maximum amplitude of the staggered polarization is of the form $CH/(T+\Theta)$, and the extention $\xi_{\rm imp}$ of this polarization away from the defect shows a similar T dependence. At optimal doping in YBCO, $\xi_{\rm imp}\approx 3$ unit cells. This value is consistent with that deduced from INS measurements of Zn doped YBCO, and compares well with the correlation length ξ of the pure system, as expected by analogy with the 1D case. In two dimensions, rigorous proofs are not available, but all approximate methods, including strong-coupling RVB-type or nearly antiferromagnetic Fermi-liquid scenarios, are, in different regimes of the phase diagram, successful in producing magnetic and transport responses close to those found experimentally (Sec. V). This underscores the importance of correlations in these materials, and the ability of impurity probes to reveal correlations which can be hard to detect in the homogeneous state.

The existence of a characteristic temperature scale Θ in the magnetic response evokes Kondo physics, and we have argued that many experimental observations from NMR and transport properties display a consistent phenomenology with a screened moment formed around a nonmagnetic impurity. For increasing doping, beyond the optimally doped regime Θ gets larger and larger and exceeds 200 K. As a result, both the amplitude of the alternating polarization and $\xi_{\rm imp}$ decrease. Similarly, the large $-\ln T$ upturns of the resistivity, which initially scale with defect content in the underdoped regime, progressively evolve upon overdoping toward the weak-localization behavior expected for a Fermi liquid metal.

Nevertheless, we have shown that a number of considerations suggest caution in taking the Kondo analogy too literally. In particular, the evolution toward the overdoped regime, as the physics gets closer to the Fermi-liquid limit, is yet to be understood. In a regular metal, a nonmagnetic impurity produces potential, rather than magnetic, scattering. Hence one does not expect magnetic signatures when interactions become weak enough, and for spinless impurities.

NMR and μSR suggest that the staggered magnetization evolves from a resonance to a bound state as hole doping is reduced, bringing the system close to the AF boundary. This behavior is precisely that found in theoretical modelings of spinless impurities in the framework of t-J or Hubbard models, which ignore processes leading to Kondo screening. Theoretical analysis based on slave bosons shows that the response of a strongly correlated system to a nonmagnetic defect is qualitatively similar in two dimensions and one dimension. Related theoretical treatments of transport neglecting Kondo screening also predict such upturns in the presence of strong Coulomb repulsions and suggest the need to be close to the AF instability.

Ultimately, these questions regarding impurity states may not be resolved until consensus is reached on the peculiar normal state of the "pure" cuprates itself. We believe, nevertheless, that the impurity experiments provide important clues as to the nature of this state. For instance, while descriptions of the impurity-induced moment phenomenon from both the weak- and strong-coupling sides have proven successful, the strength of the Coulomb repulsion U or exchange J has to be tuned to a value large enough to bring the system close to a magnetic instability. It is tempting to speculate that this is not an accident, but indicative of a renormalization-group flow. In one dimension, where U controls the magnitude of the effect or rate of approach to the fixed point, the effect is clear, but in two dimensions the connection remains unresolved.

Impurity studies offer insight into fundamental aspects of the cuprate phase diagram and offer points of reference against which theories may be compared. For example, in the pseudogap phase, magnetic properties of Cu sites located far from the impurity sites are quantitatively similar to those of the pure state. In particular, the opening of the pseudogap observed by NMR above T_c is not affected by spinless impurities. Further confirmation

of this observation comes from resistivity measurements of underdoped samples.

In the superconducting state of the cuprates, much was learned about the *d*-wave nature of the cuprate state from impurity substitutions (Sec. VI). This is because impurities in such states break Cooper pairs and mix order parameters with different signs on different parts of the Fermi surface, acting as a simple phase-sensitive probe of order parameter symmetry. Thus nonmagnetic impurities depress the critical temperature of the cuprates and reduce the area of the superconducting dome. In the optimal to overdoped cases, several scenarios have been advocated to explain the observed linear decrease of T_c, down to zero, with the defect concentration, but a consensual theoretical description is still lacking.

Single impurities in *d*-wave superconductors give rise to Andreev bound states, which overlap when sufficiently close, giving rise to a *d*-wave impurity band. In the cuprates, NMR experiments show a paramagnetic response to the impurity qualitatively similar to the normal state, albeit with a smaller Θ at a given doping. However, due to impurity resonances, the $E=0$ response (LDOS effect) gives a significant contribution to the magnetization. The enhanced (small-Θ) magnetic response observed in both the superconducting and underdoped normal states might be related to the opening of a spectral gap in both cases, leading to the formation of a nearly bound state.

At present the NMR experiments on Zn and other in-plane Cu subtituents are not consistent with STM spectroscopy on Zn impurities in BSCCO. On the one hand, the absence of a split LDOS peak is consistent with the paramagnetic (singlet) nature of the impurity state; on the other hand, the LDOS spatial pattern is at odds with what one would anticipate from NMR, namely, a maximum LDOS on the near neighbors (and no LDOS on the impurity site).

In closing, we stress that our conclusions regarding impurity-induced magnetism, carefully developed in controlled situations in quasi-1D systems, as well as cuprate materials with impurity substitutions and electron irradiation, also have implications for the nominally pure cuprates. The same kind of analysis can be applied to a wide class of other correlated electron systems, such as heavy fermions and 2D organic conductors, provided materials problems are mastered to allow introduction of controlled defects.

Generically, the material structures considered often consist of active layers (chains, ladders, planes) separated from each other by buffer regions which may contain charge reservoirs. The thickness of the buffer region and the nature of the molecular bonding determine the strength of the couplings between active layers. In quasi-1D materials it is difficult to change the carrier content of the active layer, so that hydrostatic or chemical pressure are used to change the bandwidth and hence the ratio of kinetic to Coulomb energies. In quasi-2D cuprate compounds, it is possible to tune the carrier concentration of the active layer through heterovalent charge substitutions in the buffer layers. Thus, in such materials, the very process allowing the change of the ratio of kinetic to correlation energies brings in uncontrolled disorder into the system and affects magnetic and transport properties of strongly correlated systems.

We have shown that the magnetic effects due to a single nonmagnetic impurity are enhanced by increasing electronic correlations and decreasing temperature, and that new phenomena arise due to the interference of these states in dirty systems. These effects explain the disordered spin-glass phase of the underdoped cuprates, but also underlie some observed behavior in the superconducting and pseudogap phase which have been previously attributed to the competition of homogeneous superconducting and antiferromagnetic states, or to some more exotic cause. In the superconducting state, well-defined quasiparticles allow the most controlled theoretical treatments. Here the effects of strong correlations and impurity-induced magnetism are small for optimal to overdoped systems, accounting for the success of the dirty *d*-wave approach, but they become more prominent in the underdoped regime. INS and μSR experiments on YBCO suggest that the alternating polarization fluctuates at very low frequencies, but that disordered moments freeze in LSCO, BSCCO, and other intrinsically disordered systems, creating glassy behavior and, under some circumstances, ordered antiferromagnetism coexisting with superconductivity.

One should be careful not to ignore disorder and inhomogeneity entirely and not go too far either in assigning the origin of high-temperature superconductivity itself to such effects. One can learn much from studying the "dichotomy" between those materials which are clean because they can be doped and rendered superconducting in stoichiometric form—primarily Y-123 and Y-248—and the majority of materials which are intrinsically disordered. These out-of-plane defects require further study; they may act as simple scatterers and pair breakers, or they may influence the pair interaction in more subtle ways. Unquestionably, the phase diagrams of the nominally pure materials are strongly influenced by the type of doping and defects, and one possible route to higher T_c's will be to understand and control the role of disorder.

ACKNOWLEDGMENTS

The authors are indebted to the many individuals who have contributed to the research discussed in this article. First and foremost to our long-term collaborators: B. M. Andersen, N. Blanchard, G. Boyd, W. Chen, G. Collin, D. Colson, A. Dooglav, A. Kampf, A. Keren, A. MacFarlane, A. V. Mahajan, J. F. Marucco, P. Mendels, S. Ouazi, F. Rullier-Albenque, M. Schmid, E. Semel, Y. Yoshinari, and L.-Y. Zhu. We also thank colleagues for providing insightful comments for this review or for stimulating discussions which enhanced our understanding of the subject: I. Affleck, W. A. Atkinson, A. V. Balatsky, P. Bourges, T. Giamarchi, M. Greven, K. In-

gersent, G. Khalliulin, T. S. Nunner, C. Panagopoulos, D. Poilblanc, D. J. Scalapino, J. E. Sonier, Y. Sidis, and I. Vekhter. Partial support for this research was provided by ONR Grant No. N00014-04-0060, DOE Grant No. DE-FG02-05ER46236, and by visiting scholar grants from C.N.R.S. and P.I.T.P. (P.J.H.). P.J.H. is grateful to the Laboratoire de Physique des Solides (Orsay) for hosting a sabbatical during which this work was begun.

REFERENCES

Abe, Y., K. Segawa, and Y. Ando, 1999, Phys. Rev. B **60**, R15055.
Abrahams, E., and C. M. Varma, 2000, Proc. Natl. Acad. Sci. U.S.A. **97**, 5714.
Abrikosov, A., and L. Gorkov, 1960, Zh. Eksp. Teor. Fiz. **39**, 1781 [Sov. Phys. JETP **12**, 1243 (1961)].
Adachi, S., Y. Itoh, T. Machi, E. Kandyel, S. Tajima, and N. Koshizuka, 2000, Phys. Rev. B **61**, 4314.
Affleck, I., 1989, J. Phys.: Condens. Matter **1**, 3047.
Affleck, I., T. Kennedy, E. Lieb, and H. Tasaki, 1987, Phys. Rev. Lett. **59**, 799.
Affleck, I., and J. B. Marston, 1988, Phys. Rev. B **37**, 3774.
Alet, F., and E. Sørensen, 2000, Phys. Rev. B **62**, 14116.
Alloul, H., 1977, Physica B & C **86-88**, 429.
Alloul, H., 1991, in *High Temperature Superconductivity*, Proceedings of Scottish Universities Summer School in Physics, edited by D. P. Tunstall and W. Barford (Hilger, New York), p. 207.
Alloul, H., and P. Bernier, 1973, Ann. Phys. (Paris) **8**, 169.
Alloul, H., J. Bobroff, W. MacFarlane, P. Mendels, and F. Rullier-Albenque, 2000, J. Phys. Soc. Jpn. **69**, 114.
Alloul, H., and P. Dellouve, 1987, Phys. Rev. Lett. **59**, 578.
Alloul, H., P. Mendels, H. Casalta, J.-F. Marucco, and J. Arabski, 1991, Phys. Rev. Lett. **67**, 3140.
Alloul, H., T. Ohno, J. Casalta, J. Marucco, P. Mendels, J. Arabski, G. Collin, and M. Mehbod, 1990, Physica C **171**, 419.
Alloul, H., T. Ohno, and P. Mendels, 1989, Phys. Rev. Lett. **63**, 1700.
Ami, T., M. K. Crawford, R. L. Harlow, Z. R. Wang, D. C. Johnston, Q. Huang, and R. W. Erwin, 1995, Phys. Rev. B **51**, 5994.
Andergassen, S., T. Enss, V. Meden, W. Metzner, U. Schollwöck, and K. Schönhammer, 2004, Phys. Rev. B **70**, 075102.
Andersen, B., and P. Hedegaard, 2003, Phys. Rev. B **67**, 172505.
Andersen, B., and P. Hirschfeld, 2008, Phys. Rev. Lett. **100**, 257003.
Andersen, B., P. J. Hirschfeld, A. Kampf, and M. Schmid, 2007, Phys. Rev. Lett. **99**, 147002.
Andersen, B., A. Melikyan, T. Nunner, and P. Hirschfeld, 2006, Phys. Rev. Lett. **96**, 097004.
Anderson, P., 1959, J. Phys. Chem. **11**, 26.
Anderson, P., 1961, Phys. Rev. **124**, 41.
Anderson, P., 1997, *The Theory of Superconductivity in the High-T_c Cuprate Superconductors* (Princeton University Press, Princeton).
Anderson, P., J. Liu, and R. Shelton, 1997, Phys. Rev. B **56**, 11014.
Anderson, P. W., 1991, Phys. Rev. Lett. **67**, 2092.
Ando, Y., G. Boebinger, A. Passner, T. Kimura, and K. Kishio, 1995, Phys. Rev. Lett. **75**, 4662.
Ando, Y., Y. Kurita, S. K. S. Ono, and K. Segawa, 2004, Phys. Rev. Lett. **92**, 197001.
Anfuso, F., and S. Eggert, 2006, Europhys. Lett. **73**, 271.
Arovas, D., and A. Auerbach, 1988, Phys. Rev. B **38**, 316.
Arovas, D., and S. Girvin, 1992, in *Exact Questions to Some Interesting Answers in Many Body Physics*, edited by C. Campbell and E. Krotscheck, Recent Progress in Many Body Physics Vol. 3 (Plenum, New York), pp. 315–344.
Aryanpour, K., M. Hettler, and M. Jarrell, 2002, Phys. Rev. B **65**, 153102.
Atkinson, W., 2005, Phys. Rev. B **71**, 024516.
Atkinson, W., 2007, Phys. Rev. B **75**, 024510.
Atkinson, W., P. Hirschfeld, and A. MacDonald, 2000, Physica C **341-348**, 1687.
Atkinson, W. A., 2002, private communication.
Atkinson, W. A., P. J. Hirschfeld, A. H. MacDonald, and K. Ziegler, 2000, Phys. Rev. Lett. **85**, 3926.
Atkinson, W. A., P. J. Hirschfeld, and L. Zhu, 2003, Phys. Rev. B **68**, 054501.
Auerbach, A., 1994, in *Interacting Electrons and Quantum Magnetism*, edited by J. Birman, H. Faissner, and J. Lynn, Graduate Text in Contemporary Physics (Springer-Verlag, New York).
Azuma, M., Y. Fujishiro, M. Takano, M. Nohara, and H. Takagi, 1997, Phys. Rev. B **55**, R8658.
Azuma, M., Z. Hiroi, M. Takano, K. Ishida, and Y. Kitaoka, 1994, Phys. Rev. Lett. **73**, 3463.
Balatsky, A., and M. I. Salkola, 1996, Phys. Rev. Lett. **76**, 2386.
Balatsky, A., M. I. Salkola, and A. Rosengren, 1995, Phys. Rev. B **51**, 15547.
Balatsky, A., I. Vekhter, and J.-X. Zhu, 2006, Rev. Mod. Phys. **78**, 373.
Balian, R., and N. Werthamer, 1963, Phys. Rev. **131**, 1553.
Barnes, S., 1976, J. Phys. F: Met. Phys. **6**, 1375.
Barnes, S., 1977, J. Phys. F: Met. Phys. **7**, 2637.
Basov D. N., B. Dabrowski, and T. Timusk, 1998, Phys. Rev. Lett. **81**, 2132.
Basov, D., and T. Timusk, 2005, Rev. Mod. Phys. **77**, 721.
Batista, C., K. Halberg, and A. Aligia, 1998, Phys. Rev. B **58**, 9248.
Batlogg, B., S. W. Cheong, and L. W. Rupp, Jr., 1994, Physica B **194-196**, 173.
Bernhard, C., J. L. Tallon, C. Bucci, R. D. Renzi, G. Guidi, G. V. M. Williams, and C. Niedermayer, 1996, Phys. Rev. Lett. **77**, 2304.
Bethe, H., 1931, Z. Phys. **71**, 205.
Bickers, N., 1987, Rev. Mod. Phys. **59**, 845.
Bickers, N., D. Scalapino, and R. White, 1989, Phys. Rev. Lett. **62**, 961.
Birgenau, R., and G. Shirane, 1989, in *Physical Properties of High Temperature Superconductors I*, edited by D. M. Ginsberg (World Scientific, Singapore), p. 151.
Bobroff, J., 2005, Ann. Phys. (Paris) **30**, 1.
Bobroff, J., H. Alloul, W. MacFarlane, P. Mendels, N. Blanchard, G. Collin, and J. F. Marucco, 2001, Phys. Rev. Lett. **86**, 4116.
Bobroff, J., H. Alloul, P. Mendels, V. Viallet, J. Marucco, and D. Colson, 1997, Phys. Rev. Lett. **78**, 3757.
Bobroff, J., H. Alloul, S. Ouazi, P. Mendels, A. Mahajan, N. Blanchard, G. Collin, and J. F. Marucco, 2002, Phys. Rev. Lett. **89**, 157002.
Bobroff, J., H. Alloul, Y. Yoshinari, A. Keren, P. Mendels, N. Blanchard, G. Collin, and J. Marucco, 1997, Phys. Rev. Lett.

79, 2117.
Bobroff, J., H. Alloul, Y. Yoshinari, A. Keren, P. Mendels, N. Blanchard, G. Collin, and J. F. Marucco, 1998, Phys. Rev. Lett. **80**, 3663.
Bobroff, J., W. MacFarlane, H. Alloul, P. Mendels, N. Blanchard, G. Collin, and J. Marucco, 1999, Phys. Rev. Lett. **83**, 4381.
Bonn, D., S. Kamal, K. Zhang, R. Liang, D. J. Baar, E. Klein, and W. N. Hardy, 1994, Phys. Rev. B **50**, 4051.
Bonner, J., and M. Fisher, 1964, Phys. Rev. **135**, A640.
Borkowski, L., and P. Hirschfeld, 1994, Phys. Rev. B **49**, 15404.
Borkowski, L., P. Hirschfeld, and W. Putikka, 1995, Phys. Rev. B **52**, R3856.
Boucher, J., and M. Takigawa, 2000, Phys. Rev. B **62**, 367.
Bourbonnais, C., and D. Jérome, 1999, in *Advances in Synthetic Metals, Twenty Years of Progress in Science and Technology*, edited by P. Bernier, S. Lefrant, and G. Bidan (Elsevier, New York), pp. 207–261.
Bourges, P., 1998, in *The Gap Symmetry and Fluctuations in High Temperature Superconductors*, edited by J. Bok *et al.* (Plenum, New York), pp. 349–371.
Bourges, P., Y. Sidis, B. Hennion, R. Villeneuve, J. F. Marucco, and G. Collin, 1996, Czech. J. Phys. **46**, 1155.
Bridges, F., J. B. Boyce, T. Claeson, T. H. Geballe, and J. M. Tarascon, 1989, Phys. Rev. B **39**, 11603.
Brinkman, W., and T. Rice, 1970, Phys. Rev. B **2**, 4302.
Brunel, V., M. Bocquet, and T. Jolicoeur, 1999, Phys. Rev. Lett. **83**, 2821.
Bucci, C., P. Carretta, R. de Renzi, G. Guidi, F. Licci, and L. G. Raffo, 1994, Physica C **235-240C**, 1849.
Buchholtz, L., and G. Zwicknagl, 1981, Phys. Rev. B **23**, 5788.
Bulut, N., 2000, Phys. Rev. B **61**, 9051.
Bulut, N., 2001, Physica C **363**, 260.
Bulut, N., 2003, Phys. Rev. B **68**, 235103.
Buttrey, D., J. Sullivan, and A. Reingold, 1990, J. Solid State Chem. **88**, 291.
Byers, J., M. E. Flatte, and D. J. Scalapino, 1993, Phys. Rev. Lett. **71**, 3363.
Cabra, D., and P. Pujol, 2004, in *Quantum Magnetism*, edited by U. Schollwöck, J. Richter, D. Farnell, and R. Bishop, Lecture Notes in Physics No. 645 (Springer, Berlin), p. 253.
Cardy, J., 1990, in *Les Houches, Champs, Cordes et Phénomènes Critiques (Fields, Strings and Critical Phenomena), Session XLIX*, edited by E. Brézin, and J. Zinn-Justin (North-Holland–Elsevier Science Publishers BV, Amsterdam), p. 169.
Cardy, J., and D. Lewellen, 1991, Phys. Lett. B **259**, 274.
Carlson, E., V. Emery, S. Kivelson, and D. Orgad, 2002, in *The Physics of Conventional and Unconventional Superconductors*, edited by K. H. Bennemann, and J. B. Ketterson (Springer-Verlag, Berlin).
Carretta, P., A. Rigamonti, and R. Sala, 1997, Phys. Rev. B **55**, 3734.
Casalta, H., H. Alloul, and J. Marucco, 1993, Physica C **204**, 331.
Cassanello, C., and E. Fradkin, 1997, Phys. Rev. B **56**, 11246.
Cassanello, C. R., and E. Fradkin, 1996, Phys. Rev. B **53**, 15079.
Castellani, C., C. DiCastro, P. Lee, M. Ma, S. Sorella, and E. Tabet, 1986, Phys. Rev. B **33**, 6169.
Chakhalian, J., *et al.*, 2003, Phys. Rev. Lett. **91**, 027202.
Chakravarty, S., B. Halperin, and D. R. Nelson, 1989, Phys. Rev. B **39**, 2344.
Chakravarty, S., R. Laughlin, D. Morr, and C. Nayak, 2001, Phys. Rev. B **63**, 094503.
Chang, C., J.-Y. Lin, and H. Yand, 2000, Phys. Rev. Lett. **84**, 5612.
Chang, J., Y. Su, H. Luo, H. Lu, and T. Xiang, 2004, Phys. Rev. B **70**, 212507.
Chao, K., J. Spalek, and A. Oles, 1977, J. Phys. C **10**, L271.
Chattopadhyay, A. K., R. Klemm, and D. Sa, 2002, J. Phys.: Condens. Matter **14**, L577.
Chen, Y., and C. S. Ting, 2004, Phys. Rev. Lett. **92**, 077203.
Chien, T., Z. Wang, and N. Ong, 1991, Phys. Rev. Lett. **67**, 2088.
Cho, J., F. Borsa, D. Johnston, and D. Torgeson, 1992, Phys. Rev. B **46**, 3179.
Choi, C., and P. Muzikar, 1990, Phys. Rev. B **41**, 1812.
Chou, F., N. Belk, M. Kastner, R. J. Birgeneau, and Amnon Aharony, 1995, Phys. Rev. Lett. **75**, 2204.
Chou, F., F. Borsa, J. Cho, D. Johnston, A. Lascialfari, D. Torgeson, and J. Ziolo, 1993, Phys. Rev. Lett. **71**, 2323.
Citro, R., and E. Orignac, 2002, Phys. Rev. B **65**, 134413.
Civale, L., A. Marwick, A. Worthington, T. Kirk, M. Thompson, J. Krusin-Elbaum, Y. Sun, J. Clem, and F. Holtzberg, 1991, Phys. Rev. Lett. **67**, 648.
Coleman, P., 1984, Phys. Rev. B **29**, 3035.
Cooper, J., 1991, Supercond. Sci. Technol. **4**, 1181.
Dagotto, E., 1994, Rev. Mod. Phys. **66**, 763.
Dagotto, E., 1999, Rep. Prog. Phys. **62**, 1525.
Dahm, T., P. Hirschfeld, D. Scalapino, and L.-Y. Zhu, 2005, Phys. Rev. B **72**, 214512.
Dahm, T., L.-Y. Zhu, P. Hirschfeld, and D. Scalapino, 2005, Phys. Rev. B **71**, 212501.
Damascelli, A., Z. Hussain, and Z. Shen, 2003, Rev. Mod. Phys. **75**, 473.
Damle, K., and S. Sachdev, 1998, Phys. Rev. B **57**, 8307.
Darriet, J., and L. P. Regnault, 1993, Solid State Commun. **86**, 409.
Das, J., A. Mahajan, J. Bobroff, H. Alloul, F. Alet, and E. Sørensen, 2004, Phys. Rev. B **69**, 144404.
Davidson, E., 1993, Comput. Phys. **7**, 519.
Dell'Arringa, S., E. Ercolessi, G. Morandi, P. Pieri, and M. Roncaglia, 1997, Phys. Rev. Lett. **78**, 2457.
den Nijs, M., 1988, in *Phase Transitions and Critical Phenomena*, edited by C. Domb and J. Lebowitz (Academic, London), Vol. 12, p. 219.
den Nijs, M., and K. Rommelse, 1989, Phys. Rev. B **40**, 4709.
des Cloizeaux, J., and J. Pearson, 1962, Phys. Rev. **128**, 2131.
Dooglav, A., H. Alloul, A. Volodin, and M. Eremin, 1996, Physica C **272**, 242.
Durst, A., and P. Lee, 2000, Phys. Rev. B **62**, 1270.
Eggert, S., 1993, *The Hubbard Model A: Reprint Volume* (World Scientific, Singapore).
Eggert, S., and I. Affleck, 1995, Phys. Rev. Lett. **75**, 934.
Eggert, S., and I. Affleck, 2004, J. Magn. Magn. Mater. **272-276**, e647.
Eggert, S., I. Affleck, and M. D. P. Horton, 2002, Phys. Rev. Lett. **89**, 047202.
Eggert, S., I. Affleck, and M. D. P. Horton, 2003, Phys. Rev. Lett. **90**, 089702.
Eggert, S., I. Affleck, and M. Takahashi, 1994, Phys. Rev. Lett. **73**, 332.
Eisaki, H., N. Kaneko, D. L. Feng, A. Damascelli, P. K. Mang, K. M. Shen, Z.-X. Shen, and M. Greven, 2004, Phys. Rev. B **69**, 064512.

Emery, V., 1987, Phys. Rev. Lett. **58**, 2794.
Emery, V., and S. Kivelson, 1995a, Phys. Rev. Lett. **74**, 3253.
Emery V., and S. Kivelson, 1995b, Nature (London) **374**, 434.
Eskes, H., and G. Sawatzky, 1991, Phys. Rev. B **43**, 119.
Essler, F., 1996, J. Phys. A **29**, 225.
Fabrizio, M., 1993, Phys. Rev. B **48**, 15838.
Fazekas, P., 1999, *Series in Modern Condensed Matter Physics* (World Scientific, Singapore), Vol. 5.
Fetter, A., 1965, Phys. Rev. **140**, A1921.
Finkel'shtein, A., 1983, Sov. Phys. JETP **57**, 97.
Finkelstein, A., V. E. Kataev, E. F. Kukovitskii, and G. B. Teitelbaum, 1990, Physica C **168**, 370.
Flatté, M., 2000, Phys. Rev. B **61**, R14920.
Flatté, M. E., and J. M. Byers, 1999, Solid State Phys. **52**, 137.
Fradkin, E., 1991, in *Field Theories of Condensed Matter Systems*, edited by D. Pines (Addison-Wesley, New York), Vol. 82.
Franz, M., C. Kallin, and A. J. Berlinsky, 1996, Phys. Rev. B **54**, R6897.
Friedel, J., 1958, Nuovo Cimento, Suppl. **7**, 287.
Friesen, M., and P. Muzikar, 1997, Phys. Rev. B **55**, 509.
Fujimoto, S., 2000, Phys. Rev. B **63**, 024406.
Fujimoto, S., and S. Eggert, 2004, Phys. Rev. Lett. **92**, 037206.
Fujita, K., T. Noda, K. M. Kojima, H. Eisaki, and S. Uchida, 2005, Phys. Rev. Lett. **95**, 097006.
Fujiwara, N., H. Yasuoka, Y. Fujishiro, M. Azuma, and M. Takano, 1998, Phys. Rev. Lett. **80**, 604.
Fukuzumi, Y., K. Mizuhashi, K. Takenaka, and S. Uchida, 1996, Phys. Rev. Lett. **76**, 684.
Fulde, P., L. Hirst, and A. Luther, 1970, Z. Phys. **230**, 155.
Fulde, P., P. Thalmeier, and G. Zwicknagl, 2006, Solid State Phys. **60**, 1.
Furusaki, A., and N. Nagaosa, 1993, Phys. Rev. B **47**, 4631.
Gabay, M., 1994, Physica C **235-240**, 1337.
Gabay, M., E. Semel, P. Hirschfeld, and W. Chen, 2008, Phys. Rev. B **77**, 165110.
Garg, A., M. Randeria, and N. Trivedi, 2008, Nat. Phys. **4**, 762.
Georges, A., G. Kotliar, W. Krauth, and M. Rozenberg, 1996, Rev. Mod. Phys. **68**, 13.
Giamarchi, T., 2004, in *Quantum Physics in One Dimension*, edited by J. Birman, S. Edwards, R. Friend, M. Rees, D. Sherrington, and G. Veneziano, International Series of Monographs on Physics (Physics Oxford University Press, Oxford), Vol. 121.
Giapintzakis, J., D. M. Ginsberg, M. A. Kirk, and S. Ockers, 1994, Phys. Rev. B **50**, 15967.
Glarum, S., S. Geschwind, K. Lee, M. Kaplan, and J. Michel, 1991, Phys. Rev. Lett. **67**, 1614.
Gogolin, A., A. Nersesyan, and A. Tsvelik, 1999, *Bosonization and Strongly Correlated Systems* (Cambridge University Press, Cambridge, UK), p. 209.
Golinelli, O., T. Jolicoeur, and R. Lacaze, 1994, Phys. Rev. B **50**, 3037.
Gorkov, L., and P. A. Kalugin, 1985, JETP Lett. **41**, 208 [JETP Lett. **41**, 253 (1985)].
Goto, A., W. G. Clark, P. Vonlanthen, K. B. Tanaka, T. Shimizu, K. Hashi, P. V. P. S. S. Sastry, and J. Schwartz., 2002, Phys. Rev. Lett. **89**, 127002.
Graser, S., P. Hirschfeld, T. Dahm, and L.-Y. Zhu, 2007, Phys. Rev. B **76**, 054516.
Greven, M., and R. Birgeneau, 1998, Phys. Rev. Lett. **81**, 1945.
Greven, M., R. Birgeneau, and U.-J. Wiese, 1996, Phys. Rev. Lett. **77**, 1865.
Grotendorst J., D. Marx, and A. Muramatsu, 2002, in *Quantum Simulations of Complex Many-Body Systems: From Theory to Algorithms*, edited by J. Grotendorst, D. Marx, and A. Muramatsu (J. von Neumann Institut für Computing, Jülich), Vol. 10.
Gutzwiller, M., 1963a, Phys. Rev. Lett. **10**, 159.
Gutzwiller, M., 1963b, Phys. Rev. **137**, 1726.
Hagiwara, M., K. Katsumata, I. Affleck, B. Halperin, and J. Renard, 1990, Phys. Rev. Lett. **65**, 3181.
Haldane, F., 1980, Phys. Rev. Lett. **45**, 1358.
Haldane, F., 1983, Phys. Rev. Lett. **50**, 1153.
Hanaki, Y., Y. Ando, S. Ono, and J. Takeya, 2001, Phys. Rev. B **64**, 172514.
Haran, G., and A. D. S. Nagi, 1996, Phys. Rev. B **54**, 15463.
Haran, G., and A. D. S. Nagi, 1998, Phys. Rev. B **58**, 12441.
Harashina, H., S. ichi Shamoto, T. Kiyokura, M. Sato, K. Kakurai, and G. Shirane, 1993, J. Phys. Soc. Jpn. **62**, 4009.
Harris, A., and R. Lange, 1967, Phys. Rev. **157**, 295.
Harter, J., B. Andersen, J. Bobroff, M. Gabay, and P. J. Hirschfeld, 2007, Phys. Rev. B **75**, 054520.
Hase, M., I. Terasaki, and K. Uchinokura, 1993, Phys. Rev. Lett. **70**, 3651.
Hertz, J., 1976, Phys. Rev. B **14**, 1165.
Hettler, M. H., and P. J. Hirschfeld, 1999, Phys. Rev. B **59**, 9606.
Hewson, A. C., 1993, *The Kondo Problem to Heavy Fermions* (Cambridge University Press, Cambridge, England).
Hiroi, Z., M. Azuma, M. Takano, and Y. Bando, 1991, IEEE J. Solid-State Circuits **95**, 230.
Hirsch, J., 1980, Phys. Rev. B **22**, 5259.
Hirsch, J., 1985, Phys. Rev. Lett. **54**, 1317.
Hirschfeld, P., and N. Goldenfeld, 1993, Phys. Rev. B **48**, 4219.
Hirschfeld, P., W. Putikka, and D. Scalapino, 1994, Phys. Rev. B **50**, 10250.
Hirschfeld, P., D. Vollhardt, and P. Wolfle, 1986, Solid State Commun. **59**, 111.
Hirschfeld, P. J., and W. A. Atkinson, 2002, J. Low Temp. Phys. **126**, 881.
Hodges, J., P. Bonville, P. Imbert, and A. Pinatel-Philippot, 1995, Physica C **246**, 323.
Hofstetter, W., R. Bulla, and D. Vollhardt, 2000, Phys. Rev. Lett. **84**, 4417.
Hor, P. H., R. L. Meng, Y. Q. Wang, L. Gao, Z. J. Huang, J. Bechtold, K. Forster, and C. W. Chu, 1987, Phys. Rev. Lett. **58**, 1891.
Hotta, T., 1993, J. Phys. Soc. Jpn. **62**, 274.
Hubbard, J., 1963, Proc. R. Soc. London, Ser. A **276**, 238.
Hudson, E., K. Lang, V. Madhavan, S. Pan, H. Eisaki, S. Uchida, and J. Davis, 2001, Nature (London) **411**, 920.
Hudson, E., V. Madhavan, K. McElroy, J. E. Hoffman, K. M. Lang, H. Eisaki, S. Uchida, and J. Davis, 2003, Physica B **329**, 1365.
Hudson, E., S. Pan, A. Gupta, K.-W. Ng, and J. Davis, 1999, Science **285**, 88.
Hussey, N. E., 2002, Adv. Phys. **51**, 1685.
Hybertsen, M., M. Schlüter, and N. Christensen, 1989, Phys. Rev. B **39**, 9028.
Igarashi, J., T. Tonegawa, M. Kaburagi, and P. Fulde, 1995, Phys. Rev. B **51**, 5814.
Ingersent, K., 1996, Phys. Rev. B **54**, 11936.
Inui, M., S. Doniach, and M. Gabay, 1988, Phys. Rev. B **38**, 6631.
Ishida, K., Y. Kitaoka, N. Ogata, T. Kamino, K. Asayama, J.

Cooper, and N. Athanassopoulou, 1993, J. Phys. Soc. Jpn. **62**, 2803.
Ishida, K., Y. Kitaoka, Y. Tokunaga, S. Mastumoto, K. Asayama, M. Azuma, Z. Hiroi, and M. Takano, 1994, J. Phys. Soc. Jpn. **63**, 3222.
Ishida, K., Y. Kitaoka, K. Yamazoe, K. Asayama, and Y. Yamada, 1996, Phys. Rev. Lett. **76**, 531.
Itoh, Y., T. Machi, C. Kasai, S. Adachi, N. Watanabe, N. Koshizuka, and M. Murakami, 2003, Phys. Rev. B **67**, 064516.
Itoh, Y., T. Machi, N. Watanabe, and N. Koshizuka, 2001, J. Phys. Soc. Jpn. **70**, 644.
Janossy, A., J. R. Cooper, L. Brunel, and A. Carrington, 1994, Phys. Rev. B **50**, 3442.
Johnston, D., *et al.*, 2000, e-print arXiv:cond-mat/0001147.
Joynt, R., 1997, J. Low Temp. Phys. **109**, 811.
Julien, M., T. Feher, M. Horvatic, C. Berthier, O. N. Bakharev, P. Segransan, G. Collin, and J.-F. Marucco, 2000, Phys. Rev. Lett. **84**, 3422.
Kadano, R., 1997, J. Phys. Soc. Jpn. **66**, 505.
Kakehashi, Y., 2004, Adv. Phys. **53**, 497.
Kakurai, K., S. Shamoto, T. Kiyokura, M. Sato, J. M. Tranquada, and G. Shirane, 1993, Phys. Rev. B **48**, 3485.
Kampf, A., 1994, Phys. Rep. **249**, 219.
Kampf, A. P., and T. P. Devereaux, 1997, Phys. Rev. B **56**, 2360.
Kanamori, J., 1963, Prog. Theor. Phys. **30**, 275.
Kane, C., and M. Fisher, 1992a, Phys. Rev. Lett. **68**, 1220.
Kane, C., and M. Fisher, 1992b, Phys. Rev. B **46**, 15233.
Kaplan, T., P. Horsch, and P. Fulde, 1982, Phys. Rev. Lett. **49**, 889.
Karpinski, J., E. Kaldis, E. Jilek, S. Rusiecki, and B. Bucher, 1988, Nature (London) **336**, 660.
Kee, H. Y., 2001, Phys. Rev. B **64**, 012506.
Keimer, B., A. Aharony, A. Auerbach, R. J. Birgeneau, A. Cassanho, Y. Endoh, R. W. Erwin, M. A. Kastner, and G. Shirane, 1992, Phys. Rev. B **45**, 7430.
Kennedy, T., 1990, J. Phys.: Condens. Matter **2**, 5737.
Kenzelmann, M., G. Xu, I. A. Zaliznyak, C. Broholm, J. F. DiTusa, G. Aeppli, T. Ito, K. Oka, and H. Takagi, 2003, Phys. Rev. Lett. **90**, 087202.
Keren, A., and A. Kanigel, 2003, Phys. Rev. B **68**, 012507.
Keren, A., L. Le, G. Luke, B. Sternlieb, W. Wu, Y. Uemura, S. Tajima, and S. Uchida, 1993, Phys. Rev. B **48**, 12926.
Khaliullin, G., and P. Fulde, 1995, Phys. Rev. B **52**, 9514.
Khaliullin, G., R. Kilian, S. Krivenko, and P. Fulde, 1997, Phys. Rev. B **56**, 11882.
Kilian, R., S. Krivenko, G. Khaliullin, and P. Fulde, 1999, Phys. Rev. B **59**, 14432.
Kim, Y., M. Greven, U. Wiese, and R. Birgeneau, 1998, Eur. Phys. J. B **4**, 291.
Kimura, H., M. Kofu, Y. Matsumoto, and K. Hirota, 2003, Phys. Rev. Lett. **91**, 067002.
Kluge, T., Y. Koike, A. Fujiwara, M. Kato, T. Noji, and Y. Saito, 1995, Phys. Rev. B **52**, R727.
Kojima, K., Y. Fudamoto, M. Larkin, G. M. Luke, J. Merrin, B. Nachumi, Y. J. Uemura, M. Hase, Y. Sasago, K. Uchinokura, A. R. Y. Ajiro, and J.-P. Renard, 1997, Phys. Rev. Lett. **79**, 503.
Kojima, K., A. Keren, L. P. Le, G. M. Luke, B. Nachumi, W. D. Wu, Y. J. Uemura, K. Kiyono, S. Miyasaka, H. Takagi, and S. Uchida, 1995, Phys. Rev. Lett. **74**, 3471.
Kojima, K., A. Keren, G. M. Luke, B. Nachumi, W. D. Wu, Y. J. Uemura, M. Azuma, and M. Takano, 1995, Phys. Rev. Lett. **74**, 2812.
Kojima, K., *et al.*, 2004, Phys. Rev. B **70**, 094402.
Konczykowski, M., F. Rullier-Albenque, E. Yacoby, A. Shaulov, Y. Yeshurun, and P. Lejay, 1991, Phys. Rev. B **44**, 7167.
Kontani, H., and M. Ohno, 2006, Phys. Rev. B **74**, 014406.
Kosterlitz, J., 1974, J. Phys. C **7**, 1046.
Kotliar, G., and J. Liu, 1988, Phys. Rev. Lett. **61**, 1784.
Kotliar, G., and A. Ruckenstein, 1986, Phys. Rev. Lett. **57**, 1362.
Kotliar, G., S. Savrasov, K. Haule, V. Oudovenko, O. Parcollet, and C. Marianetti, 2006, Rev. Mod. Phys. **78**, 865.
Kruis, H., I. Martin, and A. Balatsky, 2001, Phys. Rev. B **64**, 054501.
Kübert, C., and P. Hirschfeld, 1997, Solid State Commun. **105**, 459.
Kulic, M., and V. Oudovenko, 1997, Solid State Commun. **104**, 375.
Kulic, M. L., and O. V. Dolgov, 1999, Phys. Rev. B **60**, 13062.
Kyung, B., G. Kotliar, and A.-M. Tremblay, 2006, Phys. Rev. B **73**, 205106.
Laeuchli, A., D. Poilblanc, T. Rice, and S. White, 2002, Phys. Rev. Lett. **88**, 257201.
Lake, B., G. Aeppli, K. N. Clause, D. McMorrow, K. Lefmann, N. E. Hussey, N. Mangkorntong, M. Nohara, H. Takagi, T. Mason, and A. Schroder, 2001, Science **291**, 1759.
Lake, B., *et al.*, 2002, Nature (London) **415**, 299.
Lakner, M., H. v. Löhneysen, A. Langenfeld, and P. Wölfle, 1994, Phys. Rev. B **50**, 17064.
Larkin, A., 1970, Sov. Phys. JETP **31**, 784.
Laukamp, M., G. B. Martins, C. Gazza, A. L. Malvezzi, E. Dagotto, P. M. Hansen, A. C. Lez, and J. Riera, 1998, Phys. Rev. B **57**, 10755.
Lecheminant, P., 2004, in *One-Dimensional Quantum Spin Liquids*, edited by H.-T. Diep (World Scientific, Singapore).
Lederer, P., and D. Mills, 1968, Phys. Rev. **165**, 837.
Lee, P., and N. Nagaosa, 1992, Phys. Rev. B **46**, 5621.
Lee, P., N. Nagaosa, and X. Wen, 2006, Rev. Mod. Phys. **78**, 17.
Lee, P. A., and T. V. Ramakrishnan, 1985, Rev. Mod. Phys. **57**, 287.
Legris, A., F. Rullier-Albenque, E. Radeva, and P. Lejay, 1993, J. Phys. I **3**, 1605.
Leung, P., and R. Gooding, 1995, Phys. Rev. B **52**, R15711.
Liang, R., D. Bonn, and W. Hardy, 2000, Physica C **336**, 57.
Liang, S., and T. K. Lee, 2002, Phys. Rev. B **65**, 214529.
Lieb, E., T. Schultz, and D. Mattis, 1961, Ann. Phys. (N.Y.) **16**, 407.
Lieb, E., and F. Wu, 1968, Phys. Rev. Lett. **20**, 1445.
Limelette, P., P. Wzietek, S. Florens, A. Georges, T. Costi, C. Pasquier, D. Jérome, C. Mézière, and P. Batail, 2003, Phys. Rev. Lett. **91**, 016401.
Loram, J., K. Mirza, J. Cooper, W. Liang, and J. Wade, 1994, J. Supercond. **7**, 243.
Loram, J., K. Mirza, and P. Freeman, 1990a, Physica C **171**, 243.
Loram, K., K. A. Mirza, and P. F. Freeman, 1990b, Physica C **171**, 243.
Lukyanov, S., 1998, Nucl. Phys. B **522**, 533.
Lutgemeier, H., 1988, Physica C **153-155**, 95.
Luther, A., 1976, Phys. Rev. B **14**, 2153.
Luther, A., and V. Emery, 1974, Phys. Rev. Lett. **33**, 589.
Luther, A., and I. Peschel, 1975, Phys. Rev. B **12**, 3908.
Luttinger, J., 1963, J. Math. Phys. **4**, 1154.
Lyons, K. B., P. A. Fleury, J. P. Remeika, A. S. Cooper, and T. J. Negran, 1988, Phys. Rev. B **37**, 2353.

MacFarlane, W., J. Bobroff, H. Alloul, P. Mendels, N. Blanchard, G. Collin, and J. F. Marucco, 2000, Phys. Rev. Lett. **85**, 1108.
MacFarlane, W., J. Bobroff, P. Mendels, G. Collin, J. Marucco, L. Cyrot, and H. Alloul, 2002, Phys. Rev. B **66**, 024508.
Maeda, H., A. Koizumi, N. Bamba, E. Takayama-Muromachi, F. Izumi, H. Asano, K. Shimizu, H. Moriwaki, H. Maruyama, Y. Kuroda, and Y. Yamazaki, 1989, Physica C **157**, 483.
Mahajan, A., H. Alloul, G. Collin, and J. Marucco, 1994, Phys. Rev. Lett. **72**, 3100.
Mahajan, A., H. Alloul, G. Collin, and J. Marucco, 2000, Eur. Phys. J. B **13**, 457.
Manabe, K., H. Ishimoto, N. Koide, Y. Sasago, and K. Uchinokura, 1998, Phys. Rev. B **58**, R575.
Markiewicz, R., 2003, e-print arXiv:cond-mat/0312595.
Markiewicz, R., 2006, J. Phys. Chem. Solids **67**, 128.
Martin, I., A. Balatsky, and J. Zaanen, 2002, Phys. Rev. Lett. **88**, 097003.
Martins, G., M. Laukamp, J. Riera, and E. Dagotto, 1996, Phys. Rev. B **54**, 16032.
Martins, G., M. Laukamp, J. Riera, and E. Dagotto, 1997, Phys. Rev. Lett. **78**, 3563.
Martins, G., J. Xavier, L. Arrachea, and E. Dagotto, 2001, Phys. Rev. B **64**, 180513.
Mattis, D., 1993, in *The Many Body Problem: An Encyclopedia of Exactly Solved Models in One Dimension*, edited by D. Mattis (World Scientific, Singapore), p. 169.
Mayr, M., G. Alvarez, A. Moreo, and E. Dagotto, 2006, Phys. Rev. B **73**, 014509.
McElroy, K., J. Lee, J. A. Slezak, D.-H. Lee, H. Eisaki, S. Uchida, and J. C. Davis, 2005, Science **309**, 1048.
McMahan, A., J. Annett, and R. Martin, 1990, Phys. Rev. B **42**, 6268.
Meden, V., W. Metzner, U. Schollwöck, and K. Schönhammer, 2002, Phys. Rev. B **65**, 045318.
Mendels, P., and H. Alloul, 1988, Physica C **156**, 355.
Mendels, P., H. Alloul, J. H. Brewer, G. Morris, T. Duty, S. Johnston, E. Ansaldo, G. Collin, J. F. Marucco, C. Niedermayer, D. Noakes, and C. Stronach, 1994, Phys. Rev. B **49**, 10035.
Mendels, P., H. Alloul, G. Collin, N. Blanchard, J. F. Maracco, and J. Bobroff, 1994, Physica C **235-240**, 1595.
Mendels, P., H. Alloul, J. Marucco, J. Arabski, and G. Collin, 1990, Physica C **171**, 429.
Mendels, P., J. Bobroff, G. Collin, H. Alloul, M. Gabay, J. F. Marucco, N. Blanchard, and B. Grenier, 1999, Europhys. Lett. **46**, 678.
Mendels, P., X. Labouze, G. Collin, and H. Alloul, 1991, Physica C **185-189**, 1191.
Metzner, W., and D. Vollhardt, 1989, Phys. Rev. Lett. **62**, 324.
Miceli, P. F., J. M. Tarascon, P. Barboux, L. H. Greene, B. G. Bagley, G. W. Hull, M. Giroud, J. J. Rhyne, and D. A. Neumann, 1989, Phys. Rev. B **39**, 12375.
Micheluchi, U., F. Venturini, and A. Kampf, 2002, J. Phys. Chem. Solids **63**, 2283.
Mikeska, H.-J., U. Neugebauer, and U. Schollwöck, 1997, Phys. Rev. B **55**, 2955.
Mila, F., and T. Rice, 1989, Physica C **157**, 561.
Millis, A., H. Monien, and D. Pines, 1990, Phys. Rev. B **42**, 167.
Millis, A., D. Morr, and J. Schmalian, 2001, Phys. Rev. Lett. **87**, 167202.
Miller, R. I., R. F. Kiefl, J. H. Brewer, D. Callaghan, J. E. Sonier, R. Liang, D. A. Bonn, and W. Hardy, 2006, Phys. Rev. B **73**, 144509.
Milovanović, M., S. Sachdev, and R. Bhatt, 1989, Phys. Rev. Lett. **63**, 82.
Mirza, K. A., J. W. Loram, and J. R. Cooper, 1994, Physica C **235**, 1771.
Miyashita, S., and S. Yamamoto, 1993a, Phys. Rev. B **48**, 913.
Miyashita, S., and S. Yamamoto, 1993b, Phys. Rev. B **48**, 9528.
Miyazaki, T., M. Troyer, M. Ogata, K. Ueda, and D. Yoshioka, 1997, J. Phys. Soc. Jpn. **66**, 2580.
Mizuhashi, K., K. Takenaka, Y. Fukuzumi, and S. Uchida, 1995, Phys. Rev. B **52**, R3884.
Momono, N., and M. Ido, 1996, Physica C **264**, 311.
Monthoux, P., and D. Pines, 1994, Phys. Rev. B **50**, 16015.
Morr, D., J. Schmalian, R. Stern, and C. Schlichter, 1998, Phys. Rev. B **58**, 11193.
Morr, D., and N. Stavropoulos, 2002, Phys. Rev. B **66**, 140508.
Motoyama, N., H. Eisaki, and S. Uchida, 1996, Phys. Rev. Lett. **76**, 3212.
Nachumi, B., A. Keren, K. Kojima, M. Larkin, G. M. Luke, J. Merrin, O. Tchernysh, Y. J. Uemura, N. Ichikawa, M. Goto, and S. Uchida, 1996, Phys. Rev. Lett. **77**, 5421.
Nagaosa, N., and P. Lee, 1997, Phys. Rev. Lett. **79**, 3755.
Nagaosa, N., and T. Ng, 1995, Phys. Rev. B **51**, 15588.
Neef, M., S. Tornow, V. Zevin, and G. Zwicknagl, 2003, Phys. Rev. B **68**, 035114.
Nersesyan, A., A. Gogolin, and F. Essler, 1998, Phys. Rev. Lett. **81**, 910.
Nersesyan, A., A. Tsvelik, and F. Wenger, 1995, Nucl. Phys. B **438**, 561.
Ng, T.-K., 1992, Phys. Rev. B **45**, 8181.
Ng, T.-K., 1994, Phys. Rev. B **50**, 555.
Niedermayer, C., C. Bernhard, T. Blasius, A. Golnik, A. Moodenbaugh, and J. I. Budnick, 1998, Phys. Rev. Lett. **80**, 3843.
Nomura, K., and M. Yamada, 1991, Phys. Rev. B **43**, 8217.
Norman, M. R., M. Randeria, H. Ding, and J. C. Campuzano, 1995, Phys. Rev. B **52**, 615.
Nunner, T., B. Andersen, A. Melikyan, and P. Hirschfeld, 2005, Phys. Rev. Lett. **95**, 177003.
Nunner, T., and P. Hirschfeld, 2005, Phys. Rev. B **72**, 014514.
Obertelli, S. D., J. R. Cooper, and J. L. Tallon, 1992, Phys. Rev. B **46**, 14928.
Odashima, S., and H. Matsumoto, 1997, Phys. Rev. B **56**, 126.
Odashima, S., H. Matsumoto, and O. Michikami, 2000, Physica C **336**, 287.
Ogata, M., and H. Shiba, 1990, Phys. Rev. B **41**, 2326.
Ohashi, Y., 2001, J. Phys. Soc. Jpn. **70**, 2054.
Ohashi, Y., 2002, Phys. Rev. B **66**, 054522.
Ohsugi, S., Y. Tokunaga, K. Ishida, Y. Kitaoka, M. Azuma, Y. Fujishiro, and M. Takano, 1999, Phys. Rev. B **60**, 4181.
Ono, S., Y. Ando, T. Murayama, F. F. Balakirev, J. B. Betts, and G. S. Boebinger, 2000, Phys. Rev. Lett. **85**, 638.
Orignac, E., and T. Giamarchi, 1997, Phys. Rev. B **56**, 7167.
Orignac, E., and T. Giamarchi, 1998, Phys. Rev. B **57**, 5812.
Oseroff, S., S. W. Cheong, B. Aktas, M. F. Hundley, Z. Fisk, and L. W. Rupp, 1995, Phys. Rev. Lett. **74**, 1450.
Oshikawa, M., 1992, J. Phys.: Condens. Matter **4**, 7469.
Ouazi, S., J. Bobroff, H. Alloul, and W. MacFarlane, 2004, Phys. Rev. B **70**, 104515.
Ouazi, S., J. Bobroff, H. Alloul, M. L. Tacon, N. Blanchard, G. Collin, M. Julien, and M. Horvatić, 2006, Phys. Rev. Lett. **96**, 127005.
Ovchinnikov, S., and V. Val'kov, 2004, *Hubbard Operators in*

the Theory of Strongly Correlated Electrons (World Scientific, Singapore).
Paalanen, M., J. Graebner, R. Bhatt, and S. Sachdev, 1988, Phys. Rev. Lett. **61**, 597.
Paalanen, M., S. Sachdev, R. Bhatt, and A. Ruckenstein, 1986, Phys. Rev. Lett. **57**, 2061.
Pan, S., E. Hudson, K. Lang, H. Eisaki, S. Uchida, and J. Davis, 2000a, Nature (London) **403**, 746.
Pan, S., E. W. Hudson, K. M. Lang, H. Eisaki, S. Uchida, and J. Davis, 2000b, Nature (London) **403**, 746.
Pao, C.-H., and N. Bickers, 1995, Phys. Rev. B **51**, 16310.
Pavarini, E., I. Dasgupta, T. Saha-Dasgupta, O. Jepsen, and O. K., Andersen, 2001, Phys. Rev. Lett. **87**, 047003.
Payen, C., E. Janod, K. Schoumacker, C. Batista, K. Hallberg, and A. A. Aligia, 2000, Phys. Rev. B **62**, 2998.
Pennington, C., and C. Slichter, 1990, in *Physical Properties of High Temperature Superconductors*, edited by D. M. Ginsberg (World Scientific, Singapore), Vol. 2, p. 269.
Pepin, C., and P. Lee, 1998, Phys. Rev. Lett. **81**, 2779.
Pethick, C., and D. Pines, 1986, Phys. Rev. Lett. **57**, 118.
Pham, K., M. Gabay, and P. Lederer, 2000, Phys. Rev. B **61**, 16397.
Poilblanc, D., D. Scalapino, and W. Hanke, 1994a, Phys. Rev. B **50**, 13020.
Poilblanc, D., D. Scalapino, and W. Hanke, 1994b, Phys. Rev. Lett. **72**, 884.
Poilblanc, D., H. Tsunetsugu, and T. Rice, 1994, Phys. Rev. B **50**, 6511.
Polizzi, E., F. Mil, and E. Sørensen, 1998, Phys. Rev. B **58**, 2407.
Polkovnikov, A., S. Sachdev, and M. Vojta, 2001, Phys. Rev. Lett. **86**, 296.
Prelovšek, P., and I. Sega, 2004, Phys. Rev. Lett. **93**, 207202.
Qin, S., T.-K. Ng, and Z. Su, 1995, Phys. Rev. B **52**, 12844.
Ramirez, A., S.-W. Cheong, and M. Kaplan, 1994, Phys. Rev. Lett. **72**, 3108.
Read, N., 1985, J. Phys. C **18**, 2651.
Read, N., and D. M. Newns, 1983, J. Phys. C **16**, 3273.
Regnault, L., J. P. Renard, G. Dhalenne, and A. Revcolevschi, 1995, Europhys. Lett. **32**, 579.
Renard, J., K. L. Dang, P. Veillet, G. Dhalenne, A. Revcolevschi, and L.-P. Regnault, 1995, Europhys. Lett. **30**, 475.
Renard, J., M. Verdaguer, L. Regnault, W. Erkelens, J. Rossat-Mignod, J. Ribas, W. Stirling, and C. Vettier, 1988, J. Appl. Phys. **63**, 3538.
Renard, J., M. Verdaguer, L. P. Regnault, W. A. C. Erkelens, J. Rossat-Mignod, and W. G. Stirling, 1987, Europhys. Lett. **3**, 945.
Riseman, T., H. Alloul, A. Mahajan, P. Mendels, N. Blanchard, G. Collin, and J. Marucco, 1994, Physica C **235**, 1593.
Rommer, S., and S. Eggert, 1999, Phys. Rev. B **59**, 6301.
Rommer, S., and S. Eggert, 2000, Phys. Rev. B **62**, 4370.
Roos, P., and S. Miyashita, 1999, Phys. Rev. B **59**, 13782.
Rossat-Mignod, J., *et al.*, 1991, Physica C **185-189**, 86.
Rullier-Albenque, F., H. Alloul, F. Balakirev, and C. Proust, 2008, Europhys. Lett. **81**, 37008.
Rullier-Albenque, F., H. Alloul, C. Proust, P. Lejay, A. Forget, and D. Colson, 2007, Phys. Rev. Lett. **99**, 027003.
Rullier-Albenque, F., H. Alloul, and R. Tourbot, 2001, Phys. Rev. Lett. **87**, 157001.
Rullier-Albenque, F., H. Alloul, and R. Tourbot, 2003, Phys. Rev. Lett. **91**, 047001.
Rullier-Albenque, F., R. Tourbot, H. Alloul, P. Lejay, D. Colson, and A. Forget, 2006, Phys. Rev. Lett. **96**, 067002.
Rullier-Albenque, F., P. Vieillefond, H. Alloul, A. Tyler, P. Lejay, and J. F. Marucco, 2000, Europhys. Lett. **50**, 81.
Rusinov, A., 1968, Zh. Eksp. Teor. Fiz. Pis'ma Red. **9**, 146 [JETP Lett. **9**, 85 (1969)].
Sachdev, S., 1989, Phys. Rev. B **39**, 5297.
Sakaguchi, T., K. Kakurai, T. Yokoo, and J. Akimitsu, 1996, J. Phys. Soc. Jpn. **65**, 3025.
Sakai, O., Y. Shimizu, H. Shiba, and K. Satori, 1993, J. Phys. Soc. Jpn. **62**, 3181.
Sakai, T., and M. Takahashi, 1990, Phys. Rev. B **42**, 4537.
Sakurai, A., 1970, Prog. Theor. Phys. **44**, 1472.
Salkola, M., A. V. Balatsky, and J. R. Schrieffer, 1997, Phys. Rev. B **55**, 12648.
Sandvik, A., E. Dagotto, and D. J. Scalapino, 1997, Phys. Rev. B **56**, 11701.
Sauv, K., J. Conard, M. Nicolas-Francillon, and F. Bouree, 1996, Physica C **273**, 49.
Schabel, M., C.-H. Park, A. Matsuura, and Z.-X. Shen, 1998, Phys. Rev. B **57**, 6090.
Schmitt-Rink, S., K. Miyake, and C. M. Varma, 1986, Phys. Rev. Lett. **57**, 2575.
Schollwöck, U., 2005, Rev. Mod. Phys. **77**, 259.
Schollwöck, U., J. Richter, D. Farnell, and R. Bishop, 2004, in *Quantum Magnetism*, edited by U. Schollwöck, J. Richter, D. Farnell, and R. Bishop, Lecture Notes in Physics No. 645 (Springer, Berlin).
Schork, T., and P. Fulde, 1994, Phys. Rev. B **50**, 1345.
Schulz, H., 1986, Phys. Rev. B **34**, 6372.
Segawa, K., and Y., Ando, 1999, Phys. Rev. B **59**, R3948.
Seidel, A., and D.-H. Lee, 2006, Phys. Rev. Lett. **97**, 056804.
Senthil, T., and M. P. A. Fisher, 1999, Phys. Rev. B **60**, 6893.
Shender, E., and S. Kivelson, 1991, Phys. Rev. Lett. **66**, 2384.
Shimizu, T., D. E. MacLaughlin, P. C. Hammel, J. D. Thompson, and S.-W. Cheong, 1995, Phys. Rev. B **52**, R9835.
Shnirman, A., I. Adagideli, P. M. Goldbart, and A. Yazdani, 1999, Phys. Rev. B **60**, 7517.
Sidis, Y., P. Bourges, H. F. Fong, B. Keimer, L. P. Regnault, J. Bossy, A. Ivanov, B. Hennion, P. Gautier-Picard, G. Collin, D. L. Millius, and I. A. Aksay, 2000, Phys. Rev. Lett. **84**, 5900.
Sidis, Y., P. Bourges, B. Hennion, L. Regnault, R. Villeneuve, G. Collin, and J. Marucco, 1996, Phys. Rev. B **53**, 6811.
Singer, P., A. Hunt, and T. Imai, 2002, Phys. Rev. Lett. **88**, 047602.
Sirker, J., N. Laflorencie, S. Fujimoto, S. Eggert, and I. Affleck, 2006, Phys. Rev. Lett. **98**, 137205.
Sisson, D., S. Doettinger, A. Kapitulnik, R. Liang, D. A. Bonn, and W. N. Hardy, 2000, Phys. Rev. B **61**, 3604.
Slichter, C., 1998, *Principles of Magnetic Resonance* (Springer-Verlag, New York).
Sørensen, E., and I. Affleck, 1995, Phys. Rev. B **51**, 16115.
Stamp, P. C. E., 1987, J. Magn. Magn. Mater. **63-64**, 429.
Stewart, G., 2001, Rev. Mod. Phys. **73**, 797.
Strong, S., and A. Millis, 1994, Phys. Rev. B **50**, 9911.
Suh, B. J., P. C. Hammel, Y. Yoshinari, J. D. Thompson, J. L. Sarrao, and Z. Fisk, 1998, Phys. Rev. Lett. **81**, 2791.
Suhl, H., D. Fredkin, J. Langer, and B. Matthias, 1962, Phys. Rev. Lett. **9**, 63.
Sun, P., and G. Kotliar, 2005, Phys. Rev. Lett. **95**, 016402.
Takigawa, M., N. Motoyama, H. Eisaki, and S. Uchida, 1997, Phys. Rev. B **55**, 14129.
Takigawa, M., A. P. Reyes, P. C. Hammel, J. D. Thompson, R. H. Heffner, Z. Fisk, and K. C. Ott, 1991, Phys. Rev. B **43**, 247.

Tallon, J., J. Cooper, P. de Silva, G. Williams, and J. Loram, 1995, Phys. Rev. Lett. **75**, 4114.
Tallon, J., J. Loram, and G. Williams, 2002, Phys. Rev. Lett. **88**, 059701.
Tang, J.-M., and M. Flatté, 2002, Phys. Rev. B **66**, 060504.
Tang, J.-M., and M. Flatté, 2004, Phys. Rev. B **70**, 140510.
Tedoldi, F., R. Santachiara, and M. Horvatic, 1999, Phys. Rev. Lett. **83**, 412.
Thurber, K., A. Hunt, T. Imai, and F. Chou, 2001, Phys. Rev. Lett. **87**, 247202.
Timusk, T., and B. Statt, 1999, Rep. Prog. Phys. **62**, 61.
Tolpygo, S., 1994, Phys. Rev. B **53**, 12454.
Tonegawa, T., and M. Karubaki, 1995, J. Phys. Soc. Jpn. **64**, 3956.
Tranquada, J., J. Axe, N. Ichikawa, A. Moodenbaugh, Y. Nakamura, and S. Uchida, 1997, Phys. Rev. Lett. **78**, 338.
Tsuchiura, H., Y. Tanaka, M. Ogata, and S. Kashiwaya, 2001, Phys. Rev. B **64**, 140501.
Tsuei, C., and J. Kirtley, 2000, Rev. Mod. Phys. **72**, 969.
Tsvelik, A., 1987, Sov. Phys. JETP **66**, 221.
Tsvelik, A., 1995, *Quantum Field Theory in Condensed Matter Physics* (Cambridge University Press, Cambridge, UK), p. 209.
Ubbens, M., and P. Lee, 1992, Phys. Rev. B **46**, 8434.
Uchiyama, Y., Y. Sasago, I. Tsukada, K. Uchinokura, A. Zheludev, T. Hayashi, N. Miura, and P. Böni, 1999, Phys. Rev. Lett. **83**, 632.
Ueda, K., and M. Rice, 1985, in *Theory of Heavy Fermions and Valence Fluctuations*, edited by T. Kasuya and T. Saso (Springer-Verlag, Berlin), p. 216.
Uehara, M., T. Nagata, J. Akimitsu, H. Takahashi, N. Mori, and K. Kinoshita, 1996, J. Phys. Soc. Jpn. **65**, 2764.
Uemura, Y., 2004, J. Phys.: Condens. Matter **16**, S4515.
Vajk, O. P., P. K. Mang, M. Greven, P. M. Gehring, and J. W. Lynn, 2002, Science **295**, 1691.
Valles, J. M., A. E. White, K. T. Short, R. C. Dynes, J. P. Garno, A. F. J. Levi, M. Anzlowar, and K. Baldwin, 1989, Phys. Rev. B **39**, 11599.
Varma, C., 2006, Phys. Rev. B **73**, 155113.
Varma, C., P. Littlewood, S. Schmitt-Rink, E. Abrahams, and A. E. Ruckenstein, 1989, Phys. Rev. Lett. **63**, 1996.
Villain, J., R. Bidaux, J.-P. Carton, and R. Conte, 1980, J. Phys. (Paris) **41**, 1263.
Voit, J., 1995, Rep. Prog. Phys. **58**, 977.
Walker, D., A. P. Mackenzie, and J. Cooper, 1995, Phys. Rev. B **51**, 15653.
Walstedt, R., R. Bell, L. Schneemeyer, J. Waszczak, W. Warren, and R. Dupree, 1993, Phys. Rev. B **48**, 10646.
Wang, L.-L., P. Hirschfeld, and H.-P. Cheng, 2005, Phys. Rev. B **72**, 224516.
Wang, Y., L. Li, and N. Ong, 2006, Phys. Rev. B **73**, 024510.
Wang, Z., and P. Lee, 2002, Phys. Rev. Lett. **89**, 217002.
Wells, B., Z. Shen, A. Matsuura, D. King, M. Kastner, M. Greven, and R. Birgeneau, 1995, Phys. Rev. Lett. **74**, 964.
Wessel, S., and S. Haas, 2000, Phys. Rev. B **61**, 15262.
White, S., I. Affleck, and D. Scalapino, 2002, Phys. Rev. B **65**, 165122.
White, S., and R. Noack, 1994, Phys. Rev. Lett. **73**, 886.
Williams, G., J. Tallon, R. Michalak, and R. Dupree, 1998, Phys. Rev. B **57**, 8696.
Williams, G. V. M., J. L. Tallon, and R. Dupree, 2000, Phys. Rev. B **61**, 4319.
Williams, G. V. M., J. L. Tallon, E. M. Haines, R. Michalak, and R. Dupree, 1997, Phys. Rev. Lett. **78**, 721.
Xiang, T., and J. M. Wheatley, 1995, Phys. Rev. B **51**, 11721.
Xiao, G., M. Z. Cieplak, A. Gavrin, F. H. Streitz, A. Bakhshai, and C. L. Chien, 1988, Phys. Rev. Lett. **60**, 1446.
Xu, G., J. DiTusa, T. Ito, K. Oka, H. Takagi, C. Broholm, and G. Aeppli, 1996, Phys. Rev. B **54**, R6827.
Xu, J., C. Ting, and T. Lee, 1991, Phys. Rev. B **43**, 8733.
Yang, C. Y., A. R. Moodenbaugh, Y. L. Wang, Y. Xu, S. M. Heald, D. O. Welch, M. Suenaga, D. A. Fischer, and J. E. Penner-Hahn, 1990, Phys. Rev. B **42**, 2231.
Yashenkin, A., W. A. Atkinson, I. V. Gornyi, P. J. Hirschfeld, and D. V. Khveshchenko, 2001, Phys. Rev. Lett. **86**, 5982.
Yasuoka, H., T. Imai, and T. Shimizu, 1989, in *Strong Correlation and Superconductivity*, edited by H. Fukuyama, S. Maekawa, and A. P. Malozemoff (Springer-Verlag, Berlin), p. 254.
Yazdani, A., C. Howald, C. Lutz, A. Kapitulnik, and D. Eigler, 1999, Phys. Rev. Lett. **83**, 176.
Yazdani, A., B. Jones, C. Lutz, M. Crommie, and D. Eigler, 1997, Science **275**, 1767.
Zagoulaev, S., P. Monod, and J. Jégoudez, 1995, Phys. Rev. B **52**, 10474.
Zhang, F., and T. Rice, 1988, Phys. Rev. B **37**, 3759.
Zhang, G.-M., H. Hu, and L. Yu, 2002, Phys. Rev. B **66**, 104511.
Zhang, W., J. Igarashi, and P. Fulde, 1997, Phys. Rev. B **56**, 654.
Zhang, W., J. Igarashi, and P. Fulde, 1998, J. Phys. Soc. Jpn. **67**, 1537.
Zheludev, A., T. Masuda, I. Tsukada, Y. Uchiyama, K. Uchinokura, P. Böni, and S.-H. Lee, 2000, Phys. Rev. B **62**, 8921.
Zheng, G. qing, T. Odaguchi, T. Mito, Y. Kitaoka, K. Asayama, and Y. Kodama, 1993, J. Phys. Soc. Jpn. **62**, 2591.
Zhu, J.-X., C. Ting, and C. Hu, 2000, Phys. Rev. B **62**, 6027.
Zhu, L., W. A. Atkinson, and P. J. Hirschfeld, 2003, Phys. Rev. B **67**, 094508.
Zhu, L., P. Hirschfeld, and D. Scalapino, 2004, Phys. Rev. B **70**, 214503.
Ziegler, K., M. H. Hettler, and P. J. Hirschfeld, 1996, Phys. Rev. Lett. **77**, 3013.
Ziegler, W., D. Poilblanc, R. Preuss, and W. Hanke, 1996, Phys. Rev. B **53**, 8704.